

Theoretical Studies of Homogeneous Catalysis  
by Transition Metal Complexes

Thesis by

Anthony Kay Rappé

In Partial Fulfillment of the Requirements  
for the Degree of Doctor of Philosophy

California Institute of Technology

Pasadena, California

1981

(submitted October 20, 1980)

## ACKNOWLEDGEMENTS

First, I thank Bill Goddard for his enthusiasm for chemistry and trust in me.

I also thank Adria McMillan for her very skillful typing (and correcting my grammar).

I would also like to express my appreciation to all past and present members of the Goddard research group for putting up with me and for providing many stimulating discussions, much wise advice, and real comic relief. In this regard, I am particularly pleased to acknowledge Barry Olafson, Larry Harding, Terry Smedley, and Marv Goodgame.

I would further like to thank Carla Casewit and the Grubbs, Ber-caw, and Beauchamp research groups for repeated attempts to keep me in touch with the realities of experimental chemistry. I hope that they were at least partly successful.

I also thank Mom, Dad, Randy, and Jann for encouragement and moral support during this extended time.

Finally, I thank Carla to whom I am greatly indebted for her constant encouragement, support, and many lively discussions.

## ABSTRACT

CHAPTER 1: Extensive ab initio calculations (double zeta plus polarization function basis with correlated wavefunctions) on the oxidation of hydrocarbons by chromyl chloride are combined with standard thermochemical methods to predict the energetics for oxidation of alkanes, alcohols, and alkenes. Additional results are presented on the analogous oxidations by molybdenyl chloride. A common feature of all these reactions is identified and explained.

CHAPTER 2: Extensive ab initio calculations (double zeta plus polarization function basis with correlated wavefunctions) on the olefin metathesis reaction with high valent Mo and W catalysts are combined with standard thermochemical methods to predict the energetics of potential intermediates. The active catalyst is identified and explained together with several subsidiary features of the reaction manifold.

CHAPTER 3: A unifying generalized valence bond view of transition metal ligand bonding is presented as well as the energetics and structural characteristics of several ligand types. Additionally, the energetics for several ligand exchange reactions of potential synthetic utility are presented.

## PREFACE

A systematic study of chemical reactions involves a determination of all the microscopic steps along pathways from reactants to products both structurally and energetically. Secondly, a conceptual framework should be developed to understand why particular pathways are favored. Finally, one should predict and design reaction schemes that are "better" or more "desirable" in some sense.

The thesis will attempt to demonstrate that theoretical techniques may be useful in all phases of systematic studies of chemical reactions. Because reaction intermediates usually have short lifetimes and have inherently small concentrations, they are often difficult to observe and to characterize experimentally. A quantitatively accurate theoretical technique is inherently quite able to isolate and characterize reactive intermediates both structurally and energetically, bridging the gap between experimentally accessible reactants and products. A theoretical technique oriented toward presenting its results in a manner that leads directly to qualitative understanding (if coupled with chemical intuition) should be useful for both the prediction and design phases of a systematic study of chemical reactions.

Examples of this tenet are presented in Chapters 1 and 2. In Chapter 1, reaction pathways for the oxidation of alkanes, alcohols, and alkenes by chromyl chloride are structurally and energetically characterized. The resultant mechanism is outlined and compared with experimental observation. In Chapter 2, an analogous presentation is made of the olefin metathesis reaction by high valent Mo and W catalysts. Chapter 3 provides a preliminary description of a useful qualitative

view of transition metal bonding. Appendix A provides documentation of the theoretical techniques employed in the calculations discussed in Chapters 1-3.

## TABLE OF CONTENTS

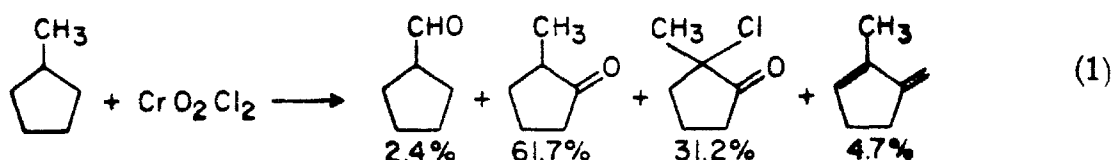
	<u>Page</u>
<u>Chapter 1: Oxidation of Chromyl Chloride</u>	
I. Introduction.....	1
II. Common Fundamental Process.....	3
III. Chromyl Chloride Oxidation of Alkanes.....	14
IV. Chromyl Chloride Oxidation of Alcohols.....	22
V. Chromyl Chloride Oxidation of Alkenes.....	26
VI. References.....	33
<u>Chapter 2: Olefin Metathesis</u>	
I. Introduction.....	35
II. Theoretical Results.....	38
III. Discussion.....	49
IV. Summary.....	51
V. References.....	53
<u>Chapter 3: Qualitative Bonding</u>	
I. Introduction.....	56
II. Ionic Sigma Bonds.....	57
III. Covalent Sigma Bonds.....	67
IV. Bonding in Saturated Complexes.....	72
V. Periodic Trends.....	102
VI. References.....	108
<u>Appendix A</u>	
I. Introduction.....	111
II. Geometrical Tests.....	113
III. Bond Strength Tests.....	115

	<u>Page</u>
IV. Retention of Bondedness.....	126
V. General Prescription.....	128
VI. References.....	129

## CHAPTER 1: Oxidation by Chromyl Chloride

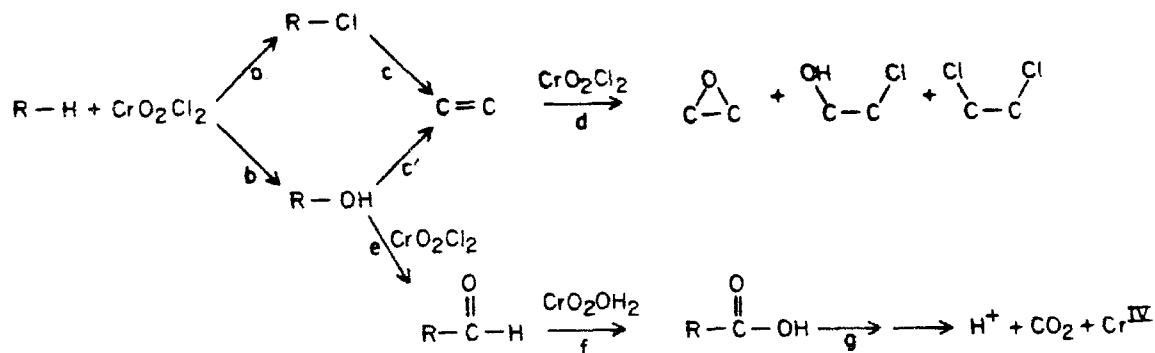
### I. Introduction

Chromic acid and related chromyl and molybdbl compounds form a class of versatile oxidizing agents<sup>1</sup> capable of delivering oxygen atoms to most types of oxidizable organic groups. This versatility can be a drawback since specificity in reaction site is at times a desirable quality. An example of this is the product distribution for the oxidation of methyl cyclopentane by chromyl chloride<sup>2</sup>



Clearly this is neither a synthetically useful nor mechanistically straightforward product mixture. Scheme I illustrates likely primary, secondary, and even higher-order reaction products of chromyl compounds reacting with a general alkane.

### Scheme I





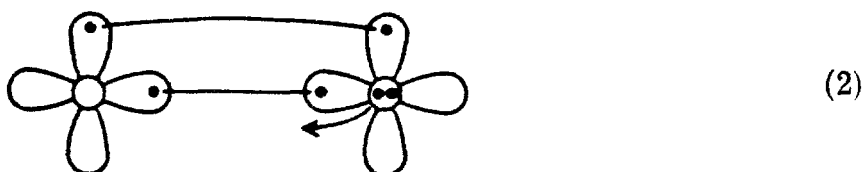
The likely primary processes a and b form alcohols (and alkyl chlorides if the oxidant is chromyl chloride). For example, propyl benzene reacts with chromyl chloride to form substantial 1-chloro, 1-phenylpropane, <sup>1b, 3</sup> whereas triphenyl methane forms predominantly triphenyl carbinol<sup>4</sup> upon hydrolysis. It is likely that alcohols and alkyl chlorides will be dehydrated under the reaction conditions<sup>1c</sup> as implied in c of Scheme I. The olefins generated in situ can be subsequently oxidized as shown in d of Scheme I. Alternatively, the alcohols may be oxidized to aldehydes and ketones as shown in e of Scheme I. Finally, aldehydes can be oxidized by chromic acid to carboxylic acids as shown in f of Scheme I and eventually to CO<sub>2</sub> and H<sub>2</sub>O as shown in g of Scheme I.

Our studies will concentrate on the energetics of chromyl chloride and molybdyl chloride oxidation of alkanes, alcohols, and alkanes. Section II provides a discussion of a significant mechanistic feature found to be common to each of the oxidation steps. Section III presents the results for alkane oxidation, Section IV, alcohol oxidation, and finally, Section V, the alkene oxidation.

## II. Common Fundamental Process

The primary reaction step common to all the reactions of chromyl chloride discussed in the sections that follow is the addition of either a sigma or pi bond across a Cr-O pi bond. As shown in Fig. 1,  $H_2$  will not react with  $CrOCl_2$ , though it will react with  $CrO_2Cl_2$  as shown in Fig. 2. It is apparent from these energetics that two seemingly similar Cr-O bonds behave surprisingly differently in reaction with  $H_2$ .

This differential reactivity is due to radically different metal-oxo bonds for  $CrOCl_2R_2$  and  $CrO_2Cl_2$  species. We find that the metal-oxygen bonds of  $CrOCl_4$ ,  $CrOCl_2$ , and  $CrHOCl_2OH$  are essentially triple bonds analogous to the triple bond in the CO diatomic, whereas the metal-oxygen bonds in  $CrO_2Cl_2$  are double bonds analogous to the C-O bond in a ketone. Since the Cr of  $CrOCl_4$  has available two singly-occupied d orbitals that can bond to the oxygen, it can form either a sigma bond and a pi bond with an oxygen pi lone pair left over



or two pi bonds and a dative sigma bond,

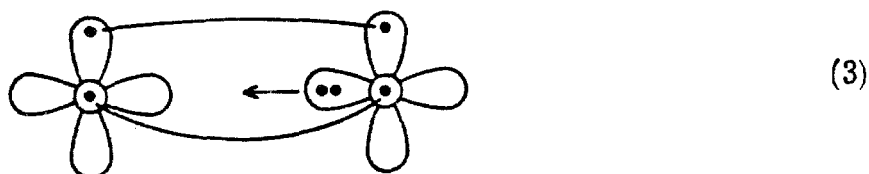


Figure 1. Energetics ( $\Delta G_{300}$ ) for addition across Cr-O triple bond.

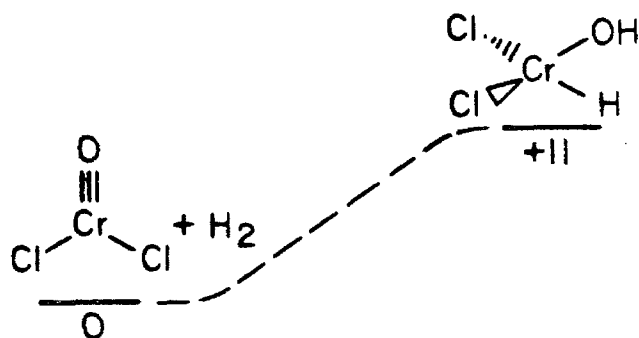
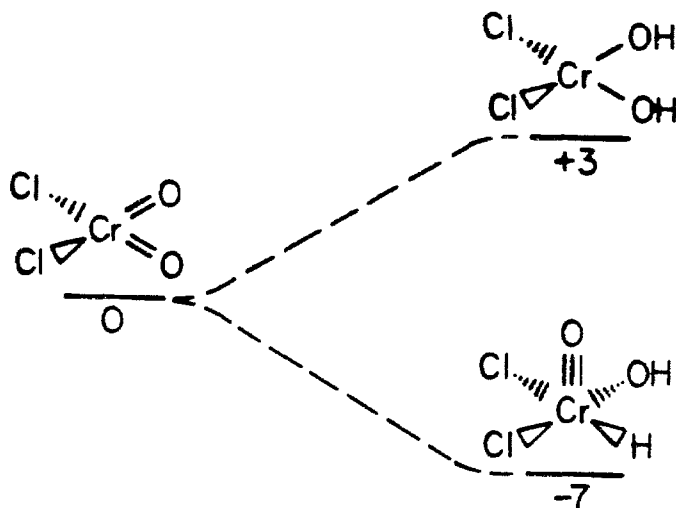
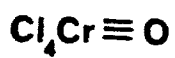


Figure 2. Energetics ( $\Delta G$ ) for addition across Cr-O double bond.

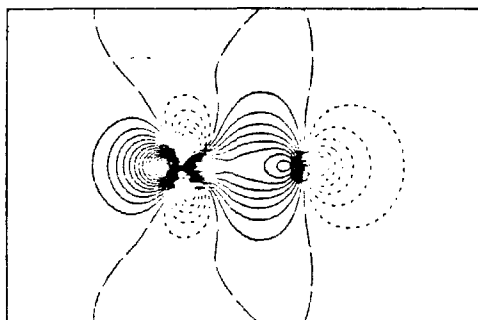


For both CO and  $\text{CrOCl}_4$ , the second bonding arrangement is substantially favored (by 50 kcal for CO and by 30 kcal for  $\text{CrOCl}_4$ ). Orbital contour plots for the oxygen-X triple bonds of  $\text{CrOCl}_4$  and CO are shown in Figs. 3 and 4, respectively. For  $\text{CrO}_2\text{Cl}_2$  there are four singly-occupied d orbitals available to bond to two oxygens, resulting in both oxygens each forming a sigma bond and one pi bond concurrent with each oxygens pi long pair slightly delocalizing into the same empty  $d\pi$  orbital. Orbital contour plots of the  $\text{CrO}_2\text{Cl}_2$  and  $\text{H}_2\text{CO}$  oxygen double bonds are shown in Figs. 5 and 6, respectively. The result is that the oxo bond in  $\text{CrOCl}_4$  is 31 kcal stronger than the first oxo bond in  $\text{CrO}_2\text{Cl}_2$  (82 kcal versus 51 kcal). Similarly, the oxo bond in  $\text{Cr}(\text{H})(\text{O})(\text{Cl})_2(\text{OH})$  is a triple bond. Thus the second oxo group in chromyl chloride is not a spectator but actually drives the formation of the hydroxy hydride intermediate. This favorable effect may be contrasted with the  $\text{CrOCl}_2 + \text{H}_2$  case where a spectator oxygen is not present in the intermediate and furthermore, addition is across a Cr-O triple bond. These two factors result in a substantial differential reactivity pattern which flavors the oxidations of alkanes, alcohols, and alkenes by chromyl chloride.

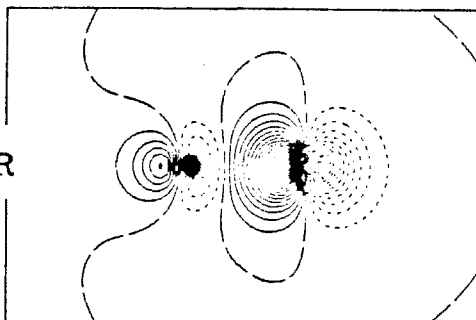
Figure 3.  $\text{Cr}(\text{O})(\text{Cl})_4$  Cr-O  $\sigma$  and  $\pi$  bond orbital contour plots. Long dashes indicate zero amplitude; the spacing between contours is 0.05 a.u.; the same convention is used in all plots.



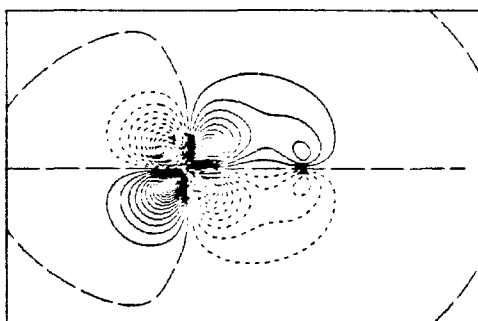
CrO  $\sigma$



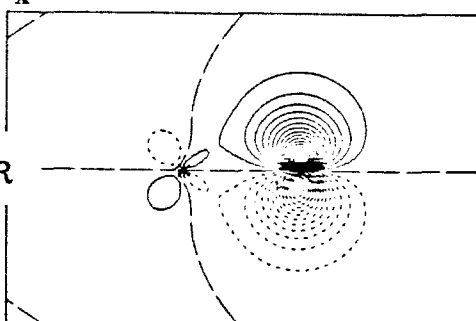
PAIR



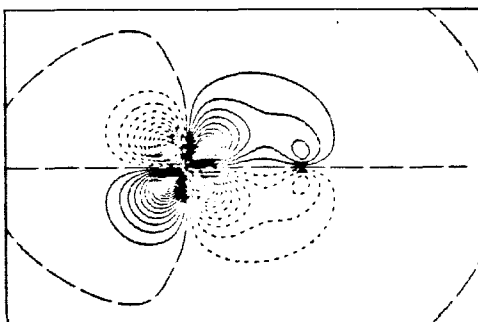
CrO  $\pi_x$



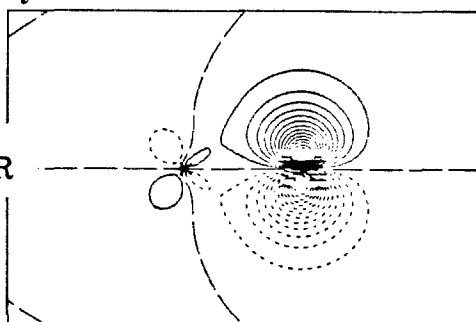
PAIR



CrO  $\pi_y$



PAIR



O L.P.

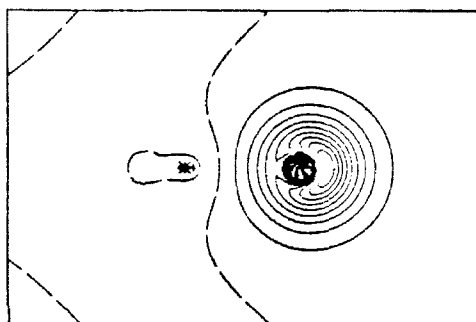
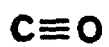
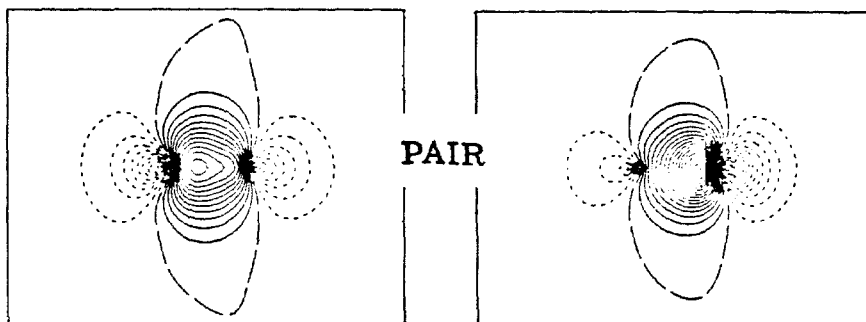


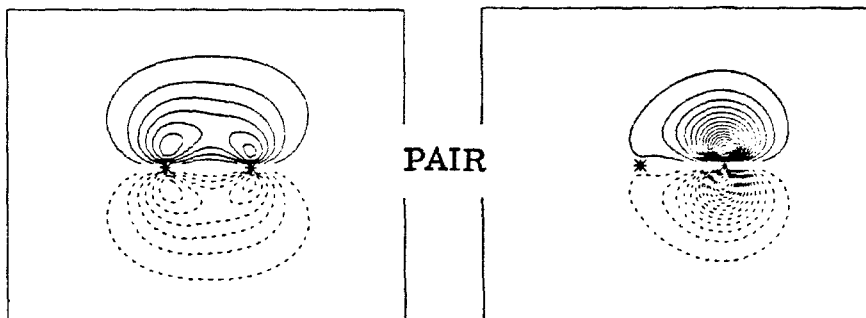
Figure 4. CO C-O  $\sigma$  and  $\pi$  bond orbital contour plots.



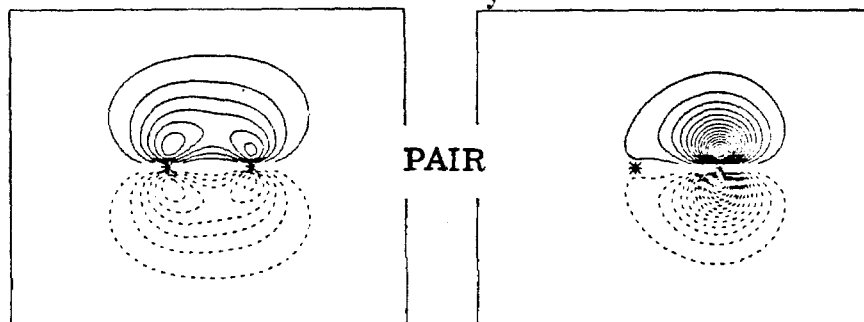
CO  $\sigma$



CO  $\pi_x$



CO  $\pi_y$



C L.P.

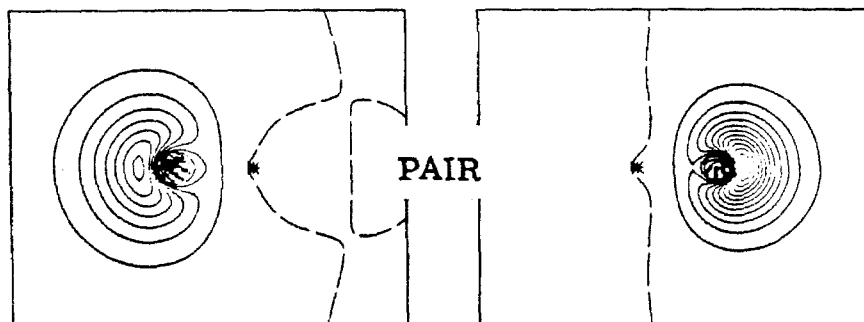
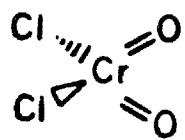
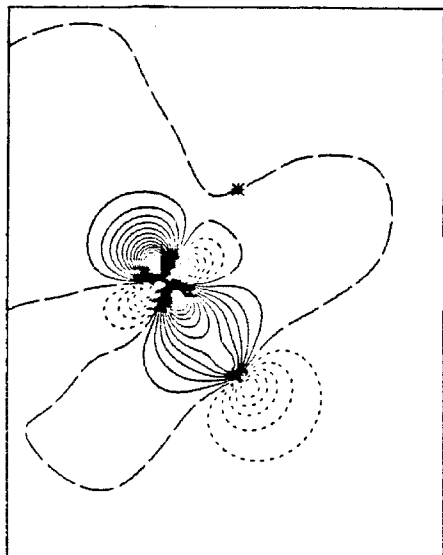




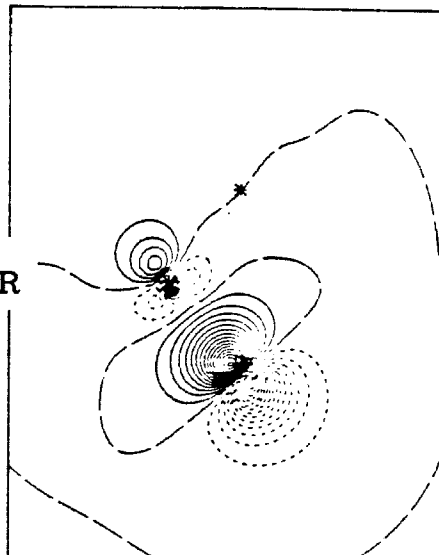
Figure 5.  $\text{Cr}(\text{O})_2(\text{Cl})_2$  Cr-O  $\sigma$  and  $\pi$  bond orbital contour plots.



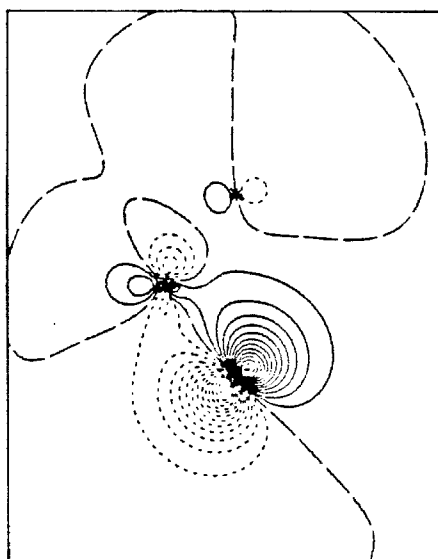
CrO  $\sigma$



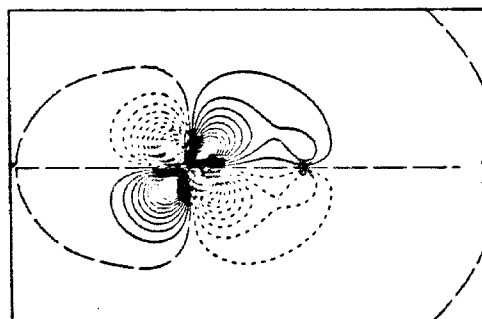
PAIR



O L.P.



CrO  $\pi$



PAIR

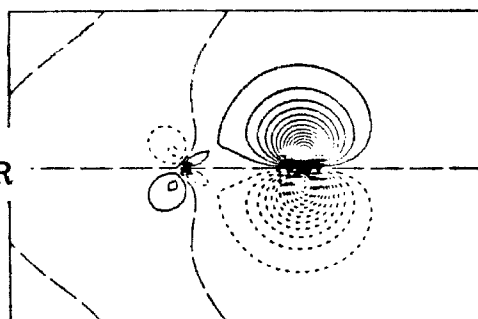
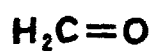
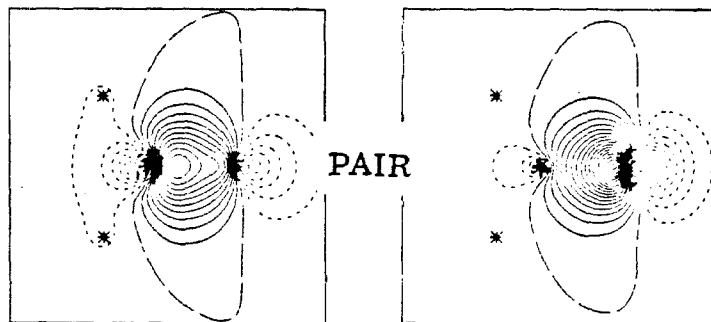


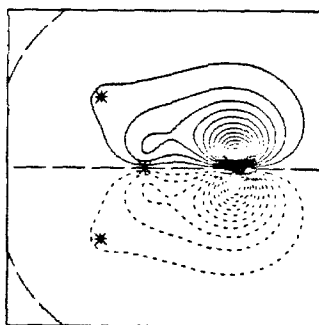
Figure 6.  $\text{H}_2\text{CO}$  C-O  $\sigma$  and  $\pi$  bond orbital contour plots.



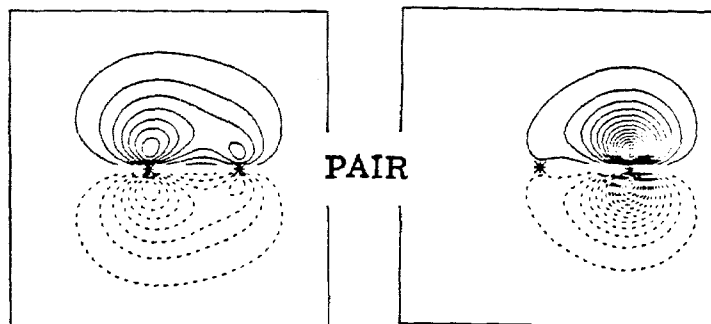
CO  $\sigma$



O L.P.

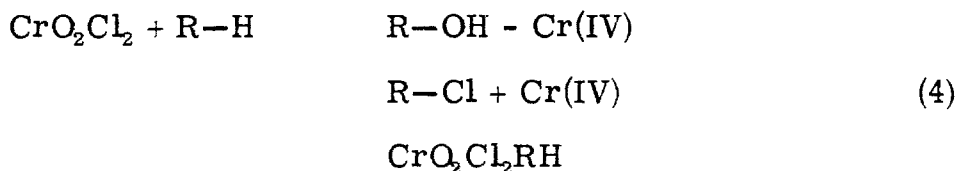


CO  $\pi$



### III. Chromyl Chloride Oxidation of Alkanes

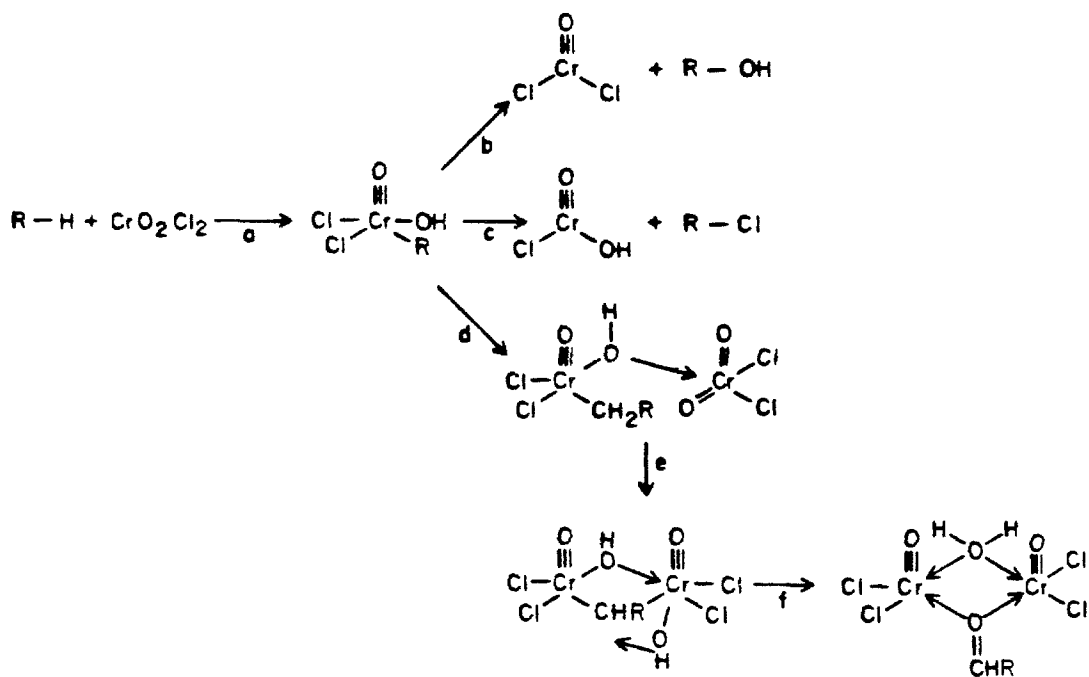
There is substantial evidence<sup>1-4</sup> that chromyl compounds react with alkanes to initially form either alcohols, alkyl chlorides, or a stable complex,



The initially formed products R-OH and R-Cl may undergo rapid secondary reactions leading to oxidation products attributable to alkene oxidation.<sup>1b,c</sup> The stable complex undoubtedly undergoes a rapid secondary reaction leading to the first "observed" intermediate, the Étard complex, an insoluble hygroscopic brown solid that can be hydrolyzed under reducing conditions to directly form aldehydes and ketones.<sup>1c</sup> The product composition usually is diverse and very dependent on reaction conditions,<sup>1b</sup> making detailed mechanistic study difficult. There is evidence for a Cr(V) intermediate<sup>3,5,6</sup> and for the Étard complex having two Cr(IV) centers.<sup>1</sup>

Based upon energetics from ab initio calculations, we propose a reaction scheme consistent with the experimental observations that consists of an initial addition of the C-H bond across one Cr-O pi bond forming an organometallic complex (reaction a of Scheme II) which either reductively eliminates an alcohol (b of Scheme II), an alkyl chloride (c of Scheme II), or reacts with a second CrO<sub>2</sub>Cl<sub>2</sub> molecule, initially forming a dative complex between the hydroxide and the second chromyl chloride (d of Scheme II). This is followed by addition across a second CH bond, leading to a complex with a bridging carbene (e of

Scheme II



Scheme II) which can rearrange to a third dative complex consisting of a bridging water and a bridging carbonyl compound (f of Scheme II), which is a feasible structure for the Etard complex.

Calculationally we have concentrated on the initial reactions stressing factors that favor the reductive elimination pathways, since use of dilute solutions or polymer supports will decrease the secondary reactions leading to Etard complex formation.

The energetics for the reaction with  $H_2$  as the substrate are shown in Fig. 7. As discussed in Sec. II, the dominant pathway is driven by the formation of a strong Cr-O triple bond, both in the Cr(VI) intermediate and the Cr(IV) product. The classic pathway consisting of either direct or stepwise addition across both Cr-O pi bonds is not energetically accessible since both Cr-O bonds and the  $H_2$  sigma bond are broken and only two O-H bonds are formed. As one can see from Fig. 7,  $H_2O$  should be the dominant product formed. The energetics for methane as the substrate are shown in Fig. 8. The major deviation from  $H_2$  is in the weaker Cr-C versus Cr-H bond strength. This will lead to large concentrations of the Cr(V) and organic radical intermediates. [We suggest that this Cr(V) intermediate implicated<sup>3, 5, 6</sup> is in fact a side reaction and is not an essential part of the reaction mechanism.] Finally, the energetics for ethane and for reaction across other terminal CH bonds are shown in Fig. 9.

A major difference between Cr and Mo compounds is the general increase in bond strength of 10-20 kcal per bond. This effect will manifest itself in that oxidation of alkanes by molybdenyl compounds should result in a smaller barrier, a smaller concentration of alkyl radicals

Figure 7. Energetics ( $\Delta G_{300}$ ) of the reaction of  $H_2$  with  $CrO_2Cl_2$ .

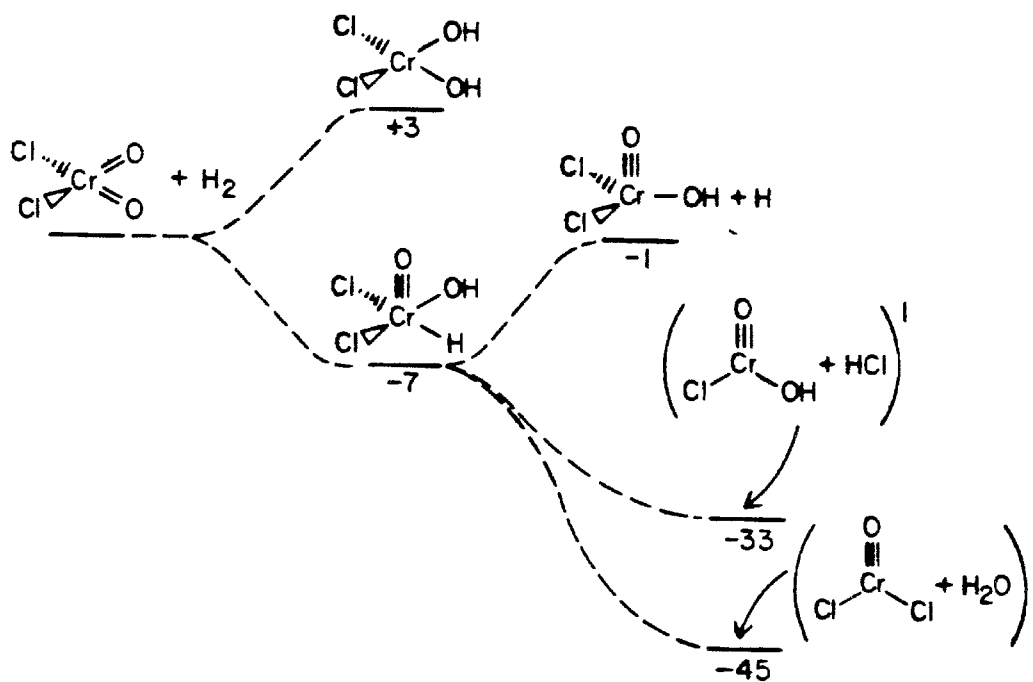




Figure 8. Energetics ( $\Delta G_{300}$ ) of the reaction of  $\text{CH}_4$  with  $\text{CrO}_2\text{Cl}_2$ .

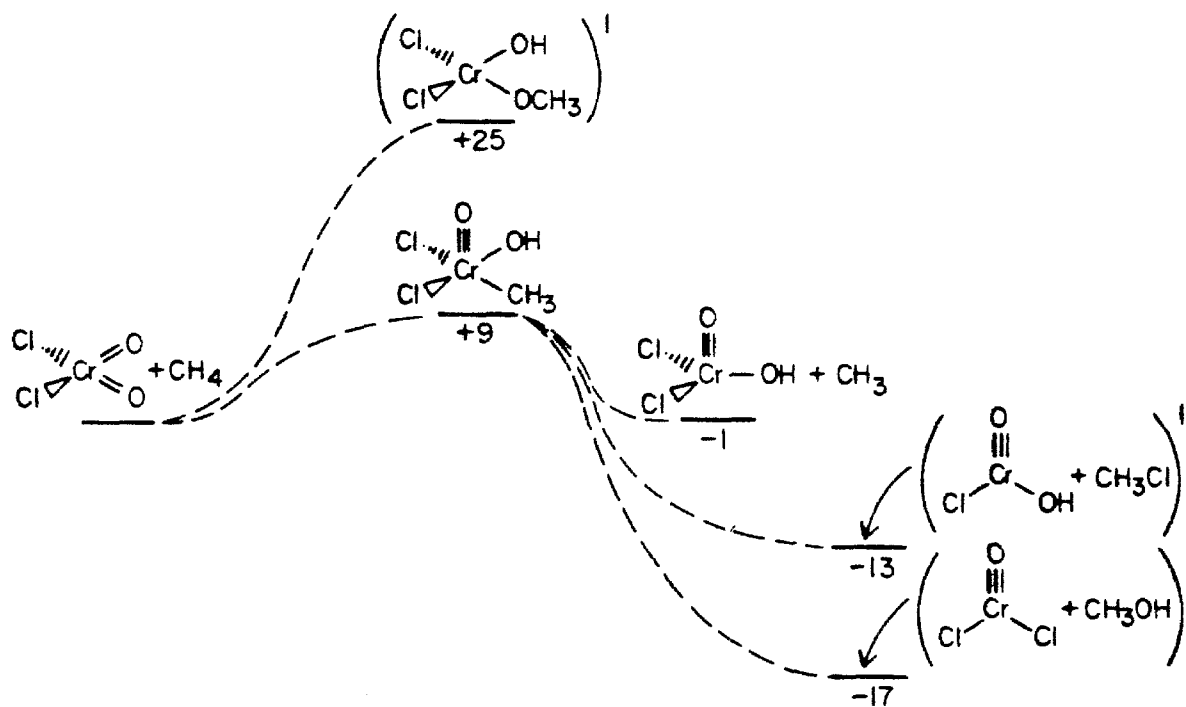
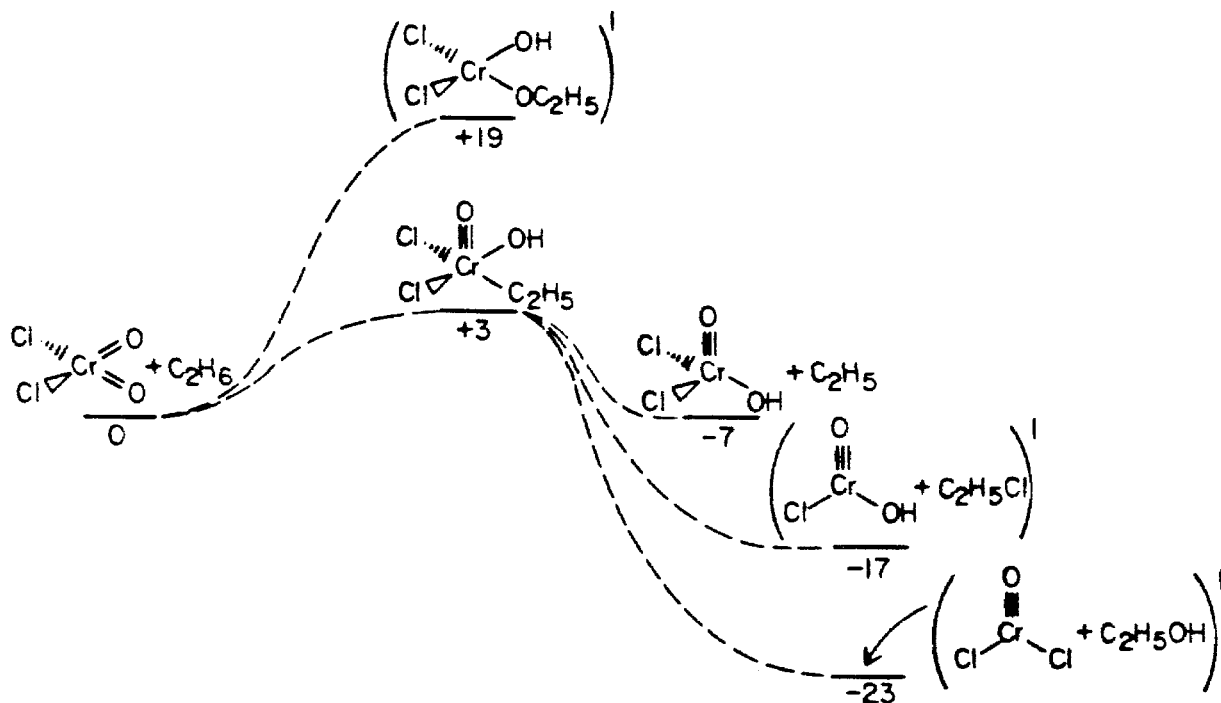
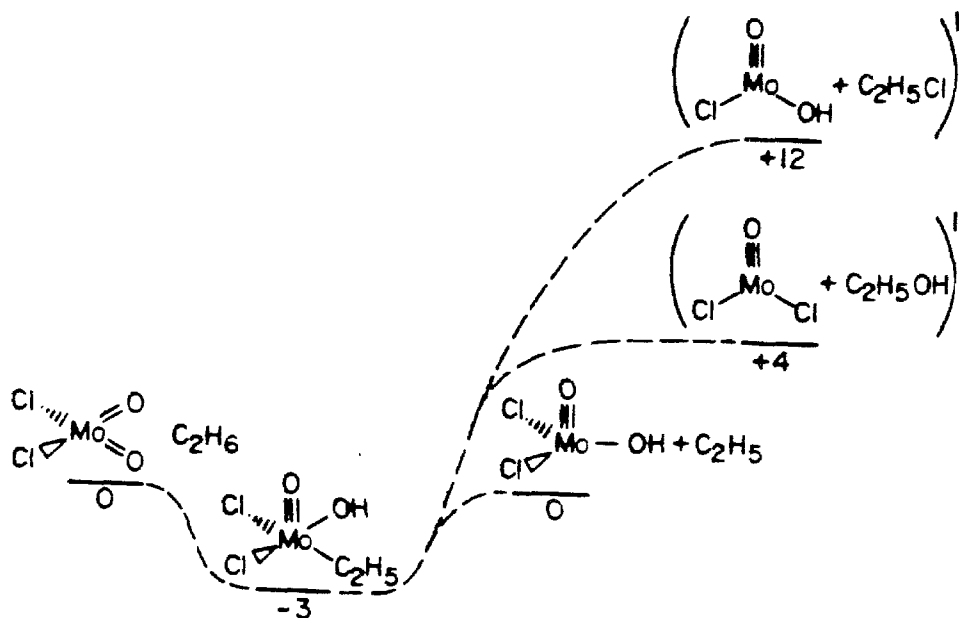


Figure 9. Energetics ( $\Delta G_{300}$ ) of the reaction of  $C_2H_6$  with  $CrO_2Cl_2$ .



and Mo(V) species, and less alkyl chloride or alcohol production with an enhanced direct formation of the Etard complex, since the final rearrangement will be the only reductive elimination step in this pathway. This general trend will be discussed in detail in Chapter 3, and Fig. 10 presents the ramifications of this effect for the oxidation of ethane by molybdenyl chloride.

Figure 10. Energetics ( $\Delta G_{300}$ ) of the reaction of  $C_2H_6$  with  $MoO_2Cl_2$ .



#### IV. Chromyl Chloride Oxidation of Alcohols

Though chromyl chloride is not a standard alcohol oxidizing reagent, study of this reaction is mechanistically significant since at least small quantities of free alcohol should be formed during alkane oxidation. As mechanistic studies on the oxidation of alcohols by chromyl chloride have not been carried out, analogy to other chromyl compounds and the general reactivity of high valent early transition metal complexes suggests likely alternatives. The most probable processes are substitution of the alkoxide for a chloride (a of Scheme III), addition across the OH bond (b of Scheme III), or finally addition across a CH bond (c of Scheme III), followed by reductive elimination forming either a hydroxychloride (d of Scheme III) or a hydrate (e of Scheme III), either of which will dehydrate, forming the aldehyde or ketone.

The energetics for these pathways for  $C_2H_5OH$  as the substrate are shown in Fig. 11. The energetics suggest that chromyl chloride is a viable oxidizing reagent for water-insoluble alcohols and that if formed during alkane oxidation, alcohols will subsequently be oxidized to aldehydes and ketones, explaining why they are generally not observed. The energetics for the molybdyl chloride oxidation of ethanol are shown in Fig. 12. Again, the increased Mo bond strengths favor formation of the organometallic intermediate and disfavor the reductive elimination pathways.

Scheme III

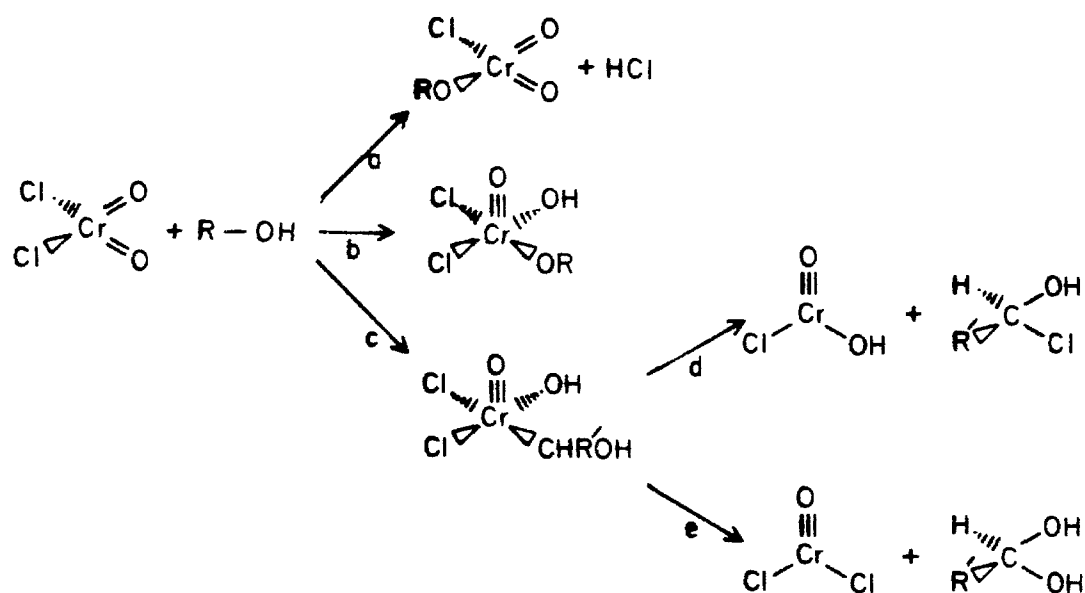


Figure 11. Energetics ( $\Delta G_{300}$ ) for the reaction of  $C_2H_5OH$  with  $CrO_2Cl_2$ .

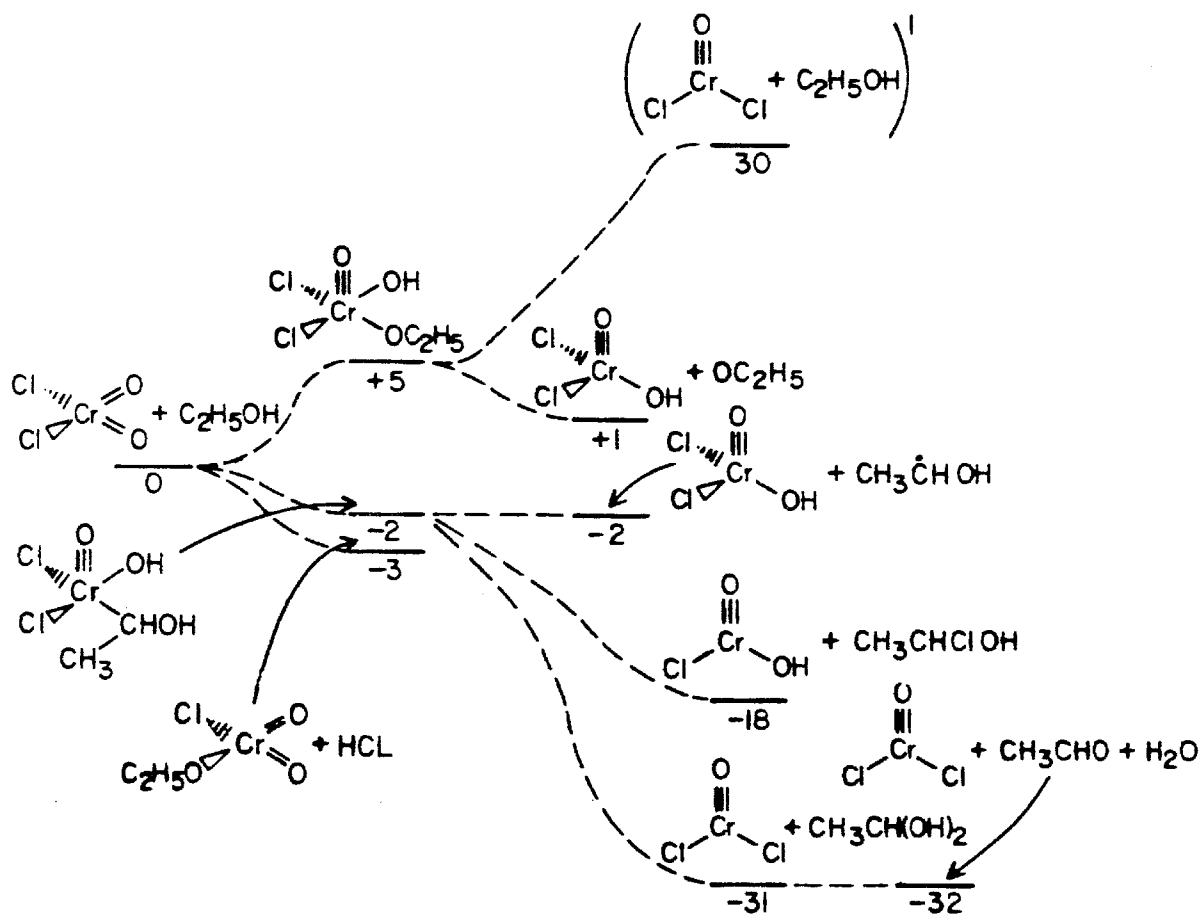
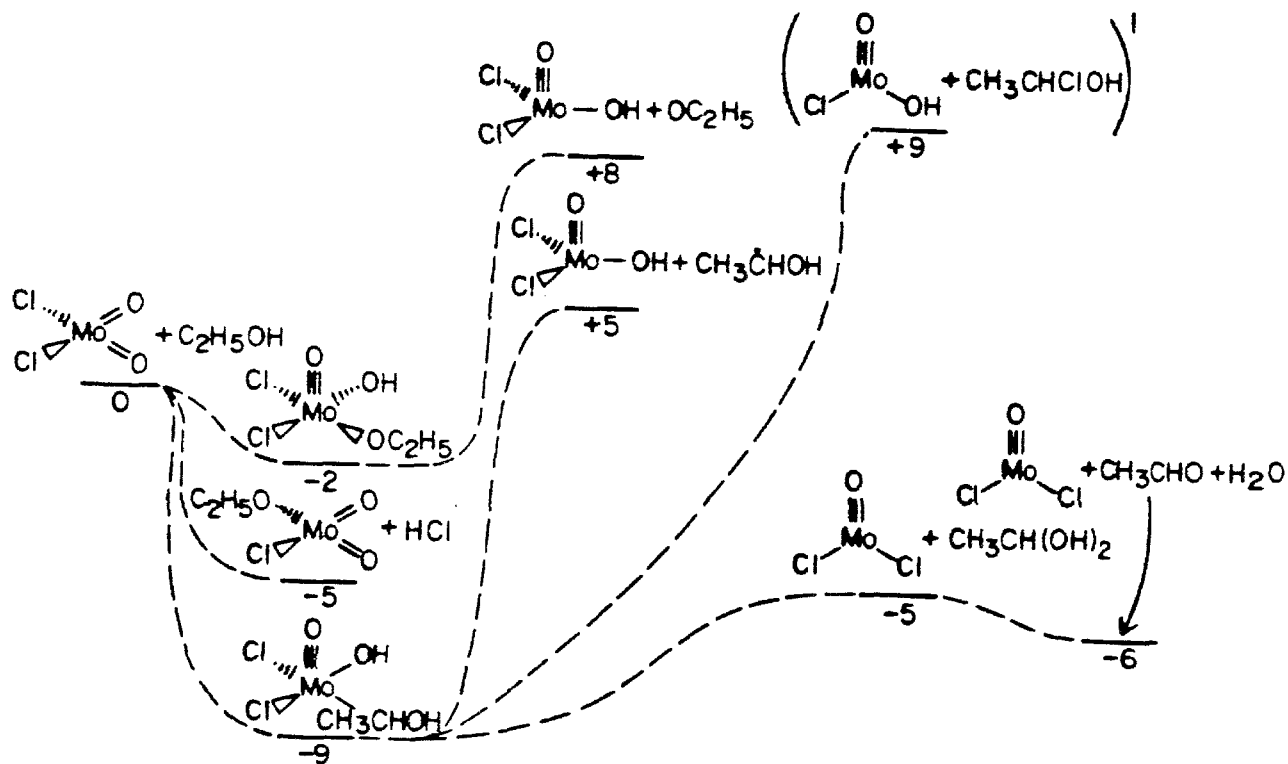


Figure 12. Energetics ( $\Delta G_{300}$ ) for the reaction of  $C_2H_5OH$  with  $MoO_2Cl_2$ .





## V. Chromyl Chloride Oxidation of Alkenes

Olefins are oxidized by chromyl chloride to dominantly form epoxides and chlorohydrides. Because of the possibility of selectively attaching an oxygen atom to an olefin (predominantly cis addition), olefin oxidation has received far more mechanistic study than other organic substrates. A novel aspect of olefin oxidation is the proposal of a metallocyclic intermediate analogous to the metallocyclobutane proposed for olefin metathesis (a of Scheme IV) that can decompose to form either a carbonyl compound (b of Scheme IV), an epoxide (c of Scheme IV), or the precursor to a chlorohydrin (d of Scheme IV). Experimentally, each of these products has been observed in alkene oxidation by chromyl chloride.<sup>6</sup>

The energetics for the oxidation of ethylene by chromyl chloride are shown in Fig. 13. These energetics confirm the proposal that the metallocyclooxetane is a likely common precursor for all of the observed oxygen-containing products and rule out the direct addition reaction characteristic of oxidations by  $\text{OsO}_4$  (e of Scheme IV).

As discussed in Sec. III, a major difference between Cr and Mo compounds is the general increase in bond strength of 15 kcal per bond. This effect manifests itself in a strong relative disfavor of any reductive elimination pathway for molybdenum. The C-C bond cleavage pathway will dominate the reductive elimination of epoxides or chlorohydrins, and it is very likely that it is through this pathway that  $\text{MoO}_3$  and  $\text{WO}_3$  are activated for metathesis on a polymer support<sup>9</sup>

Scheme IV

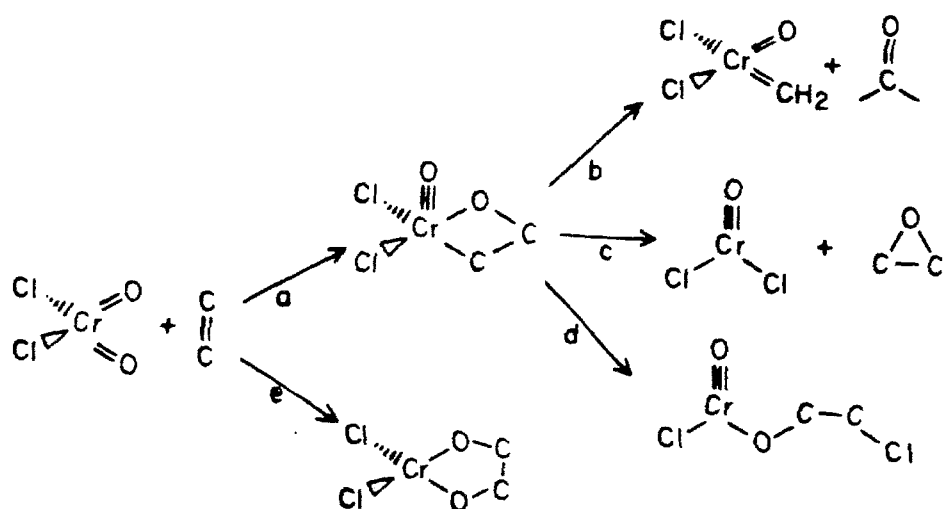
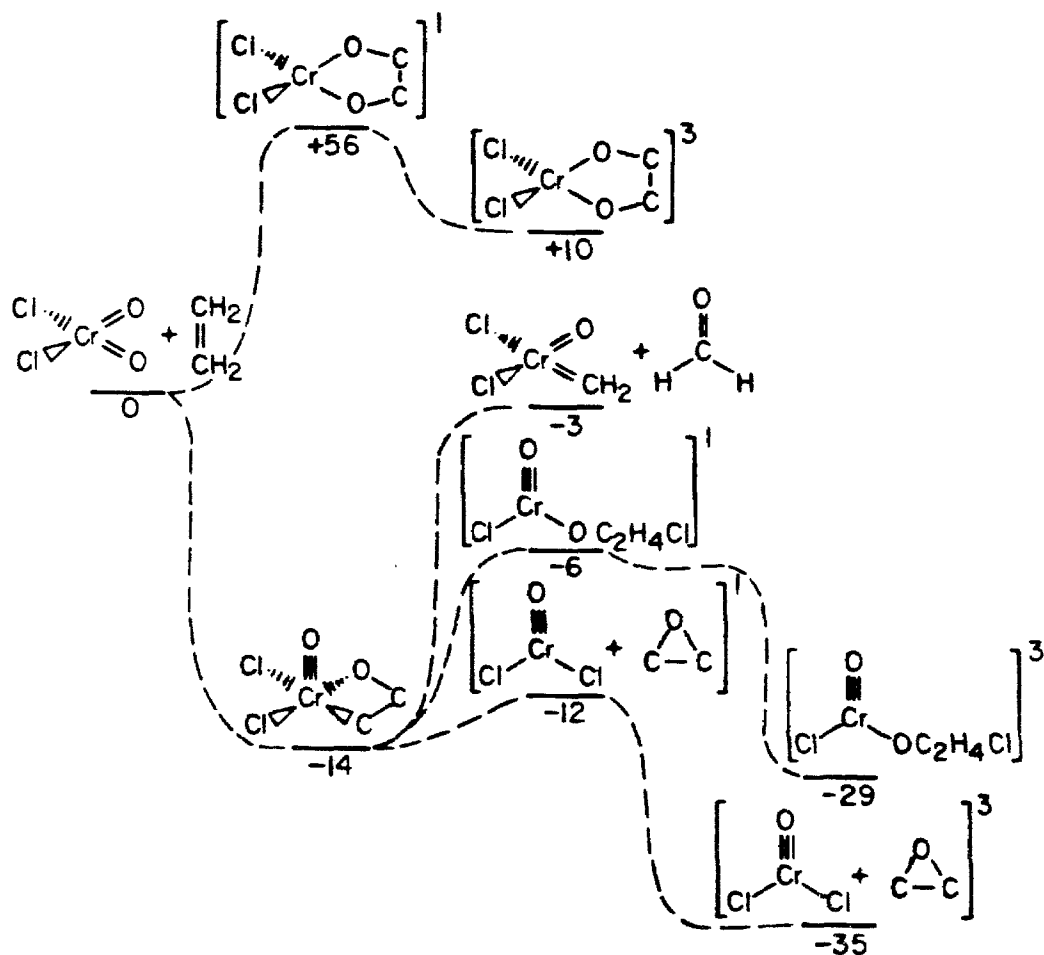
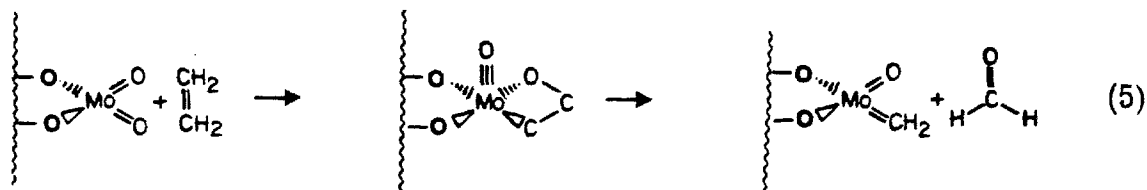


Figure 13. Energetics ( $\Delta G_{300}$ ) for the reaction of  $C_2H_4$  with  $CrO_2Cl_2$ .





The energetics for these processes are summarized in Fig. 14 for molybdenum. In fact, under appropriately chosen operating conditions, olefins such as propene are allylicly oxidized to carbonyls such as acrolein over supported  $\text{MoO}_3$  and  $\text{WO}_3$  catalysts.<sup>10</sup> The addition across a C-H bond (as discussed in Sec. III) may be competitive with addition across the C-C pi bond. The energetics for this dilemma are presented in Fig. 15 for  $\text{CrO}_2\text{Cl}_2$ , indicating that reaction across the C-C pi bond should be favored over reaction across the C-H bond. Molybdenum as shown in Fig. 16 should result in a more competitive situation. Experimentally, the products observed (C-C reaction versus C-H reaction) are very dependent upon the reaction conditions.<sup>11-13</sup> Imra<sup>14</sup> has found that for nonstoichiometric  $\text{MoO}_3$  and  $\text{WO}_3$  the dominant product is the oxidative C-C bond cleavage product; that is, propene forms formaldehyde and acetaldehyde. Furthermore, San Filippo<sup>15</sup> has found that chemisorbed chromyl chloride oxidatively cleaves the C-C double bond.

Our interpretation of these results is that the true surface sites responsible for metathesis initiation and C-C bond cleavage are as described in (5) with adjacent sites being needed to achieve quantitative yields of C-C bond cleavage through a process analogous to the bimolecular decomposition of homogeneous alkylidene complexes.<sup>16</sup>

Figure 14. Energetics ( $\Delta G_{300}$ ) for the reaction of  $C_2H_4$  with  $MoO_2Cl_2$ .

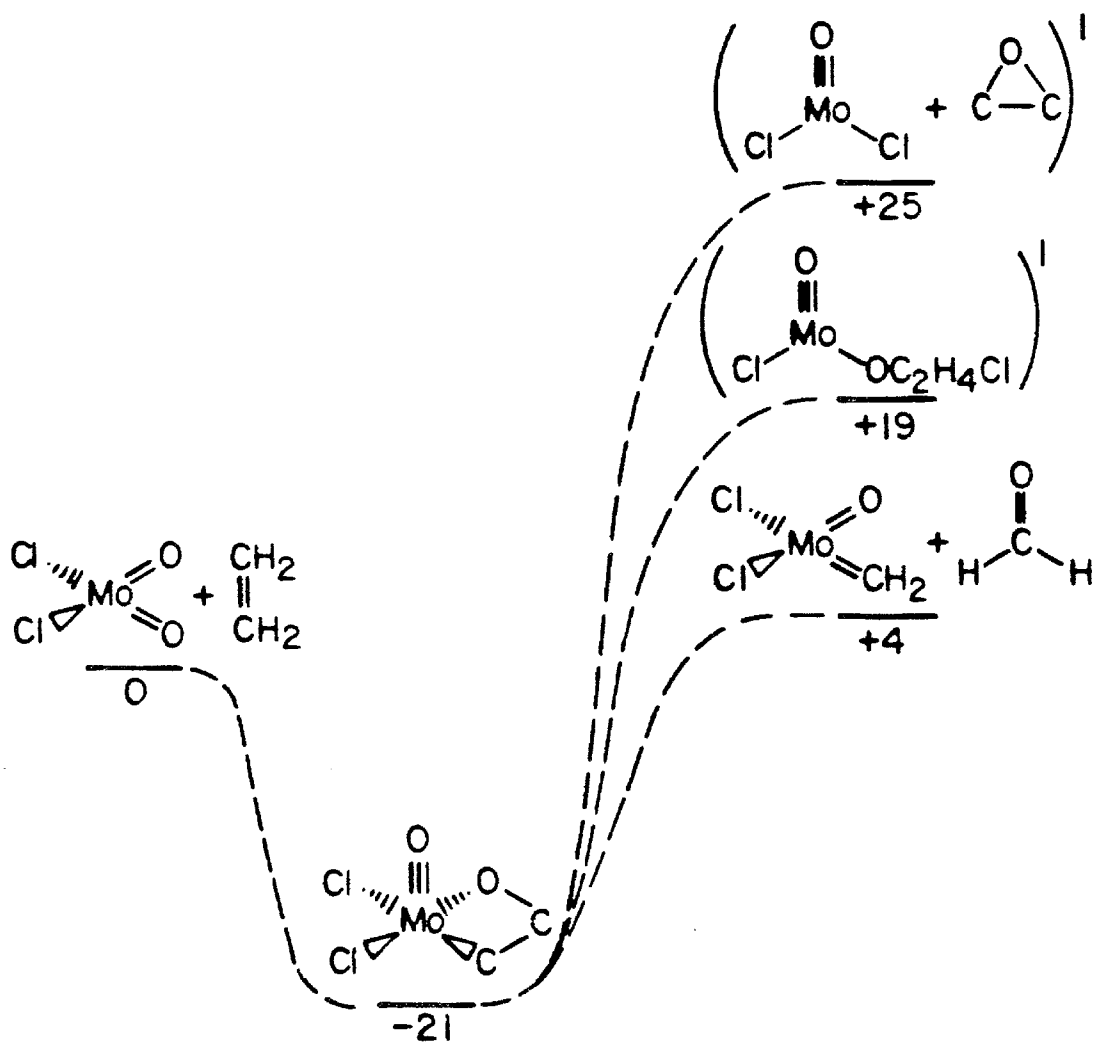


Figure 15. Energetics ( $\Delta G_{300}$ ) for the reaction of  $\text{CH}_3\text{CHCH}_2$  with  $\text{CrO}_2\text{Cl}_2$ .

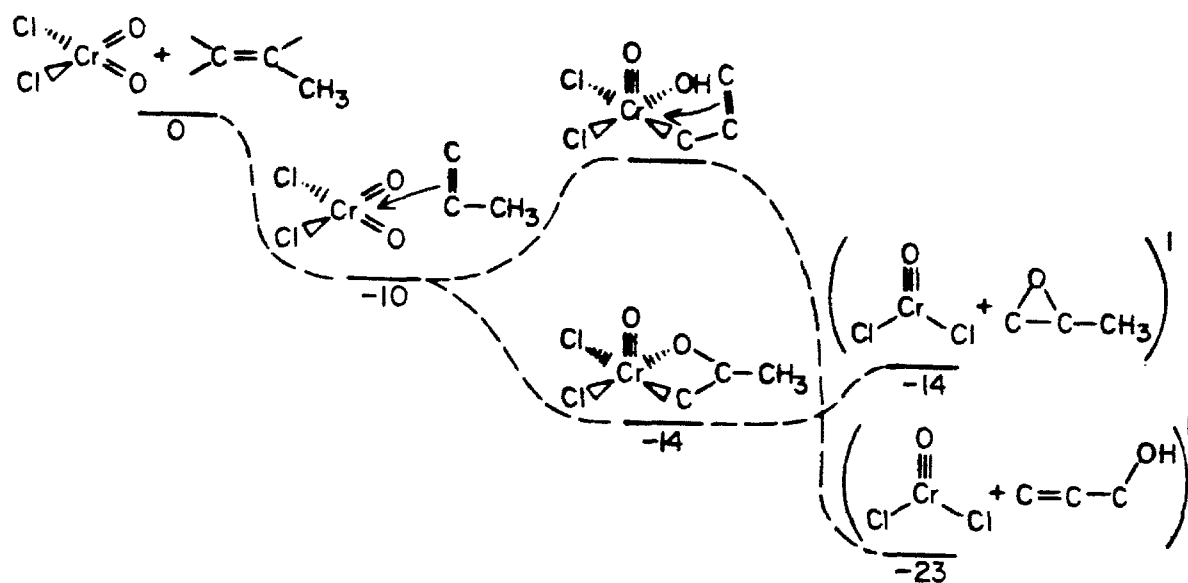
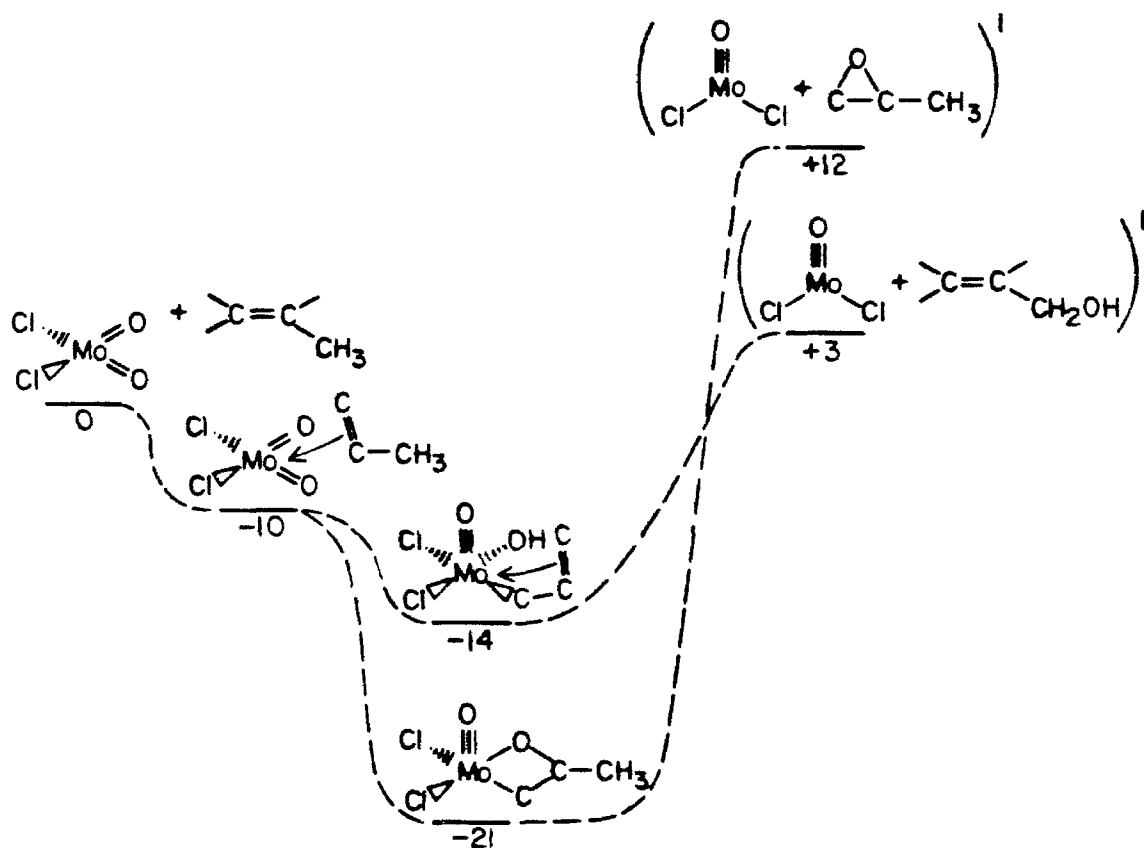


Figure 16. Energetics ( $\Delta G_{300}$ ) for the reaction of  $\text{CH}_3\text{CHCH}_2$  with  $\text{MoO}_2\text{Cl}_2$ .



## References

1. (a) W. H. Hartford and M. Darrin, Chem. Rev., 58, 1-61 (1958);  
(b) K. B. Wiberg, "Oxidation in Organic Chemistry"; Part A,  
Academic Press: New York, 1965; pp. 69-184; (c) F. Freeman,  
Rev. React. Species Chem. React., 1, 37-64 (1973).
2. V. Psemetschi, I. Necsoiu, M. Rentea, and C. D. Nenitzescu,  
Rev. Roum. Chem., 14, 1567-1574 (1969).
3. L. M. Stephenson, J. Egnatchik, and D. R. Speth, J. Org.  
Chem., 44, 346-349 (1979).
4. I. Necsoiu, V. Przemetchi, A. Ghenciulescu, C. N. Rentea,  
and C. D. Nenitzescu, Tetrahedron, 22, 3037-3045 (1966).
5. I. P. Gragerov and M. P. Ponomarchuk, J. Org. Chem. USSR  
(English translation), 3, 440-445 (1967); I. P. Gragerov and M.  
P. Ponomarchuk, ibid., 5, 1125 (1969).
6. F. Freeman, C. R. Armstead, M. G. Essig, E. L. Karchefski,  
C. J. Kojima, V. C. Manopoli, and A. H. Wickman, J. Chem.  
Soc. Chem. Comm., 65 (1980).
7. R. A. Walton, "Progress in Inorganic Chemistry", 16, 1-226  
(1972).
8. K. B. Sharpless, A. Y. Teranishi, and J. E. Bäckvall, J. Am.  
Chem. Soc., 99, 3120-3128 (1977).
9. (a) E. A. Lombardo, M. Lo Jacono, and W. K. Hall, J. Catal.,  
64, 150-162 (1980); (b) R. H. Grubbs and S. J. Swetnick, J.  
Mol. Catal., 8, 25-36 (1980).
10. L. D. Krenze and G. W. Keulks, J. Catal., 61, 316-325 (1980);  
ibid., 64, 295-302 (1980).

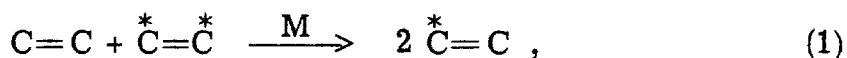


11. S. De Rossi, E. Iguchi, M. Schiavello, and R. J. D. Tilley, J. Catal., 61, 256-263 (1980).
12. P. E. Dai and J. H. Lungford, J. Catal., 64, 173-183 (1980).
13. J. Engelhardt, J. Catal., 62, 243-252 (1980).
14. L. Imra and K. F. Wedemeyer, U. S. Patent No. 3,946,081.
15. J. San Filippo, Jr., and C. Chern, J. Org. Chem., 42, 2182-2183 (1977).
16. R. R. Schrock, S. Rocklage, J. Wengrovius, G. Rupprecht, and J. Fellmann, J. Mol. Catal., 8, 73-83 (1980).

## CHAPTER 2: Olefin Metathesis

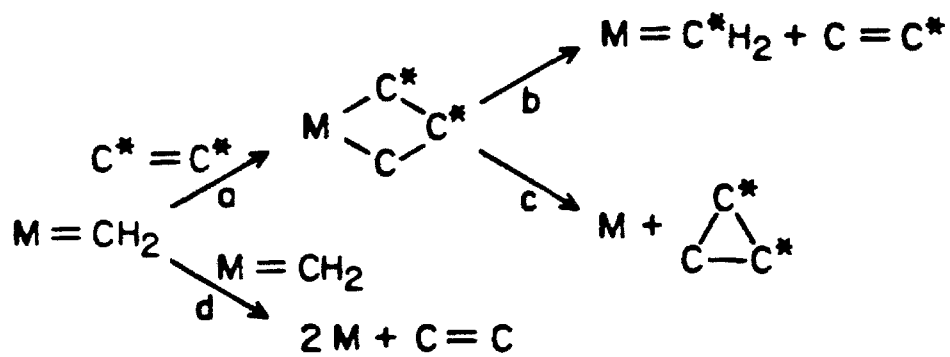
### I. Introduction

One of the most intriguing and best studied catalytic reactions in organometallic chemistry is the olefin metathesis reaction.<sup>1</sup> It is of at least potential synthetic utility<sup>2</sup> and is of true industrial importance.<sup>3</sup> The reaction involves at least formally a simultaneous cleave of two olefin double bonds followed by the formation of the alternate double bonds



where M is some metal complex. The currently accepted mechanism was proposed by Herisson and Chauvin<sup>4</sup> and has been established through detailed (and ingenious) study of isotopic scrambling<sup>5, 6</sup> and indirect evidence such as synthesis of carbene<sup>7</sup> and metallocyclobutane<sup>8-11</sup> complexes and analysis of the character of polymeric products of cycloolefins.<sup>12</sup> Furthermore, Casey<sup>13</sup> has synthesized low-valent carbene complexes that will directly metathesize olefins  $[W(CO)_5CO_2]$ . The mechanism involves a metal carbene complex as the active chain carrying catalyst which reacts with an olefin to form a metallocyclobutane intermediate (a of Scheme I) which decomposes to form the product olefin (b of Scheme I). Potential side reactions are the unimolecular decomposition of the metallocycle forming a cyclopropane plus the reduced metal complex (c of Scheme I) and the bimolecular decomposition of two carbene complexes (d of Scheme I). There are two general classes of metathesis catalysts, high-valent (generally d0) which are industrially important, and low-valent (oxidation state zero) which have been mechanistically significant even though this second type of

Scheme I

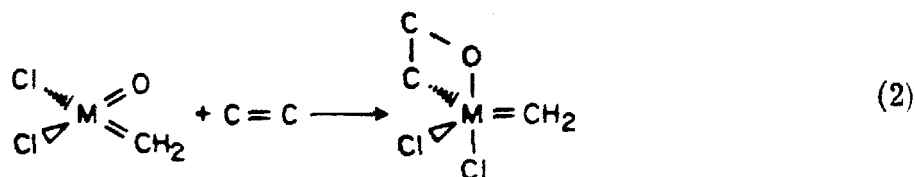


carbene is significantly different from the high-valent type. The remainder of this chapter will deal exclusively with the high-valent class of metathesis catalysts.

Typical recipes for active homogeneous<sup>14</sup> high-valent Mo and W metathesis catalysts involve a combination of various sources of metal [M(0) through M(VI)] with Lewis acids such as  $\text{AlCl}_2\text{C}_2\text{H}_5$  under a variety of conditions. A result of this diversity is that a detailed understanding of the ligand environment and even the oxidation state of the active catalyst (if there is just one active catalyst) is still lacking. Since the true catalyst may not be in large concentration,<sup>15</sup> physical studies on the catalytic system are difficult if not impossible. In fact, for supported catalyst it has been shown by Hall<sup>16</sup> that the metathesis sites correspond to less than 1% of the Mo present at the surface. The theoretical calculations presented here<sup>17a</sup> will concentrate on determining the detailed ligand environment of high-valent metathesis catalysts and developing an understanding of why particular ligands are desirable.

## II: Theoretical Results

The energetics for two possible Cr metathesis catalysts are shown in Fig. 1. As discussed in Chapter I, Sec. II, for an analogous system (oxidation of hydrocarbons by chromyl chloride), the oxygen ligand in  $\text{CrO}(\text{Cl})_2(\text{CH}_2)$  is not a spectator but in fact drives the formation of the metallocyclic intermediate through its change in character (and energetics) from a double bond to a triple bond. This effect changes a ludicrous pathway for  $\text{Cr}(\text{Cl})_4(\text{CH}_2)$  into an accessible one for  $\text{Cr}(\text{O})(\text{Cl})_2(\text{CH}_2)$ . For Mo and W the energetics change as indicated in Figs. 2 and 3, clearly dictating chemistry different from the Cr oxo-carbene for Mo and W oxo-carbene complexes, though for both Mo and W the tetrachloro carbene complex is still not a viable intermediate. For example, Cr will not form a stable metathesis catalyst due to the energetic accessibility of the reductive elimination pathway (c of Scheme I). In contrast, for Mo and W metathesis will dominate cyclopropane formation. As we have seen in Chapter 1 (and as will be discussed in detail in Chapter 3), the origin of this dramatic difference is the increased bond strengths in Mo complexes and a further increase for W compounds. In considering  $\text{M}(\text{O})(\text{Cl})_2(\text{CH}_2)$  as metathesis catalysts, we must consider the competition of the side reaction



As shown in Fig. 1, this pathway is energetically inaccessible. Table I

Figure 1. Energetics for the Reaction of  $C_2H_4$  with  $Cl_4CrCH_2$  and  $Cl_2OCrCH_2$ .

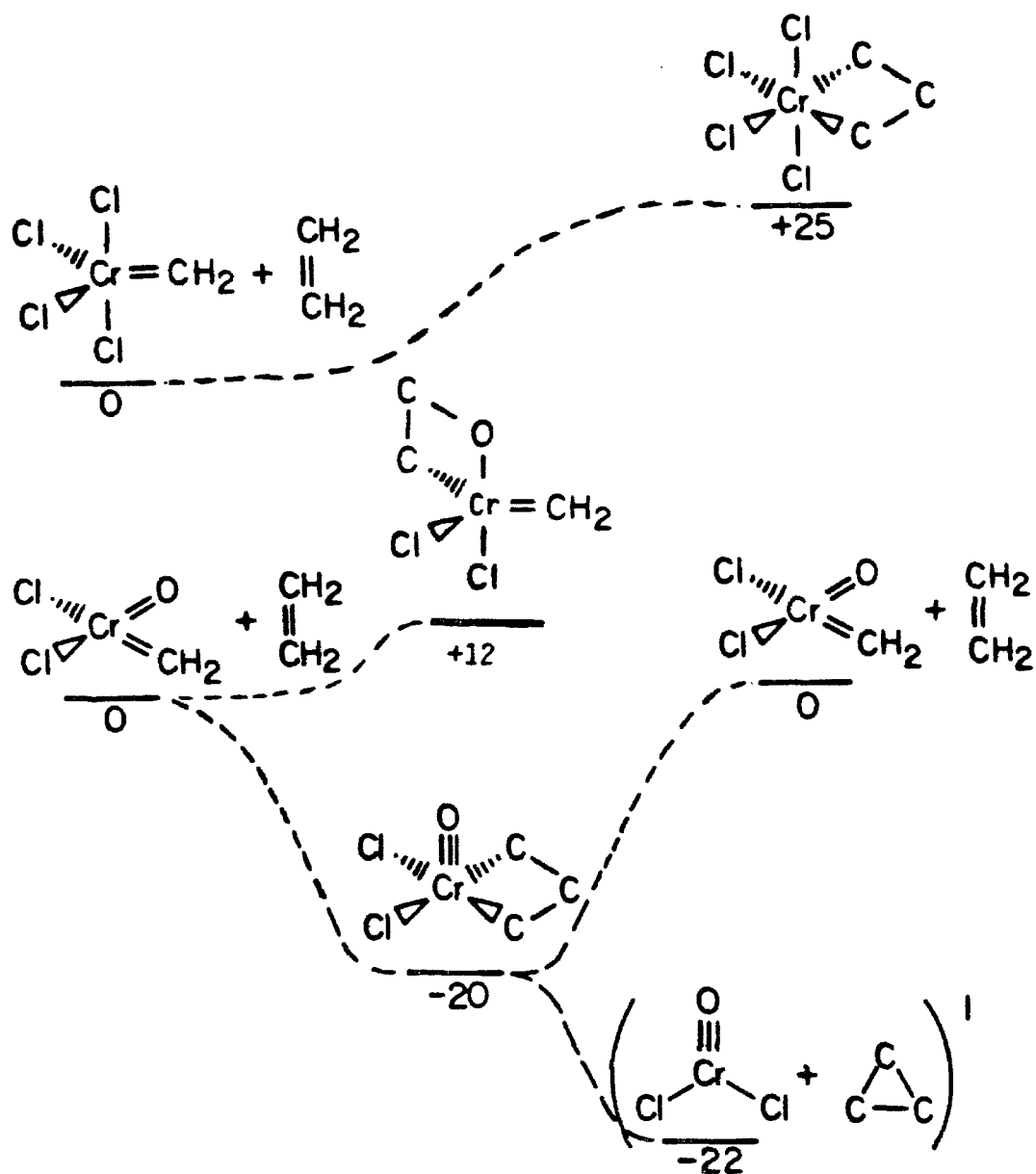


Figure 2. Energetics for the reaction of  $C_2H_4$  with  $Cl_4MoCH_2$  and  $Cl_2OMoCH_2$ .

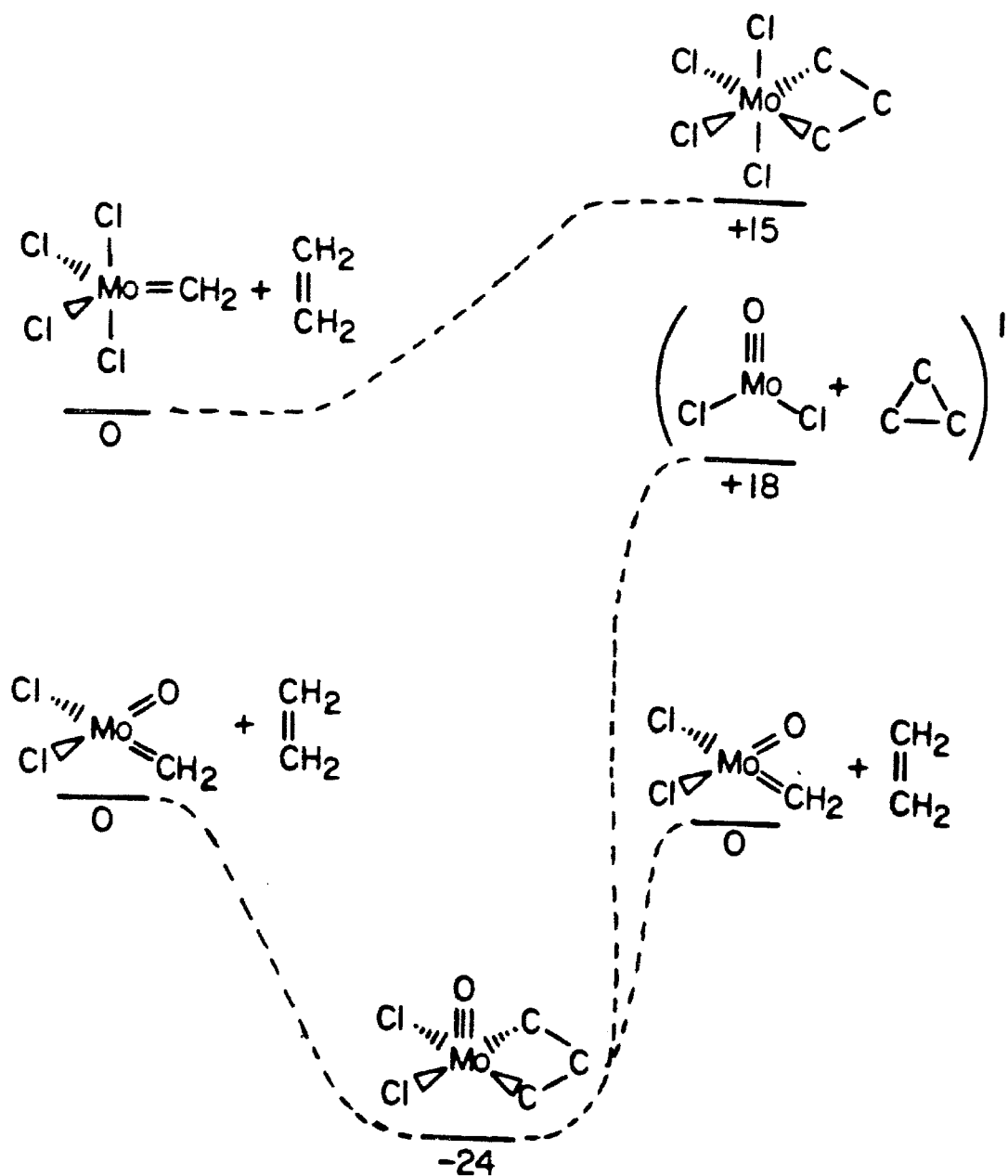
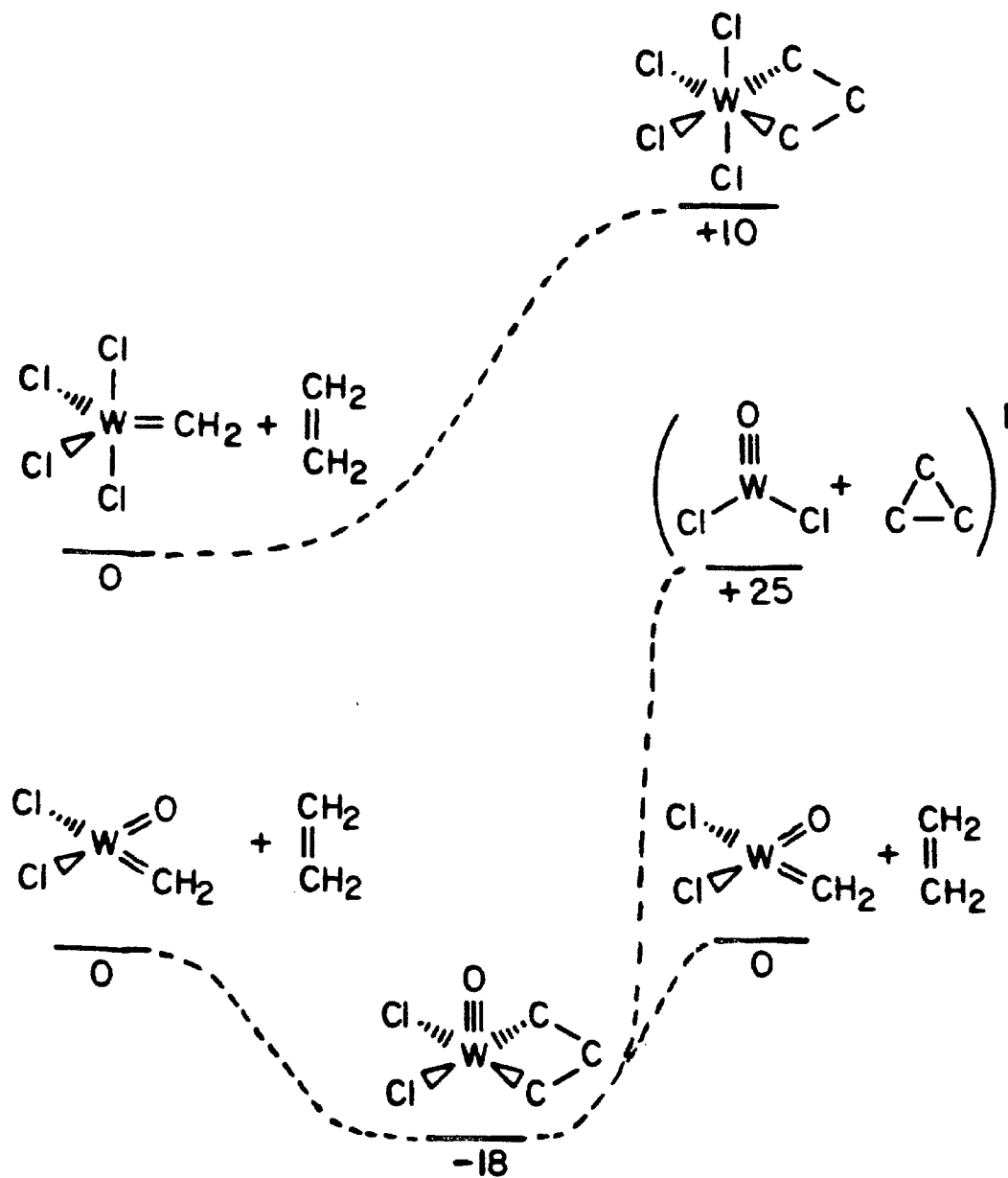
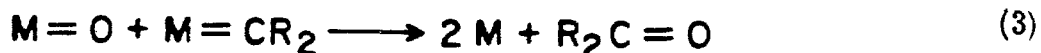


Figure 3. Energetics for the reaction of  $C_2H_4$  with  $Cl_4WCH_2$  and  $Cl_2OWCH_2$ .





presents the energetics for the bimolecular decomposition pathway d of Scheme I and the analogous



for Cr, Mo, and W. As expected, this mode becomes less exothermic as one proceeds down the column. There will still be substantial chain terminating olefin formation even for tungsten if the concentration of carbene complex becomes significant.

As is apparent from Figs. 1-3, we appear to be predicting that the chain carrying catalyst is the metallocyclic complex. These energetics have ignored solvation effects such as prior coordination of the olefin to the oxo carbene complex. This must be an attractive interaction since  $d^0$  metal complexes are strong Lewis acids and olefins are fair Lewis bases. The magnitude of the attraction is as yet unknown, though extrapolation of calculations on  $TiCl_2O + C_2H_4$ <sup>17b</sup> would predict an attraction of  $\sim 10$  kcal. As can be seen from Figs. 4-6, this still leaves the metallocycle in a 10 kcal well, still an unrealistic surface. There is another solvation effect which we have ignored, the effect of auxiliary Lewis bases such as  $Cl^-$ , amines, or phosphines in solution. If there the Lewis base has a differential effect on the oxo carbene and the metallocycle, the metallocycle well will be diminished. The reaction surfaces for a differential effect of 10 kcal are shown in Figs. 7-9.

**Figure 4.** Energetics ( $\Delta G_{300}$ ) for the reaction of  $C_2H_4$  with  $Cl_4CrCH_2$  and  $Cl_2OCrCH_2$  with inclusion of pi complexation of olefin.

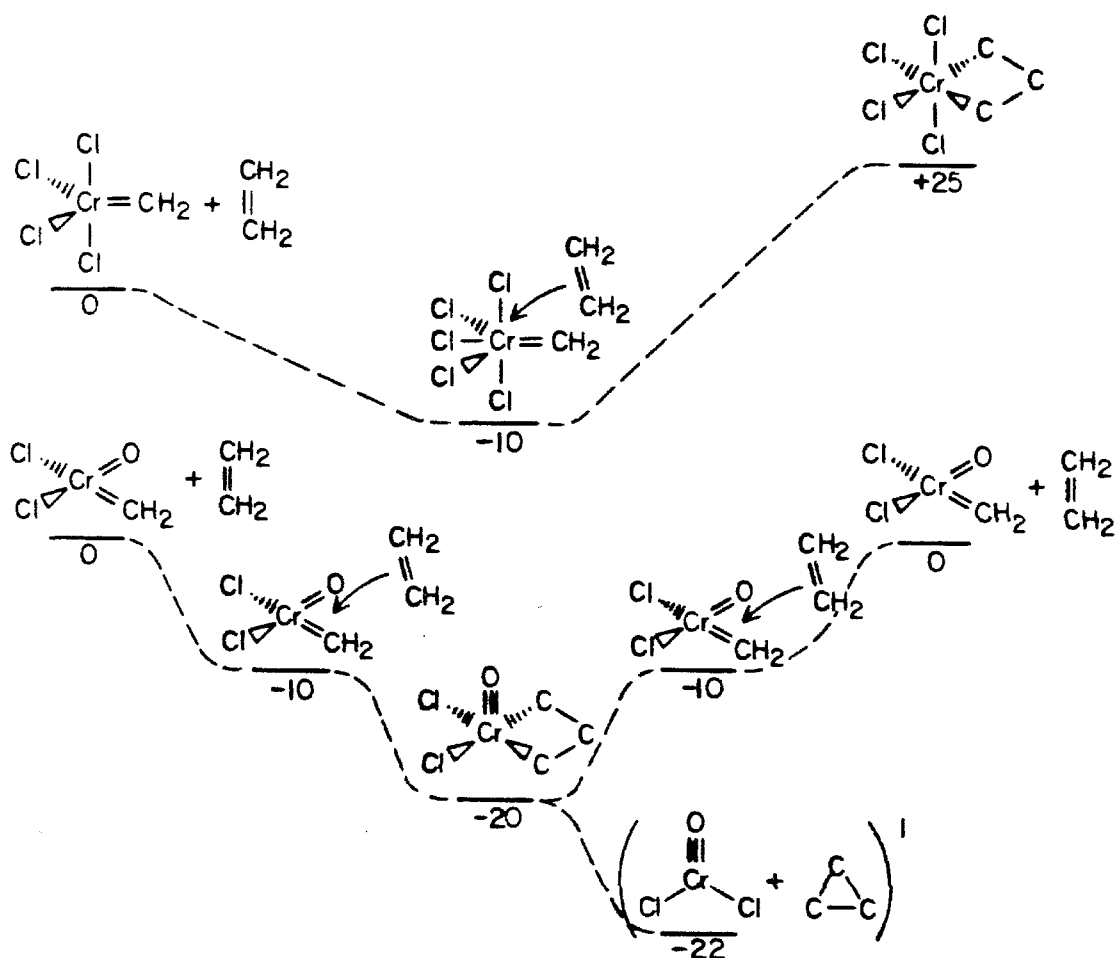


Figure 5. Energetics ( $\Delta G_{300}$ ) for the reaction of  $C_2H_4$  with  $Cl_4MoCH_2$  and  $Cl_2OMoCH_2$  with inclusion of pi complexation of olefin.

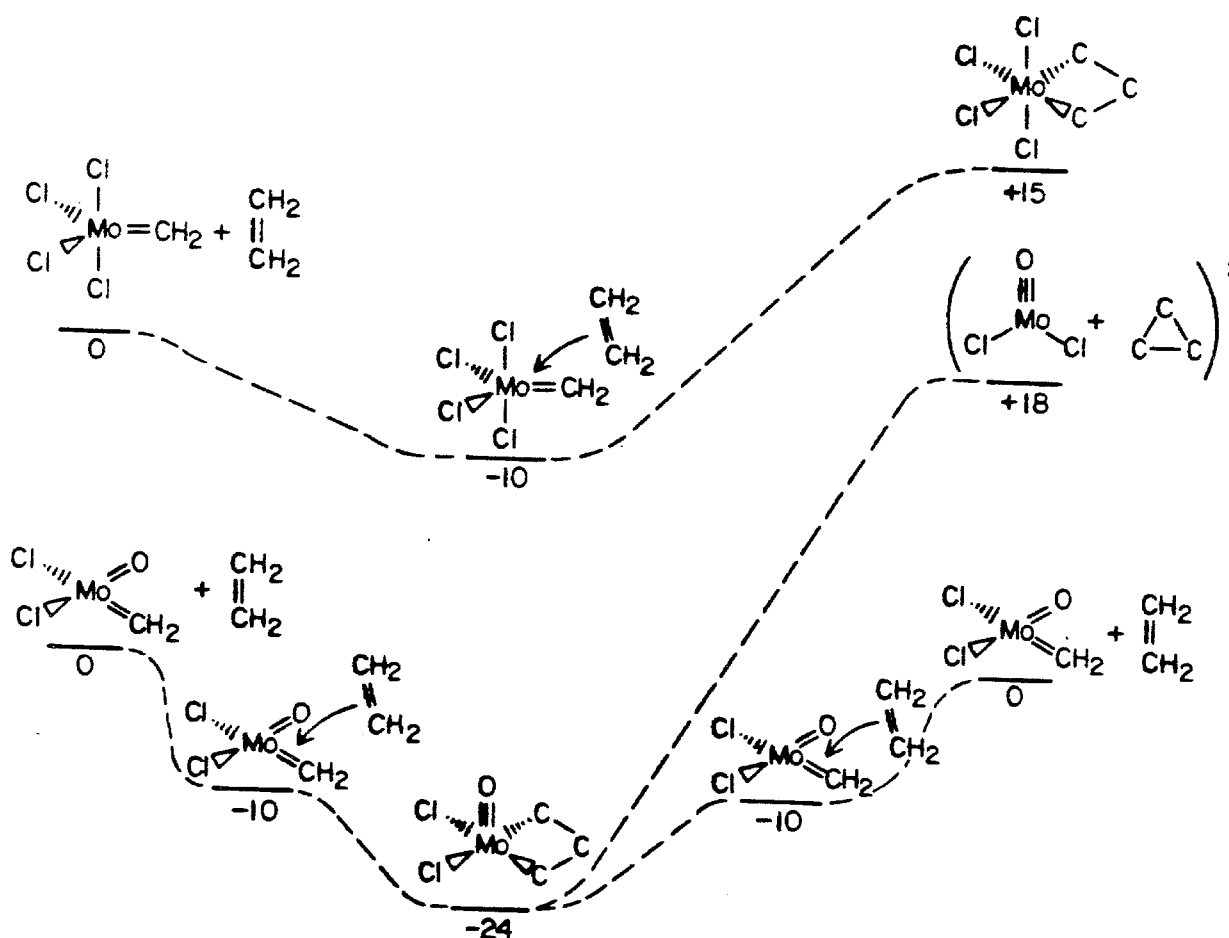
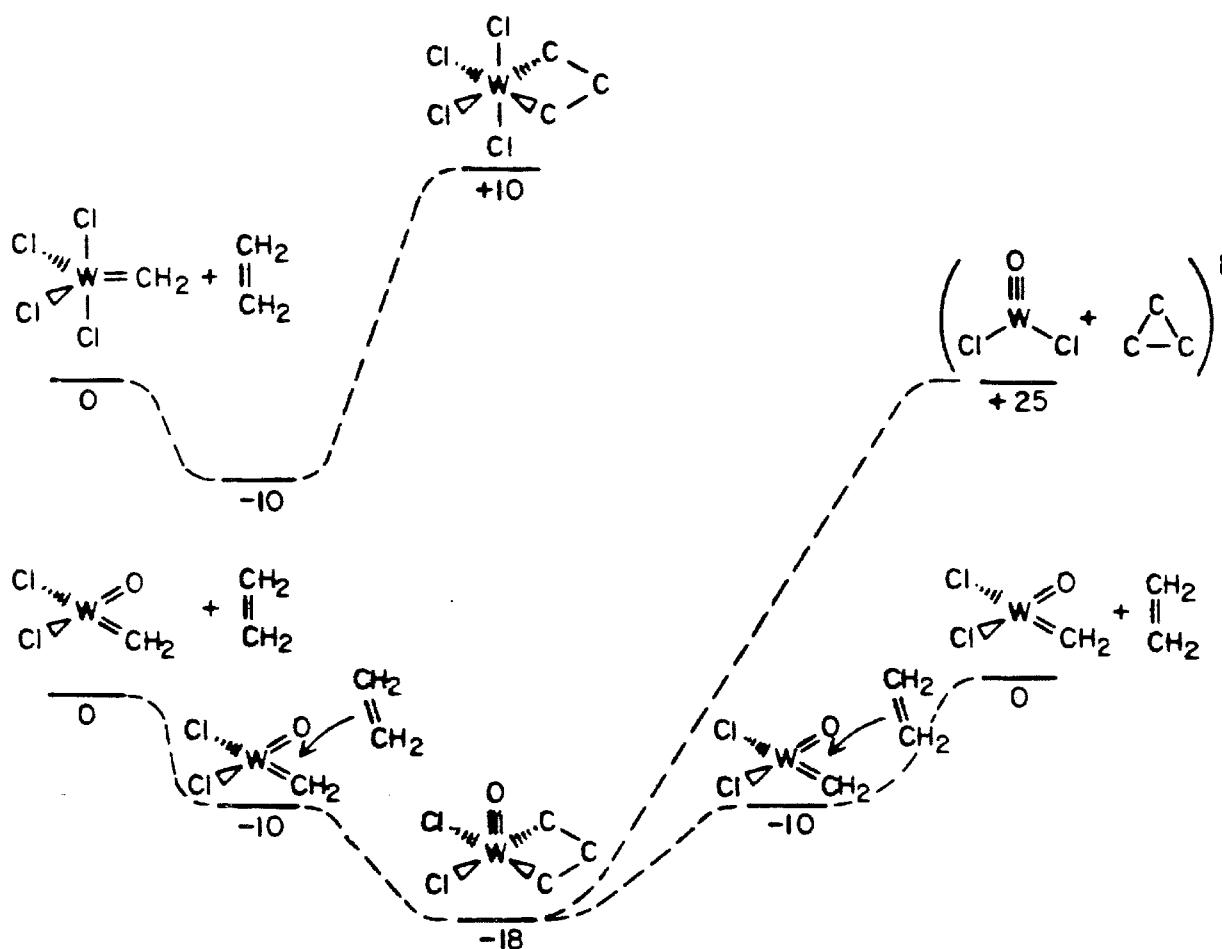


Figure 6. Energetics ( $\Delta G_{300}$ ) for the reaction of  $C_2H_4$  with  $Cl_4WCH_2$  and  $Cl_2O_2CH_2$  with inclusion of pi complexation of olefin.



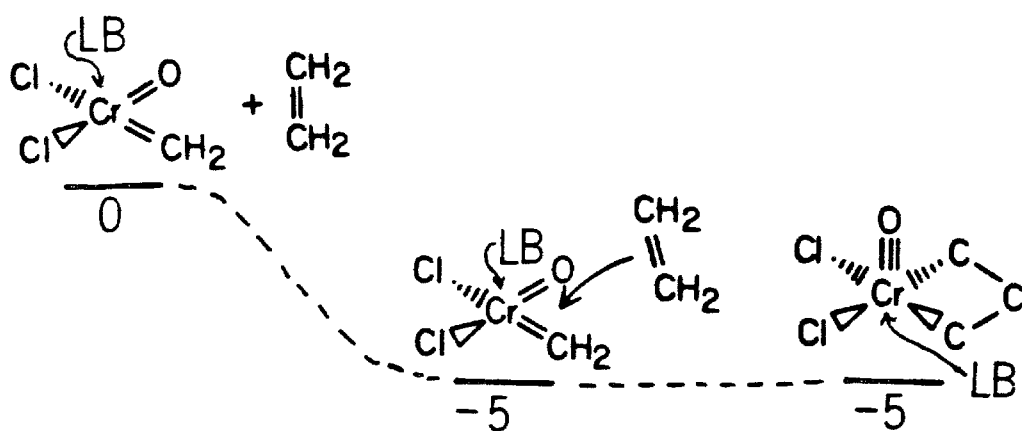


Figure 7. Energetics ( $\Delta G_{300}$ ) for the reaction of  $\text{C}_2\text{H}_4$  with  $\text{Cl}_2\text{OCrCH}_2$  with inclusion of pi complexation of olefin and the effect of a Lewis Base (LB).

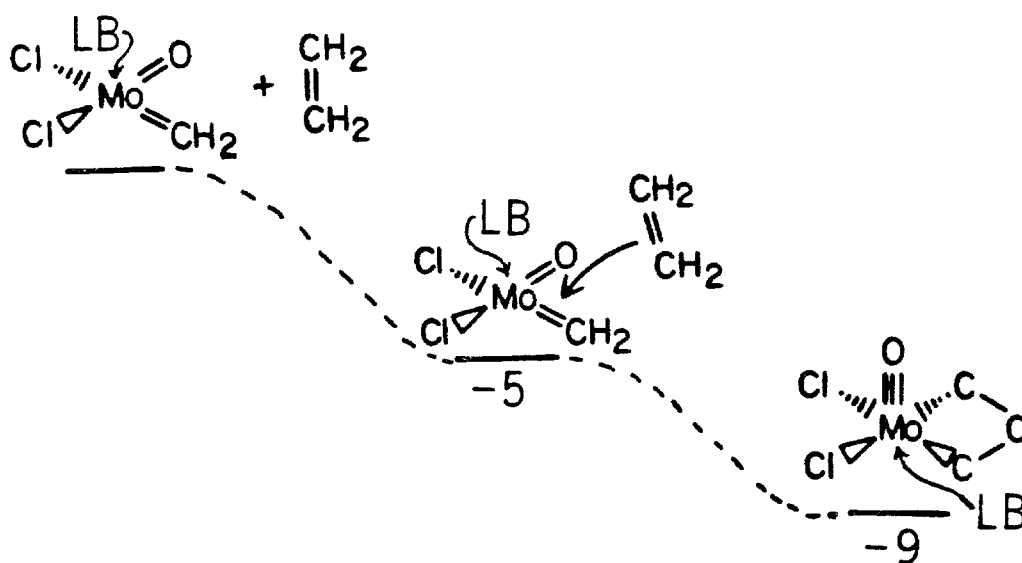


Figure 8. Energetics ( $\Delta G_{300}$ ) for the reaction of  $\text{C}_2\text{H}_4$  with  $\text{Cl}_2\text{OMoCH}_2$  with inclusion of pi complexation of olefin and the effect of a Lewis Base (LB).

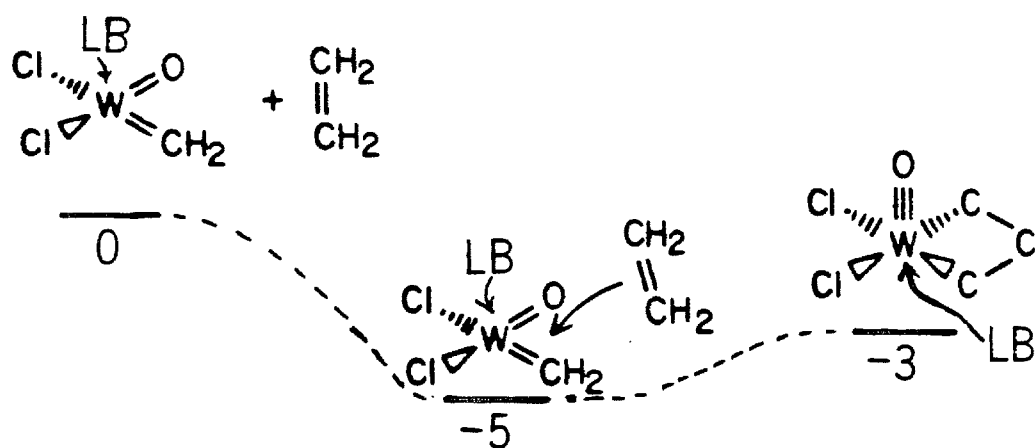
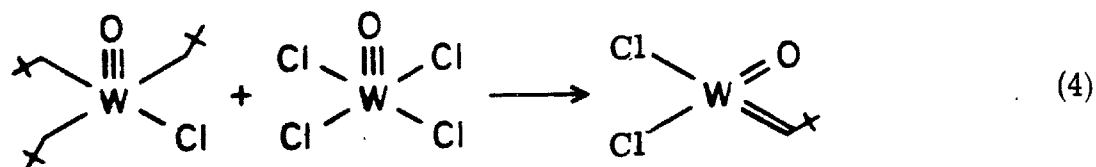


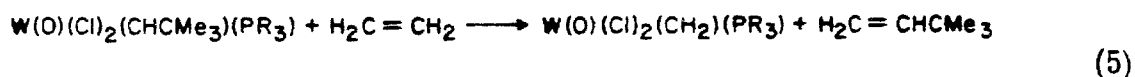
Figure 9. Energetics ( $\Delta G_{300}$ ) for the reaction of  $\text{C}_2\text{H}_4$  with  $\text{Cl}_2\text{OWCH}_2$  with the inclusion of pi complexation of olefin and the effect of a Lewis Base (LB).

### III. Discussion

Several experiments confirm our finding that the stable high-valent metathesis catalyst is an oxo-carbene. First, Basset<sup>18</sup> found that oxygen-containing compounds (O<sub>2</sub> or alcohols) accelerate the metathesis reaction. Second, Muetterties<sup>19</sup> has shown that in fact oxygen and perhaps chlorine are essential for the generation of active stable metathesis catalysts for high-valent tungsten. We feel that the chlorine probably can be replaced by other electronegative ligands such as alkoxides of the carbon portion of the ligand could be made inert. More recently Osborn<sup>20</sup> has generated Mo and W complexes that will metathesize olefins without standard co-catalysts; we interpret this as forming an oxo-carbene complex through a straightforward ligand exchange<sup>21</sup> followed by alpha abstraction<sup>22</sup> process



Finally (and most significantly), Schrock<sup>23</sup> has synthesized high-valent complexes of Mo and W that will metathesize olefins without co-catalysts,



The likely role of the Lewis base PR<sub>3</sub> in (5) is to increase electron density of the metal center.<sup>24</sup> This probably strengthens the M-C double bond, decreasing the energy gap between the carbene and metallocyclic complexes (a of Scheme I) (vide supra) and decreasing the



importance of the bimolecular decomposition pathway for homogeneous systems. The general accelerating effect of Lewis bases (amines) is well documented for heterogeneous catalysts.<sup>25</sup>

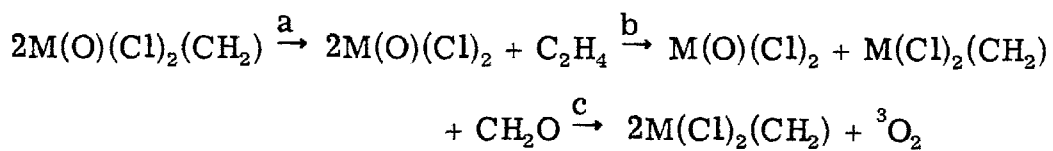
To verify the energetic similarity of dioxo and oxo-carbene complexes, we suggest that reaction of ketones with Schrock's oxo-carbene complex should generate olefins and a dioxo complex. If isolated, this dioxo complex should react with olefins to regenerate an oxo-carbene complex. This reaction has precedent in Tebbe's stabilized titanium carbene complex<sup>26</sup> which has been developed into a reasonable synthetic reagent for the formation of olefins.<sup>27</sup> The titanium system is not reversible due to secondary reactions and the tremendous difference in bond strengths between the oxo and carbene complexes (this will be discussed in Chapter 3). Furthermore, we suggest the molybdenyl and tungstenyl chlorides should be very useful in generating supported catalysts that can be systematically studied since a major difficulty with standard catalyst preparations is that the percentage of metal sites that actually participate in metathesis may be small ( $\sim 1\%$ ).<sup>16</sup> San Filippo has found that chromyl chloride can be chemisorbed to a support under exceedingly mild conditions and that the chemisorbed chromyl chloride will stoichiometrically oxidatively cleave C-C double bonds.<sup>28</sup> We suggest that low loading of the support will prevent the intermolecular decomposition pathways, d of Scheme I and (4). If the surface loading is high stoichiometric, C-C bond cleavage will dominate. Finally, we suggest that the concentration-dependent rate acceleration<sup>25</sup>/inhibition<sup>16</sup> found for amines is due to an initial formation of a mono-amine complex that is a better catalyst (as discussed earlier for phosphines), followed

by the eventual formation of the di-amine which should be catalytically inactive (this has been shown to be true for phosphines by Schrock<sup>23, 24</sup>).

#### IV. Summary

In summary, we suggest that oxo-carbene complexes are the stable metathesis catalysts for high-valent Mo, W, and Re complexes and that the oxygen ligand is intimately involved in the catalytic process. Furthermore, we suggest that oxo-carbene complexes are even formed on supported catalysts and that dioxo precursors may provide a convenient route to formation of well-defined surface catalysts for olefin metathesis and oxidation reactions.

Table I. Energetics for Bimolecular Decomposition Modes of Oxo-Carbenes.



M	a	b	c
Cr	-44	-44	+15
Mo	- 6	- 1	+69
W	- 2	+ 3	+73

## References

1. (a) R. H. Grubbs, Prog. Inorg. Chem., 24, 1-50 (1978); (b) N. Calderon, J. P. Lawrence, and E. A. Ofstead, Adv. Organomet. Chem., 17, 449-492 (1979).
2. J. Tsuji and S. Hashiguchi, Tetrahedron Lett., 21, 2955-2958 (1980).
3. G. W. Parshall, "Homogeneous Catalysis"; Wiley, New York, 1980; pp. 174-176.
4. J. L. Herisson and Y. Chauvin, Makromol. Chem., 141, 161-176 (1970).
5. R. H. Grubbs, P. L. Burk, and D. D. Carr, J. Am. Chem. Soc., 97, 3265-3267 (1975); R. H. Grubbs, D. D. Carr, C. Hoppin, and P. L. Burke, ibid., 98, 3478-3483 (1976).
6. T. J. Katz and J. McGinnis, J. Am. Chem. Soc., 97, 1592-1594 (1975); T. J. Katz, J. McGinnis, and C. Altus, ibid., 98, 606-608 (1976).
7. R. R. Schrock, J. Am. Chem. Soc., 96, 6796-6797 (1974); ibid., 98, 5399-5400 (1976); R. R. Schrock and P. R. Sharp, ibid., 100, 2389-2399 (1978).
8. M. Ephritikhine, M. L. H. Greene, R. E. MacKenzie, Chem. Commun., 619-621 (1976); M. Ephritikhine, B. R. Francis, M. L. H. Green, R. E. MacKenzie, and M. J. Smith, J. Chem. Soc., Dalton Trans., 1131-1135 (1977).
9. R. J. Puddephatt, M. A. Quyser, and C. F. H. Tippar, J. Chem. Soc., Chem. Commun., 626-627 (1976).
10. P. Foley and G. M. Whitesides, J. Am. Chem. Soc., 101,

2732-2733 (1979).

11. J. Rajaram and J. A. Ibers, J. Am. Chem. Soc., 100, 829-838 (1978).
12. C. P. Casey and R. L. Anderson, Chem. Commun., 895- (1975).
13. (a) C. P. Casey and T. J. Burkhardt, J. Am. Chem. Soc., 95, 5833-5834 (1973); (b) ibid., 96, 7808-7809 (1974); (c) C. P. Casey, L. D. Albin, and T. J. Burkhardt, ibid., 99, 2533-2539 (1979).
14. There is some question whether those catalysts thought to be homogeneous actually are; see, for example, Ref. 1a.
15. Indications are that the active catalyst has a rapid bimolecular decomposition pathway, and hence a stable catalytic system must have the catalyst in small concentration. See, for example, Ref. 7.
16. E. A. Lombardo, M. LoJacono, and W. K. Hall, J. Catal., 64, 150-162 (1980).
17. (a) A preliminary account of this work has been published; see A. K. Rappé and W. A. Goddard III, Nature, 285, 311-312 (1980); J. Am. Chem. Soc., 102, 5114-5115 (1980); (b) A difficulty in determining the binding energy of olefins or other Lewis bases to  $d^0$  metal complexes is that they are usually irreversibly oxidized; see D. J. Salmon and R. A. Walton, Inorg. Chem., 17, 2379-2382 (1978). An exception to this is  $TiCl_4$  where several Lewis acid-base complexation energies have been determined (28-45 kcal); see B. Hessett and P. G. Perkins, J. Chem. Soc. A, 3229-3234 (1970).

18. J. M. Basset, G. Coudurier, R. Mutin, H. Proliand, and Y. Trambouze, J. Catal., 34, 196-202 (1974).
19. M. T. Mocella, R. Rovner, E. L. Muetterties, J. Am. Chem. Soc., 98, 1689-1690 (1976).
20. J. R. M. Kress, M. J. Russell, M. G. Wesolek, and J. A. Osborn, J. Chem. Soc., Chem. Commun., 431-432 (1980).
21. R. A. Walton, "Progress in Inorganic Chemistry", 16, 1-226 (1972).
22. R. R. Schrock, Acc. Chem. Res., 12, 98-104 (1979).
23. (a) R. Schrock, S. Rocklage, J. Wengrovius, G. Rupprecht, and J. Fellmann, J. Mol. Catal., 8, 73-83 (1980); (b) J. H. Wengrovius, R. R. Schrock, M. R. Churchill, J. R. Missert, and W. J. Youngs, J. Am. Chem. Soc., 102, 4515-4516 (1980).
24. R. R. Schrock and J. Wengrovius, "Symposium on the Chemistry of Early Transition Metal Oxides, Polyoxoanions, and Oxo Complexes", Division of Inorganic Chemistry, Second Chemical Congress of the North American Continent and 180th National Meeting of the American Chemical Society, Las Vegas, Nevada, 27 August 1980.
25. J. Fathikalajahi and G. B. Willis, J. Mol. Catal., 8, 127-134 (1980).
26. F. N. Tebbe, G. W. Parshall, and G. S. Reddy, J. Am. Chem. Soc., 100, 3611-3613 (1978).
27. S. H. Pine, R. Zahler, D. A. Evans, and R. H. Grubbs, J. Am. Chem. Soc., 102, 3271-3272 (1980).
28. J. San Filippo, Jr., and C. Chern, J. Org. Chem., 42, 2182-2183 (1977).

## CHAPTER 3: Qualitative Bonding

### I. Introduction

Valence bond ideas have formed the foundation for conceptual discussions of organic molecular structures and chemical reactivities for many years<sup>1</sup> and have been quantified through ab initio theoretical studies.<sup>2</sup> For transition metal systems, molecular orbital concepts have dominated qualitative thinking<sup>3,4</sup> due to lack of satisfactory valence bond concepts capable of describing the bonding modes commonplace for transition metals. We will attempt to present a preliminary description of a qualitative view of transition metal bonding which is consistent with ab initio calculations and experimental realities. We begin with a discussion of sigma bonding both ionic, described in Section II, and covalent, described in Section III. This will be followed by a section describing fully ligated systems, first sigma bonding and then both sigma and pi bonding ligands. Finally, we will discuss trends across rows of the periodic table and down columns that are useful in extrapolating results from one element to another.

## II. Ionic Sigma Bonds

Bonds in general can be classified as either ionic or covalent. In this section we will discuss ionic bonding in general and will show that transition metal s orbital bonds to ligands can qualitatively be considered as ionic (though, as we will show, even these bonds are not purely ionic). A qualitative (semi-quantitative) energetic description of ionic bonding,<sup>5</sup> if it is idealized as  $A^+B^-$ , is

$$E_{\text{ionic}} = IP - EA - 1/R + PR, \quad (1)$$

where IP is the ionization potential of the species likely to lose the electron (A), EA is the electron affinity of the species that receives the electron (B),  $1/R$  is the electrostatic attraction between the two species, A and B, and PR is the Pauli Repulsion between the cores of the two species. To have a strong ionic bond, one needs a small IP, a large EA, or a small distance between the charges. To investigate the utility of this concept, we will consider NaCl as a prototype ionic system. The first IP of Na is 5.14 eV<sup>6</sup> and the EA of Cl is 3.62 eV,<sup>7</sup> so for distances less than 9.5 Å there will be a net favorable ionic interaction between Na and Cl. Figure 1 shows potential curves for both ionic and covalent descriptions of the NaCl bond;<sup>8</sup> clearly, the ionic bond is far more favorable. Covalent bonds are far more sensitive to orbital overlaps, and since there is a large mismatch in the size of an Na 3s orbital and a Cl 3p orbital, the overlap is never large (the overlap at the optimum covalent bond distance is 0.13).<sup>8</sup> Another factor in the poor overlap is the orthogonality of the 3s orbital on Na to the core of Cl and the 3p orbital on Cl to the core of Na. Figure 2 presents a partitioning of the ionic bonds into its two components; note that the



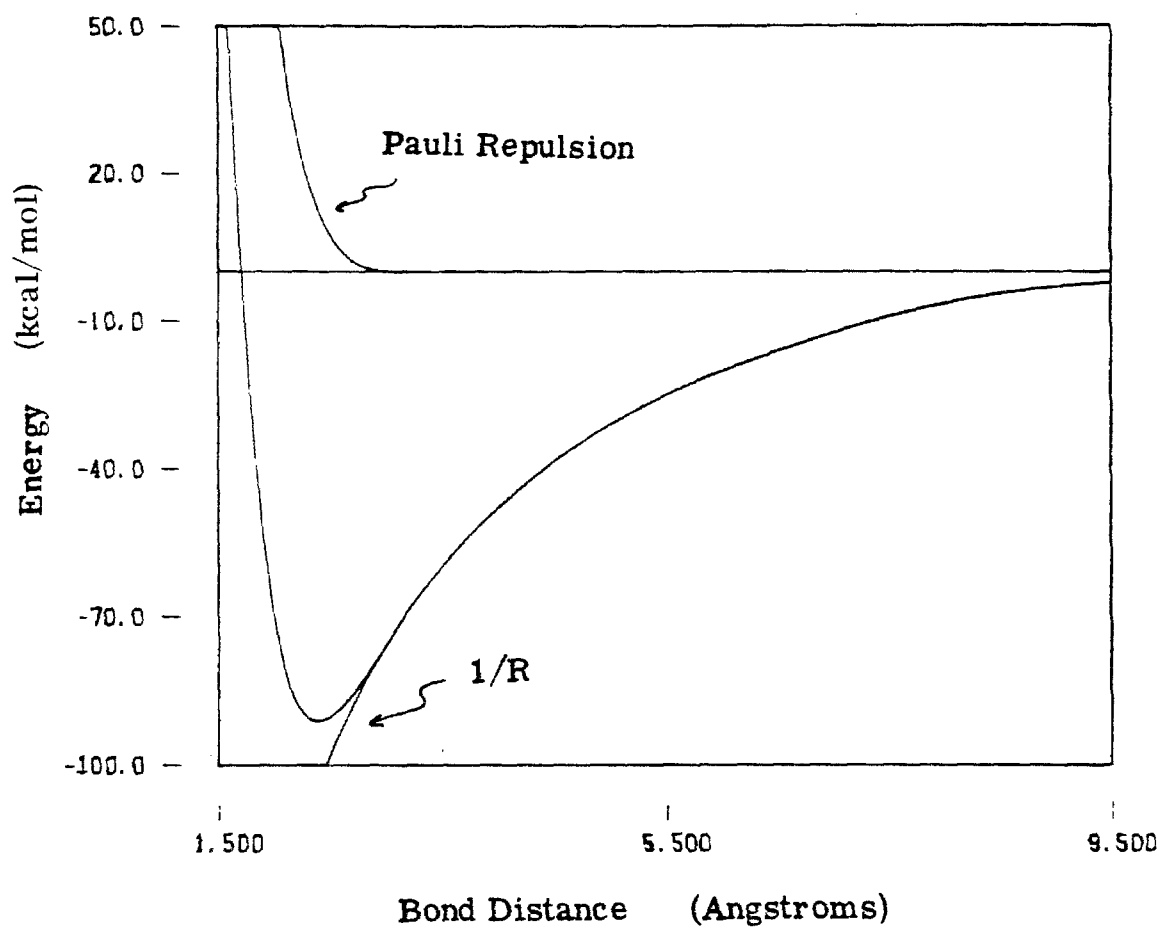


Figure 2. Partitioning of NaCl ionic bond.

Pauli Repulsion contribution is very short range. Table I presents bond energies and bond distances for the covalent bond, the ionic bond, and the optimum mixture of the two for NaCl.<sup>8</sup> For our purposes we will consider this to be an ionic bond.

Since the first ionization potential of a transition metal atom is rather low (6-8 eV), we suggest that the first M-Cl bond is dominantly ionic. The second ionization potential is substantially larger, so to investigate what will be a reasonable description of a second M-Cl bond, let us consider bonding a Cl to  $\text{Sc}^+\text{Cl}^-$ ; that is, we will examine what character the second bond has if we consider the first to be purely ionic. The first ionization of Sc is 6.56 eV,<sup>6</sup> leading to an estimated ionic bond strength of about 80 kcal. The second ionization of Sc is 12.89 eV;<sup>6</sup> this should imply substantially less ionicity in this bond. Figure 3 shows a purely ionic second bond and an ionic plus covalent second bond; clearly the second Cl bond to Sc has substantial covalent character even though the Cl is predominantly bonding to an Sc 4s orbital. Figure 4 shows the partitioning of the ionic bond, indicating that the large ionization potential has severely dampened the importance of the ionic bonding contribution (through the IP-EA-electrostatic term). For convenience we will consider all bonds to transition metal s orbitals as just that, bonds to s orbitals, even though there is substantial ionic character in both s orbital bonds.

In summary, the important factors for ionic bonding are a short distance (large  $1/R$  term) (implying that first-row transition metals will form stronger ionic bonds than second-row transition metals), a large EA (Table II lists various common sigma bonding ligands in the

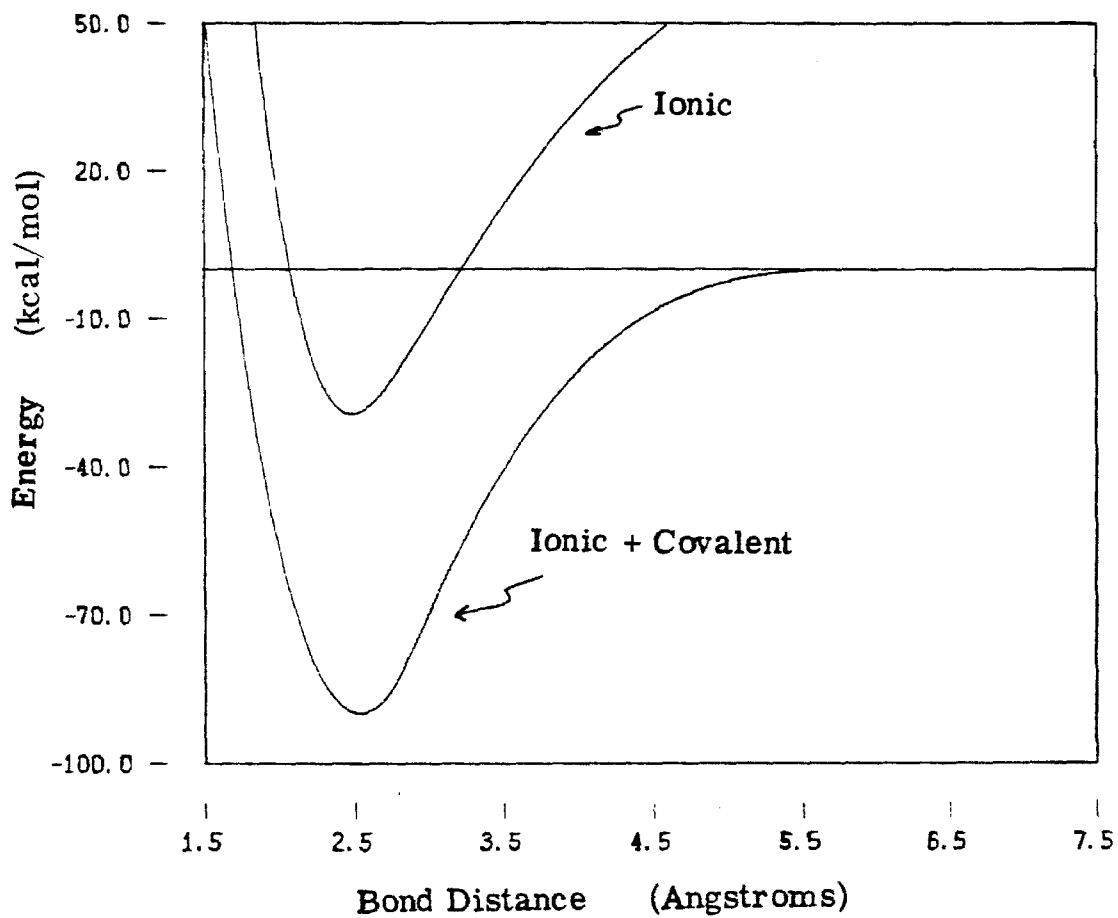


Figure 3.  $\text{ScCl}_2$  ionic second bond and ionic + covalent second bond.

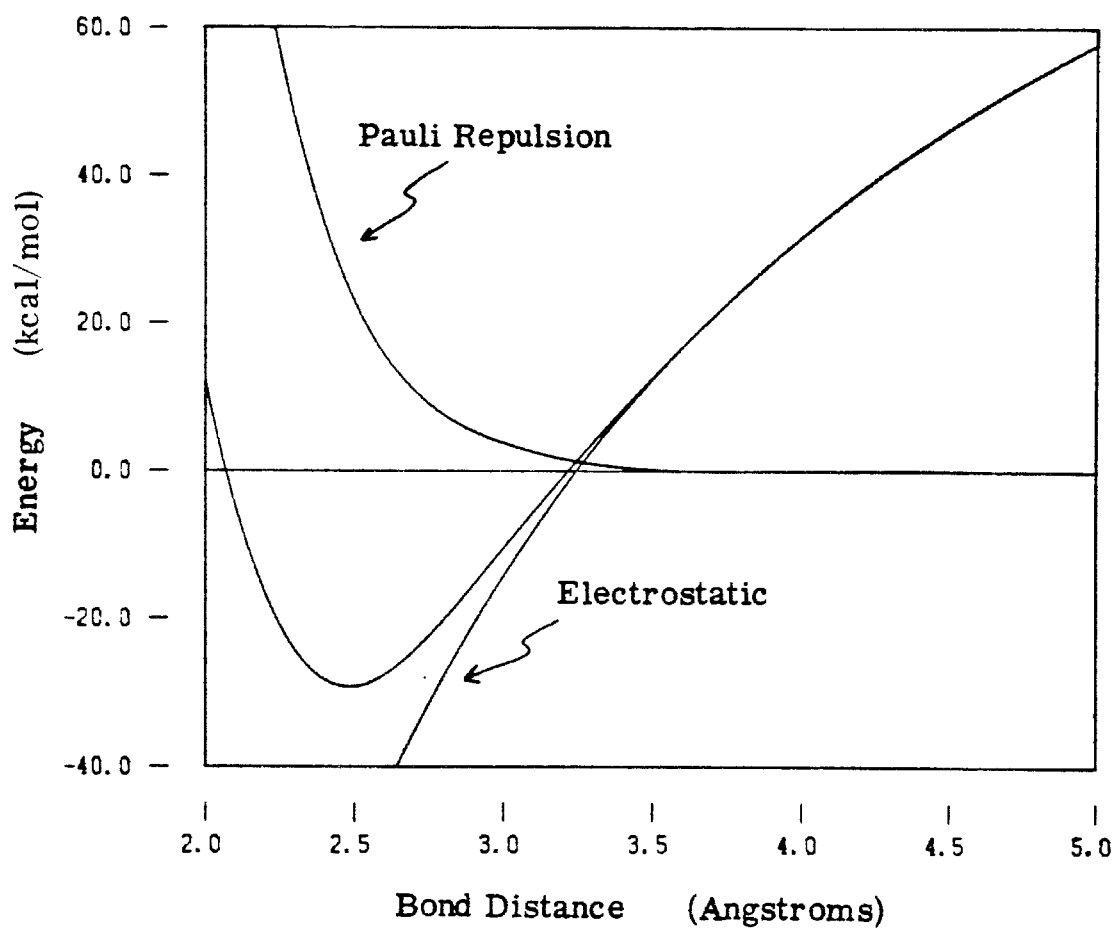


Figure 4. Partitioning of  $\text{ScCl}_2$  ionic second bond.

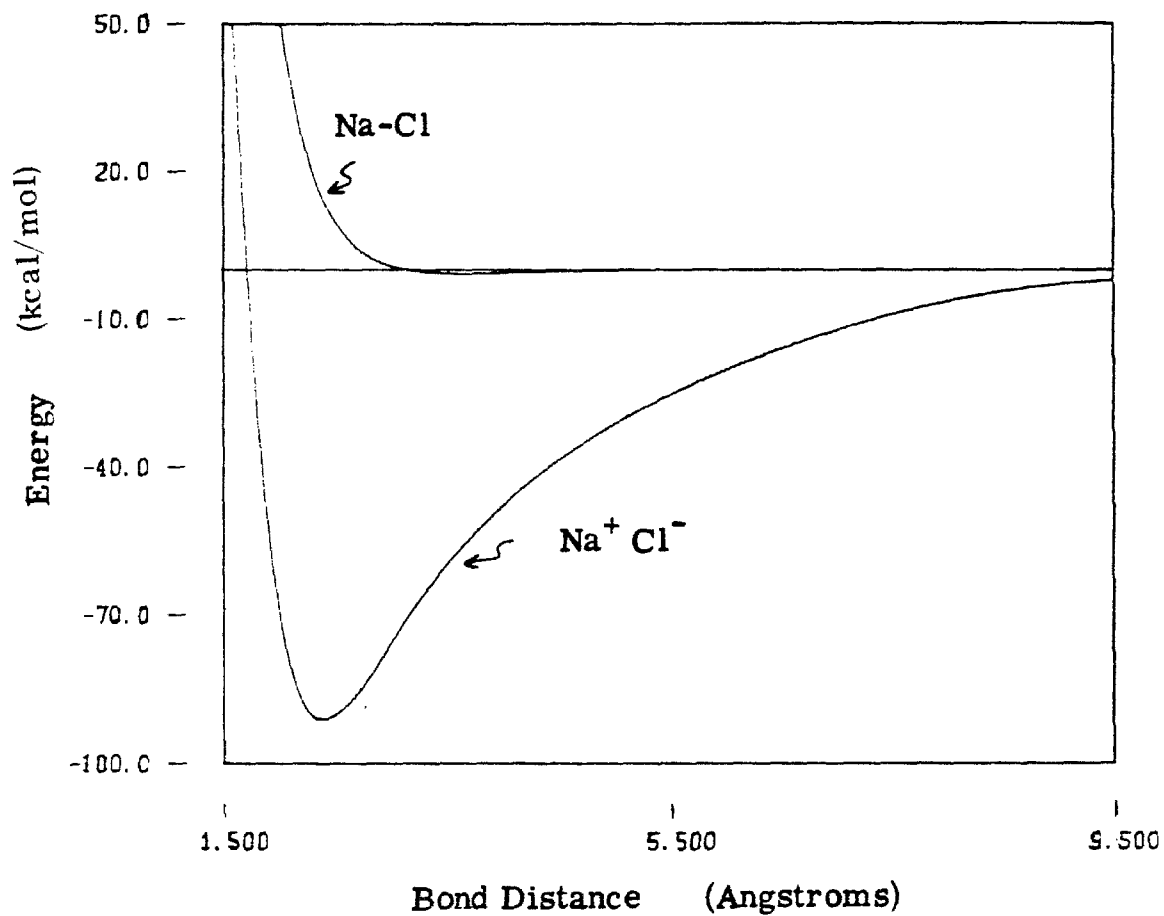


Figure 1. NaCl Ionic and Covalent Bonds.

TABLE I.<sup>a</sup> Bond Energy and Bond Distances for Ionic and Covalent Bonds for NaCl.

Bond	$R_e(\text{\AA})$	B. D. E. (kcal/mol)
covalent	3.7	0.6
ionic	2.38	90.6
covalent + ionic	2.38	94.9
experiment <sup>b</sup>	2.36	97.5

<sup>a</sup> From Ref. 8.

<sup>b</sup> From Ref. 22.

TABLE II.<sup>a</sup> Electron Affinities for Common Sigma Bonding Ligands.

Ligand	EA (eV)	Ligand	EA (eV)
Cl	3.62	CCl <sub>3</sub>	>2.1
F	3.4	CF <sub>3</sub>	2.1
Br	3.36	OH	1.83
I	3.06	BH <sub>2</sub>	1.39
SiH <sub>3</sub>	2.73	H	0.78
SH	2.32	NH <sub>2</sub>	0.75
C <sub>5</sub> H <sub>5</sub>	2.2	CH <sub>3</sub>	0.08 <sup>b</sup>

<sup>a</sup> Atomic electron affinities from Ref. 7; molecular electron affinities from Ref. 23.

<sup>b</sup> From Ref. 24.

order of decreasing EA), and a small IP (Table III lists the first, second, and average ionization potentials for various "metals"). Finally, Table IV presents approximate first ionic bond strengths for various metals and halides, and the trends are consistent with ionic bond strengths decreasing in the order  $F > Cl > Br > I$  and also decreasing as one goes down a column of the periodic table.

TABLE III.<sup>a</sup> Ionization Potentials of Metals.

Atom	First IP (eV)	Second IP (eV)	Average IP (eV)
H	13.6	---	---
Li	5.39	---	---
Na	5.14	---	---
K	4.34	---	---
Rb	4.18	---	---
Ca	6.11	11.87	8.99
Sc	6.56	12.89	9.73
Ti	6.83	13.63	10.23
V	6.74	14.2	10.47
Cr	6.76	16.49	11.63
Mn	7.43	15.64	11.54
Fe	7.90	16.18	12.04
Co	7.86	17.05	12.46
Ni	7.63	18.15	12.89
Cu	7.72	20.29	14.01
Sr	5.69	11.03	8.36
Y	6.5	12.4	9.45
Zr	6.95	14.03	10.49
Nb	6.71	14.	10.39
Mo	7.10	16.15	11.63
Tc	7.28	15.26	11.27
Ru	7.36	16.76	12.06
Rh	7.46	18.07	12.77
Pd	8.33	19.42	13.88
Ag	7.57	21.48	14.53

<sup>a</sup> Ref. 6.



TABLE IV. Approximate Ionic Bond Strengths<sup>a</sup> (kcal/mol).

Metal	Halides			
	F	Cl	Br	I
Li	148(136) <sup>b</sup>	104(112)	87(100)	66(82)
Na	175(123)	85(98)	71(86)	54(69)
K	104(117)	84(100)	72(90)	57(76)
Rb	99(115)	82(100)	70(90)	56(76)
Ca	86(126)	59(94)	45(73)	28(> 64)
Sr	87(129)	62(96)	50(79)	33(> 65)
Sc	72	46	33	16
Y	62(143)	40	28	12
Ti	74	45	32	14
Zr	60	35	23	6
V	84	52	38	20
Nb	74	46	32	15
Cr	91	56	42	23
Mo	71	41	27	9
Mn	82	45	30	10
Tc	73	40	26	8

<sup>a</sup> Using  $EA - IP + 1/R - 20$  kcal/mole; EA's from Ref. 7, IP's from Ref. 6, bond distances from Refs. 1 and 22.

<sup>b</sup> The numbers in parentheses are experimental bond energies from Ref. 22.

### III. Covalent Sigma Bonds

Consider now covalent bonding to transition metals. This will dominantly involve bonding to d orbitals as the d IP's are too large to form ionic bonds (around 10 eV).<sup>6b</sup> Intuitively, sigma bonding to all d orbitals is not the same; one would expect that bonding along the z axis to the  $d_{z^2}$  orbital is better than bonding along the x axis to one of the lobes of the  $d_{x^2-y^2}$  orbital. For the  $\text{Sc}^{+2}\text{H}$ , the d sigma bond is 9 kcal stronger than bonding to one of the lobes of another d orbital and the bond to d sigma is 0.13 Å shorter (1.75 Å versus 1.88 Å); thus bonding to d sigma is best, but it is not highly unfavorable to bond to the lobe of another d orbital. Orbital contour plots of these two cases are shown in Figs. 5 and 6.

Consider forming two covalent bonds to transition metal d orbitals. From main group chemistry it is known that there are well-defined angular characteristics for s and p orbital bonds, and understanding deviations from these is useful in probing novel chemistry.<sup>2</sup> s orbital bonds prefer to have angles of 180° ( $\text{BeH}_2$ ), and p orbital bonds prefer angles of 90° ( $\text{SiH}_2$ ,  $\text{PH}_2$ , or  $\text{SH}_2$ ). We will now consider the preferences, if any, of d orbitals.

Since bonding to d sigma is best, an important question is if it is possible to form two d sigma bonds, one to the  $d_{z^2}$  and another to a combination of the remaining d orbitals combined to form a pure d sigma orbital orthogonal to  $d_{z^2}$ . As one might expect, it is possible, and in the yz plane the other d sigma is  $1/\sqrt{3}(d_{x^2-y^2} \pm \sqrt{2}d_{yz})$ , and contour plots of  $d_{z^2}$  (d sigma) and d sigma' are shown in Fig. 7. The angle between the maxima of these two d sigma orbitals is 54.7 or

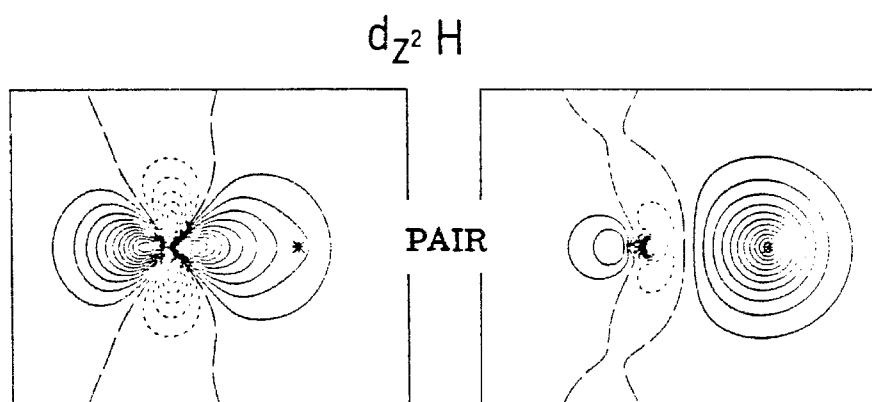
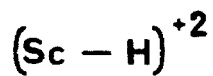


Figure 5.  $(\text{ScH})^{+2}$  D sigma bond orbital contour plot. Long dashes indicate zero amplitude; the spacing between contours is 0.05 a.u.; the same convention is used in all plots.

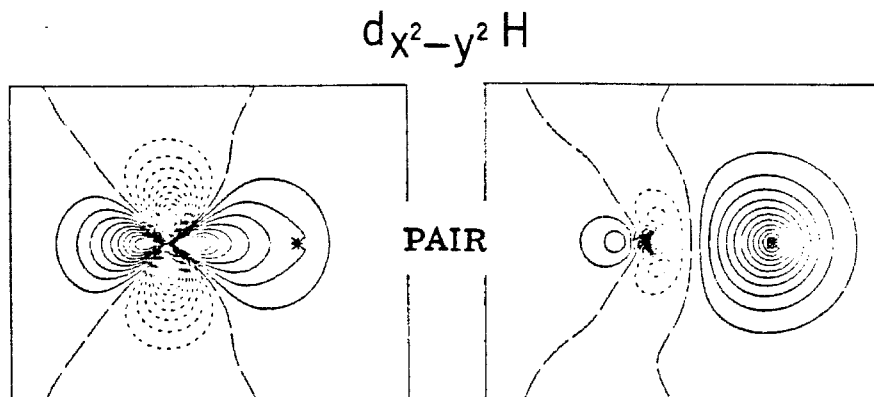
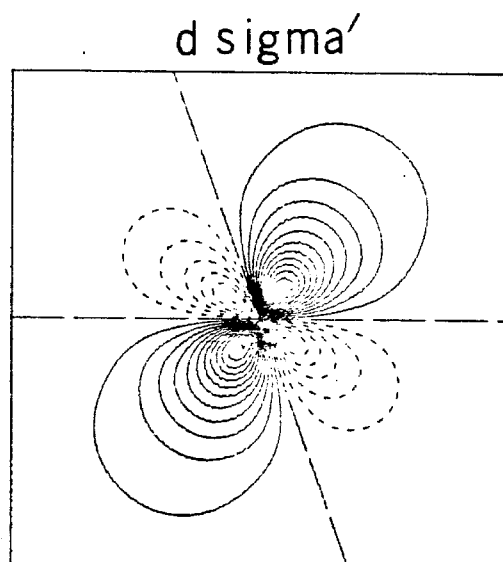
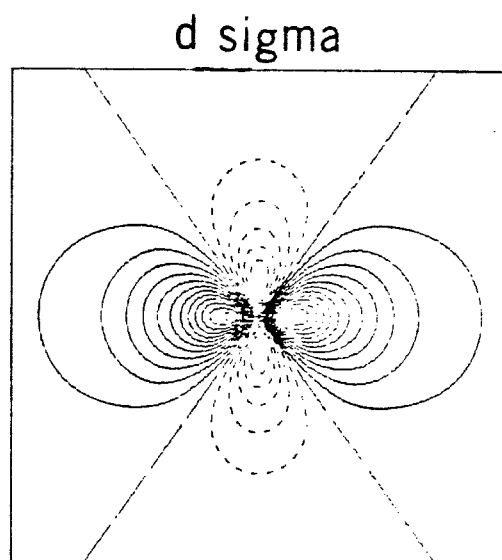


Figure 6.  $(\text{ScH})^{+2}$  D delta bond orbital contour plots.

Figure 7.  $\text{Sc}^{+2}$  D sigma and D sigma' orbital contour plots.



125.3°. Thus the optimum angle for  $MH_2$  should be 54.7 or 125.3°. The bending curve for  $MoH_2^+$  is shown in Fig. 8 where it can be seen that there are minima in the proper places, indicating that transition metal d bonds do have angular preferences. Bond angles of less than 90° are common for transition metal complexes, and in fact these small angles are strong evidence for covalent d ligand bonds.

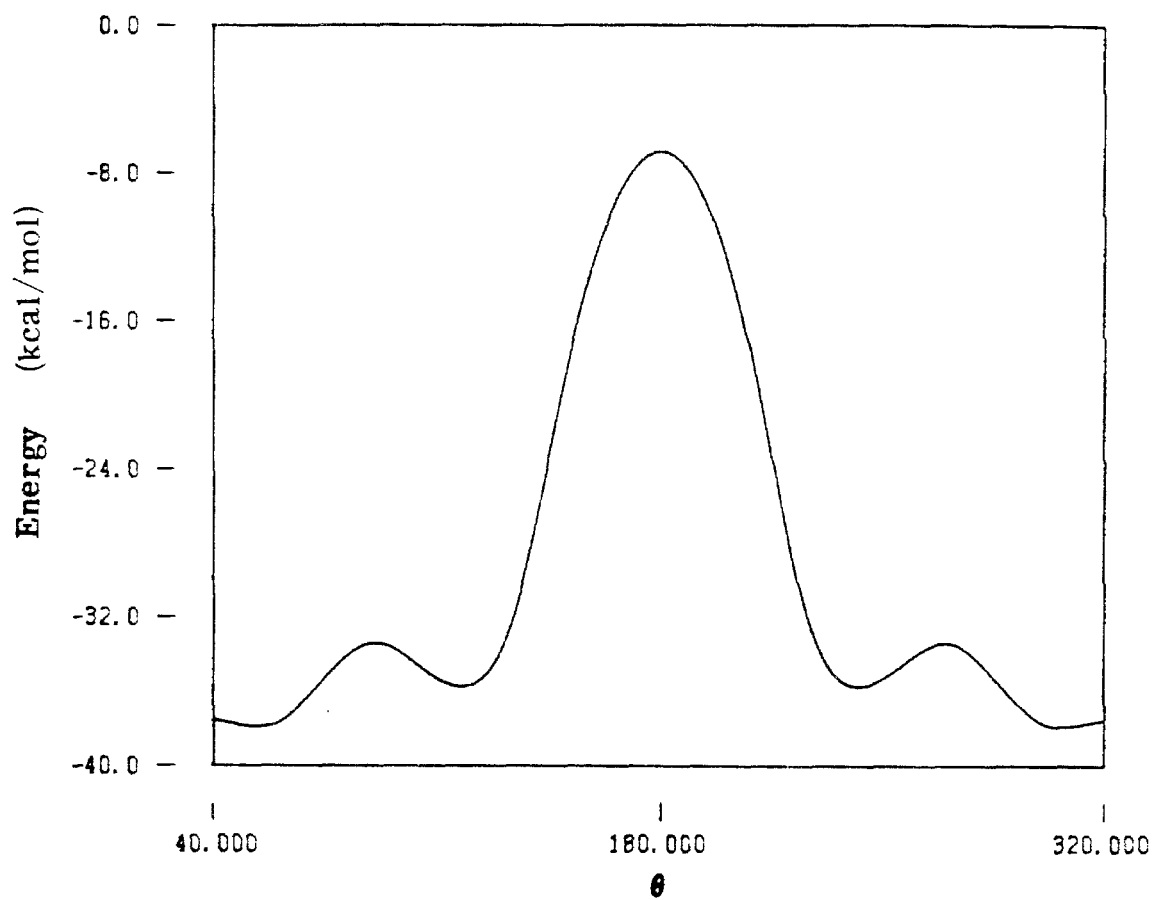
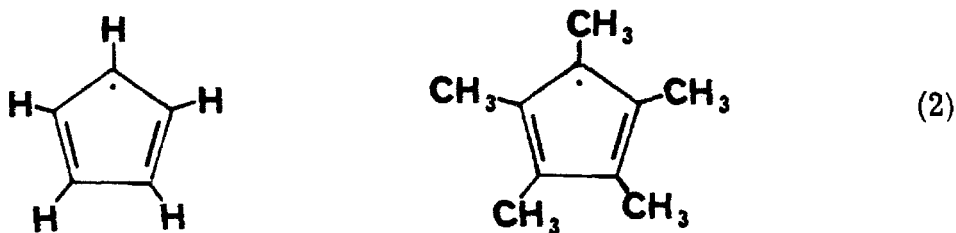


Figure 8.  $(\text{MoH}_2)^+$  bonding curve.

#### IV. Bonding in Saturated Complexes

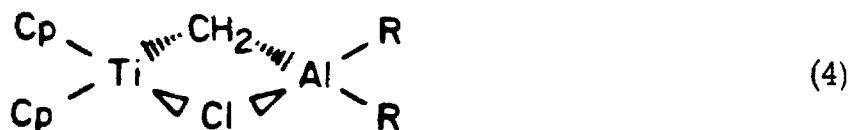
There is substantial interesting and relevant chemistry that involves transition metal complexes where all (or almost all) ligands are attached to the metal through covalent bonds. A major portion of this chemistry exploits the stability characteristics of the cyclopentadienyl ligand (either perhydro or permethyl),



Systems such as



(a known anti-tumor agent<sup>9</sup>) and



(commonly referred to as "Tebbe's Complex"<sup>10</sup>) are useful as mechanistic probes for the industrially important olefin metathesis<sup>11</sup> and Ziegler-Natta olefin polymerization<sup>12</sup> processes because their stability

allows isolation of intermediates that are too "hot" for the chloroanalog. Furthermore, Tebbe's Complex has been developed into a useful synthetic reagent for the deoxygenation of carbonyl compounds and epoxides.<sup>13</sup> There are numerous other examples<sup>14-17</sup> where (3) has found use as a substitute for  $\text{TiCl}_4$  and is in fact preferable due to the decreased reactivity and hence greater selectivity.

Since cyclopentadienyl (Cp) ligands are currently at the fringe of accessibility for ab initio theoretical techniques and since "hotness" of a compound is no problem to theoretical study, we have chosen to model Cp with a Cl atom. The ionic bond strength for Cl is comparable to that for Cp (217 kcal versus 219 kcal) so the orbitals left for bonding to other ligands should be comparable and one would expect trends learned for dichloro systems should apply to bis-Cp systems.

As a preface to bonding a sigma ligand such as H to  $\text{ScCl}_2$ , Fig. 9 shows the splitting of the d orbital levels as two Cl ligands approach Sc. Figure 10 shows the effect of bending the chlorides back to facilitate bonding a ligand to the front. Note that the total splitting of the d levels is 0.8 kcal, not a dramatic effect, suggesting that the sigma ligand to be bonded could form a bond wherever it wanted to bond, the limiting factor being steric interactions. Now consider bonding two sigma ligands (H's) to  $\text{TiCl}_2$ . Titanium atom has a ground state  $s^2d^2$  configuration, so we will consider that the two Cl's bond to the s orbitals, leaving a  $d^2$  configuration. For a triplet spin state, this leads to  $^3F$  and  $^3P$  states for the free metal ion. These states split as the two Cl's are brought up to the Ti and then bent back. This is shown in Fig. 11. As is apparent from Fig. 11, the  $^3F$  and  $^3P$  states are only minimally



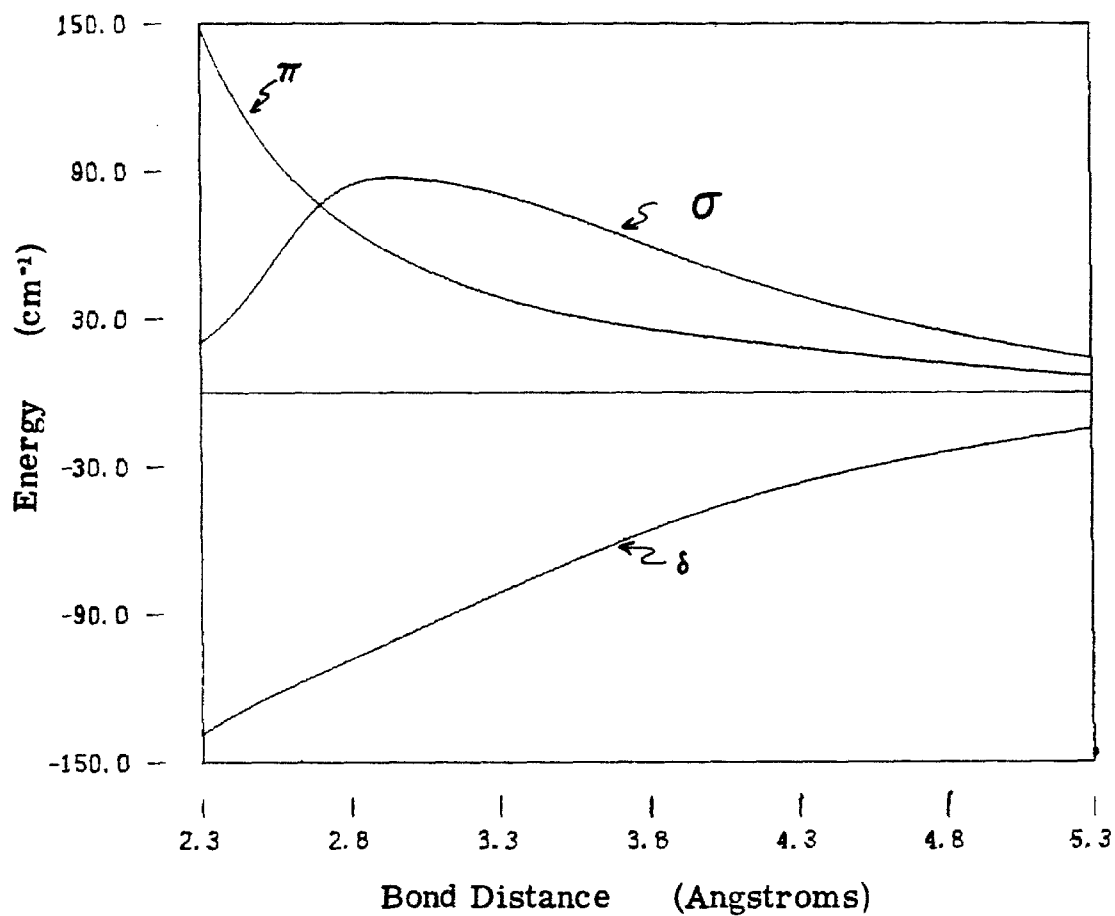


Figure 9. ScCl<sub>2</sub> D orbital levels as a function of internuclear distance.

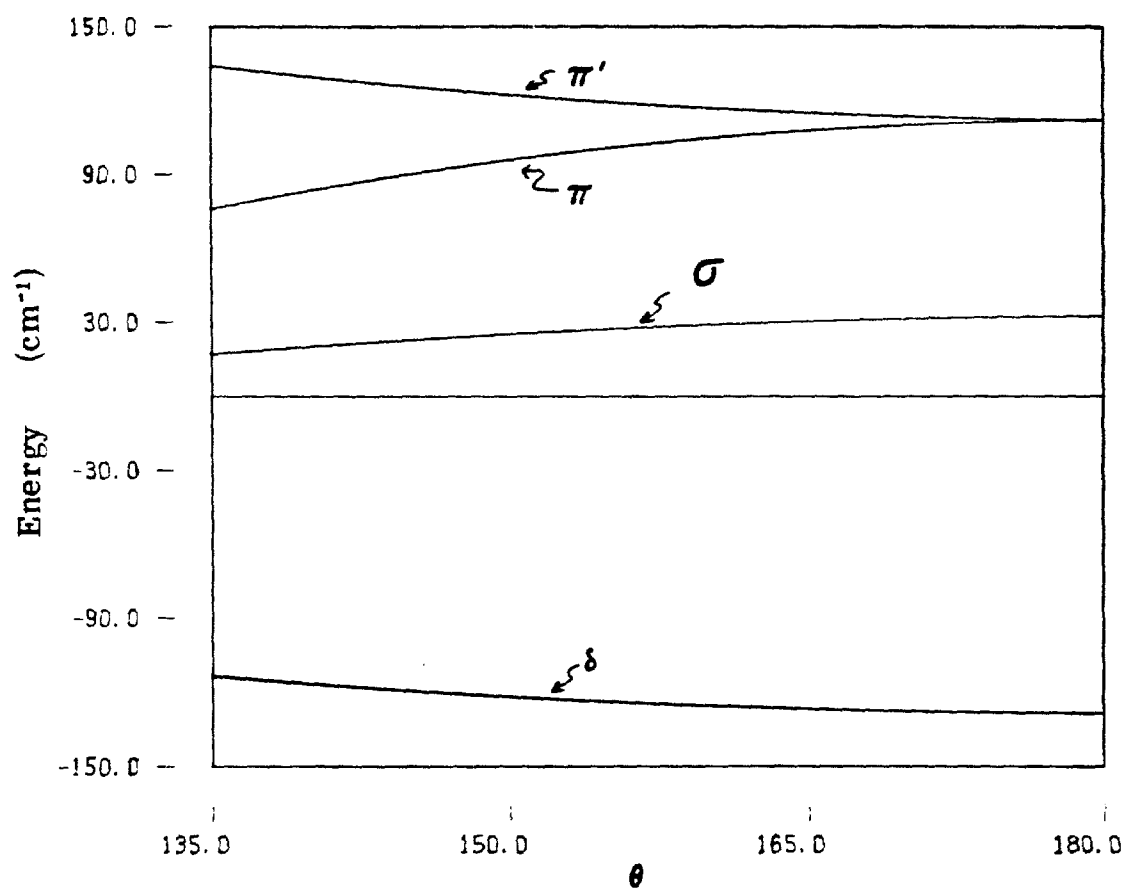


Figure 10.  $\text{ScCl}_2$  D orbital levels as a function of bond angle.

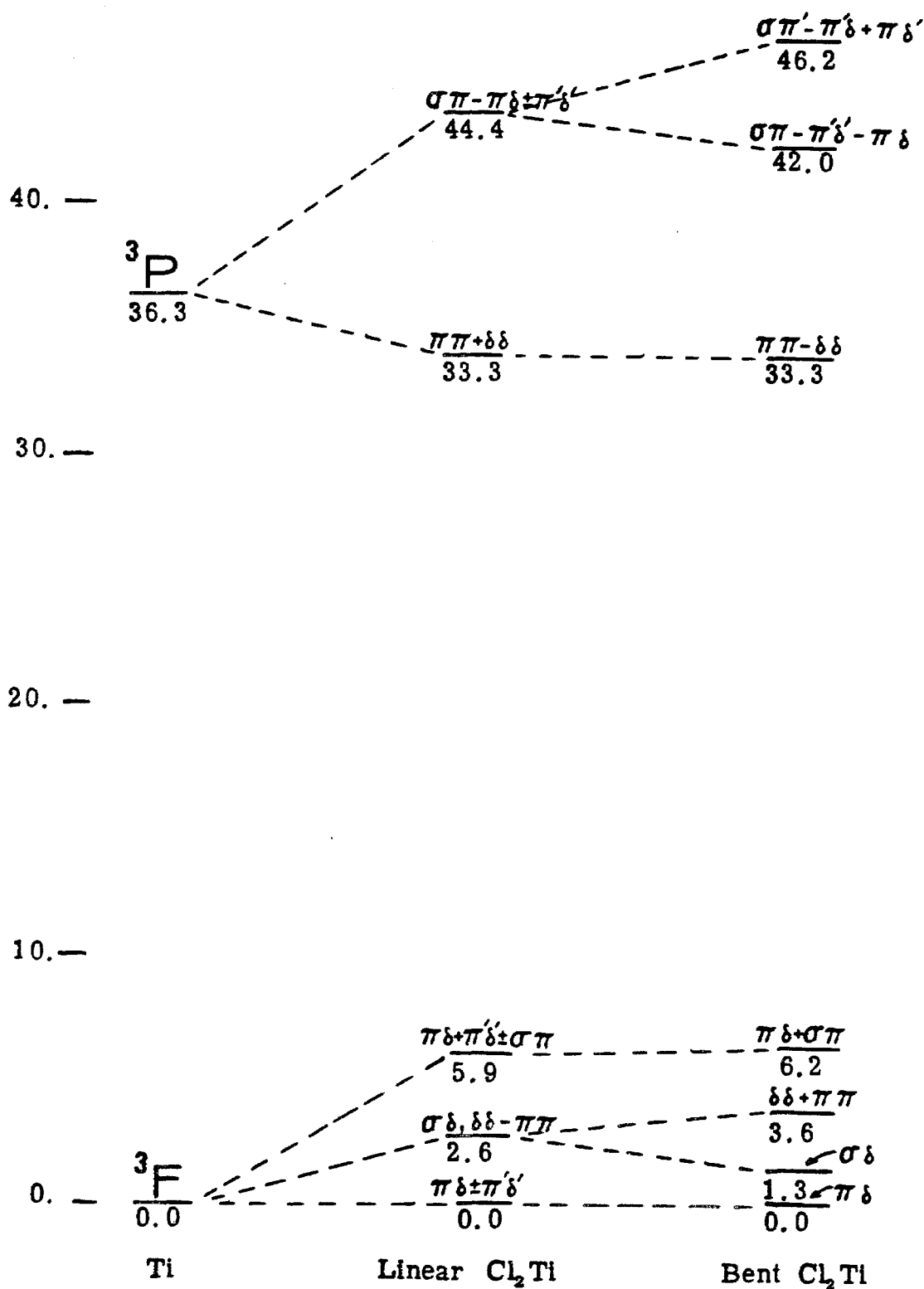
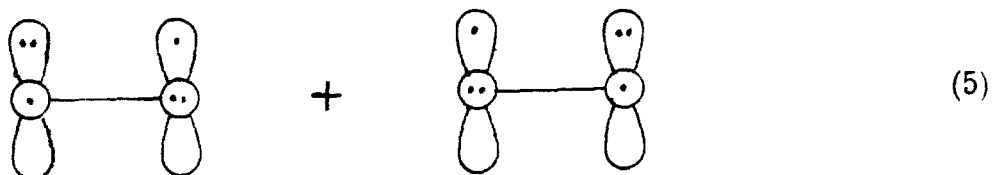


Figure 11.  $\text{TiCl}_2$  triplet d-d states.

perturbed (as we have already seen for  $\text{ScCl}_2$ ), a total splitting of 6 kcal for the  $^3\text{F}$  state. Since this is not a large effect, one would anticipate that the chlorides (or Cps) would provide very little geometrical effect other than steric. This is in sharp contrast to the semi-empirical results used to formulate the molecular orbital description of bent sandwich compounds generally used as an interpretive tool for such systems.<sup>4</sup>

It is difficult though for sigma ligands such as H's to bond to a pure atomic state, since pure states may be a mixture of various "real" d orbital states and ligands can only bond to individual d orbital states. A molecular example of this is bonding an H to  $^3\Sigma^- \text{O}_2$ . A valence bond description of  $\text{O}_2\text{H}^{18}$  involves two resonance structures



If the hydrogen approaches along the y axis, only one of the two resonance structures remains important



and the O-H bond is substantially weaker than a normal O-H bond (47 kcal as compared with 104-120 kcal<sup>19</sup>) due to the quenching out of the

resonance energy. As the two sigma bonding ligands approach, the mixing of the various d orbital configurations will be quenched out. The energies for the quenched orbital states are shown in Fig. 12. This is a significant effect; one can see from Fig. 12 that the best orbital states to bond to are sigma-delta and sigma-delta'. To form a d sigma bond in the equatorial plane (d sigma), one must hybridize the d sigma and d delta orbitals; that is, d sigma and d delta in the coordinate systems of Fig. 12. The hybridized d sigma\* and d delta\* are

$$\begin{aligned} d\sigma^* &= 0.7 d\sigma - 0.3 d\delta \\ d\delta^* &= 2/3 d\delta + 1/3 d\sigma. \end{aligned} \tag{7}$$

Since both sigma-delta and sigma-delta' are low energy states, making one d sigma\* bond is favorable; however, making d sigma\* and d sigma\*' bonds requires hybridization involving the other d delta orbital. This will require mixing in the delta-delta' orbital state as well as sigma-delta and sigma-delta' states. This leads to an 8 kcal destabilization since the delta-delta' state is 12 kcal above the sigma-delta and sigma-delta' states. Bonding to the pure sigma-delta and sigma-delta' states will result in one d sigma\* and one bond to the lobe of a d delta\* orbital. For Sc we found that this is 9 kcal less favorable than two d sigma bonds. Figure 13 shows pictorially these two opposing effects, and implies that we would predict an optimum angle of 75° for two sigma bonds to TiCl<sub>2</sub>. Calculationally we find an optimum H-Ti-H angle of 76.3° for Ti(H)<sub>2</sub>(Cl)<sub>2</sub>. Furthermore, the optimum C-Ti-C angle for Ti(Cl)<sub>2</sub>(C<sub>3</sub>H<sub>6</sub>) is 75.4°. Other parameters for

40. —

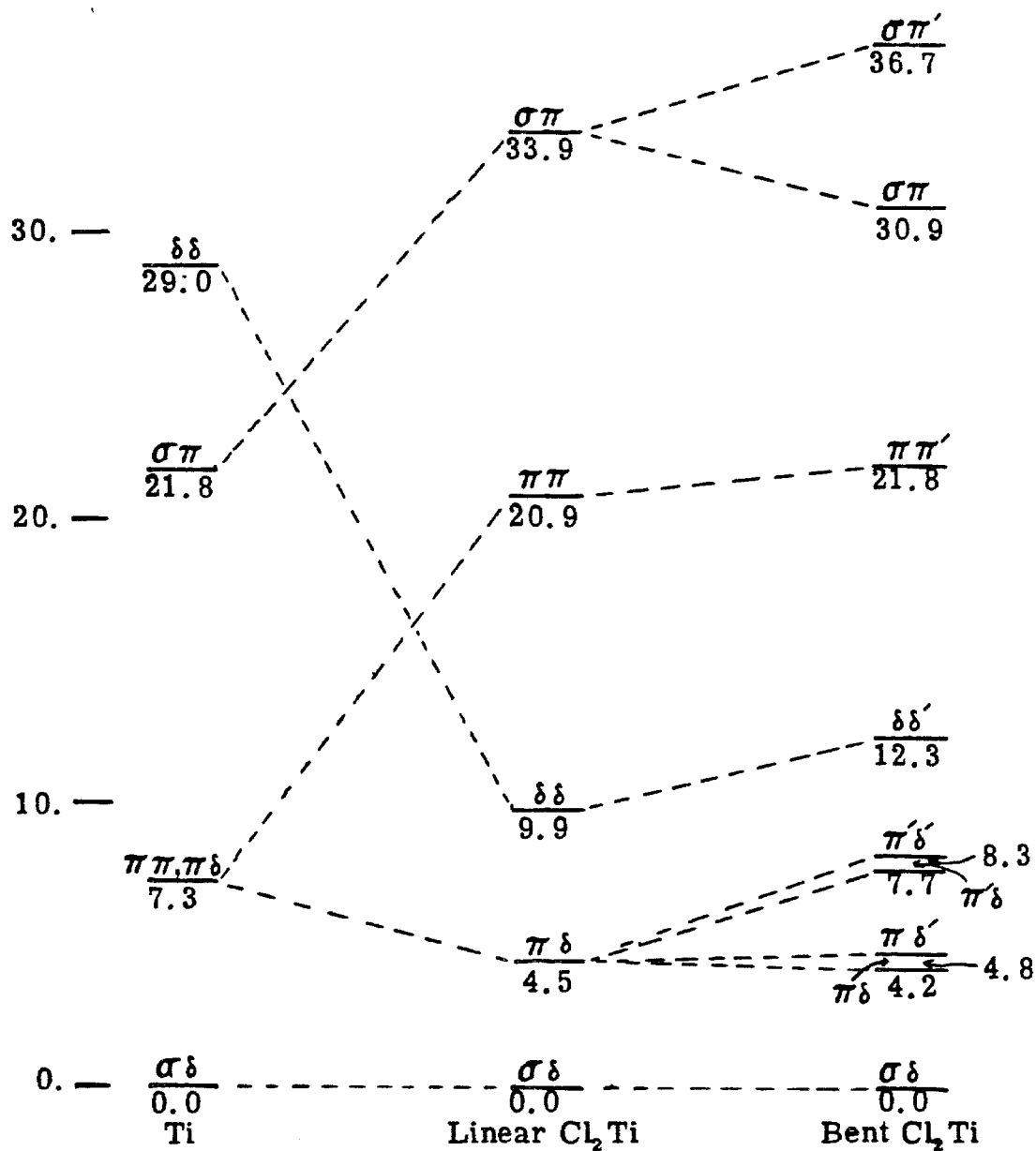


Figure 12.  $\text{TiCl}_2$  triplet single configuration states.

Figure 13.  $\text{Cl}_2\text{TiH}_2$  M-H bond strength as a function of  $\theta$  and d-d hybridization energy as a function of  $\theta$ .

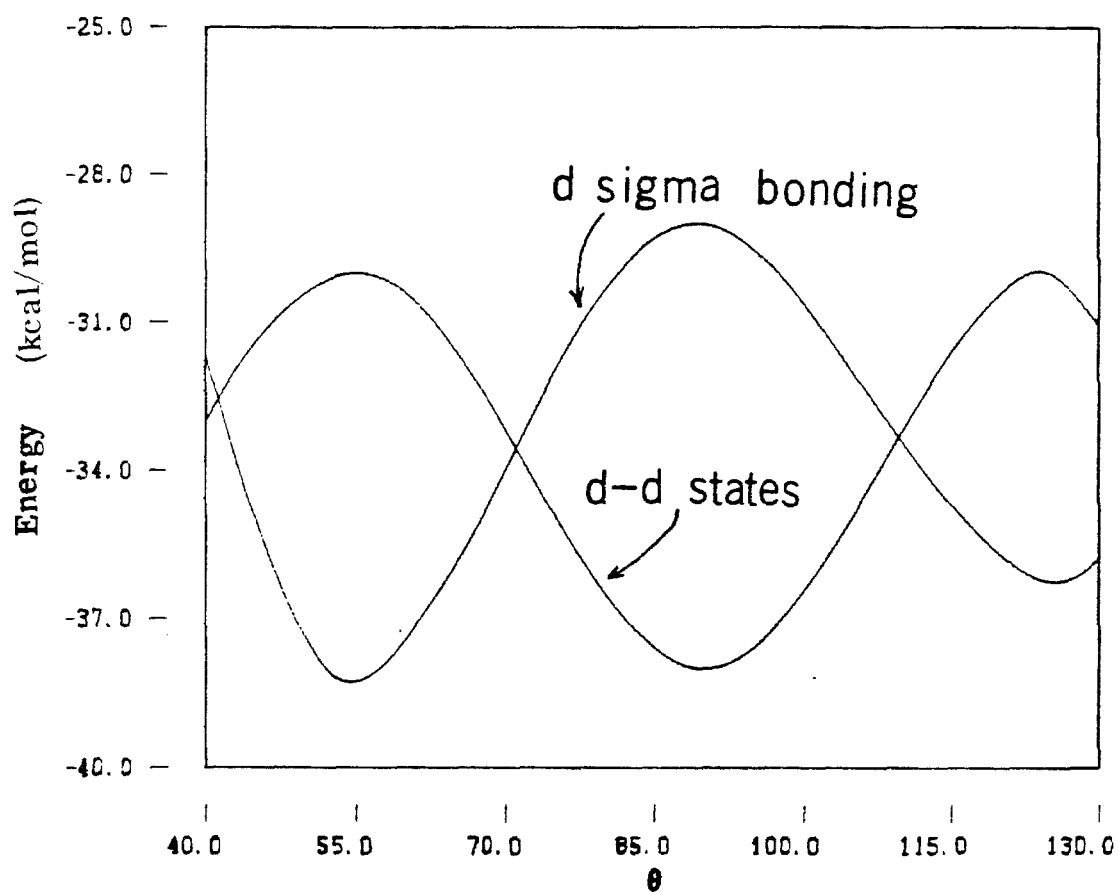
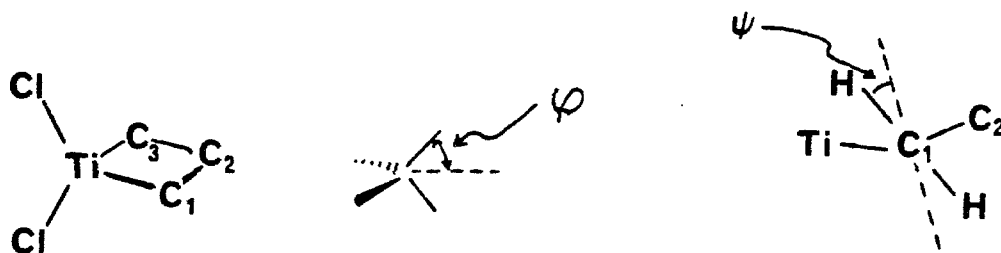


TABLE V. Bond distances ( $\text{\AA}$ ) and Bond Angles for a Planar and Pucker Titanacyclobutane.



Bond Distances		
	Planar	Puckered $10^\circ$
Ti-C <sub>1</sub>	2.02	2.01
Ti-Cl	2.328	2.328
C-H	1.09	1.09
C <sub>1</sub> -C <sub>2</sub>	1.56	1.56

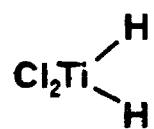
  

Bond Angles		
	Planar	Puckered $10^\circ$
C <sub>1</sub> -Ti-C <sub>3</sub>	75.6	75.6
H-C-H	111.0	111.0
$\varphi_{\text{H}}$	--	2.8
$\varphi_{\text{Cl}}$	--	1.3
$\psi$	--	4.9

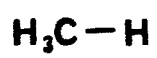
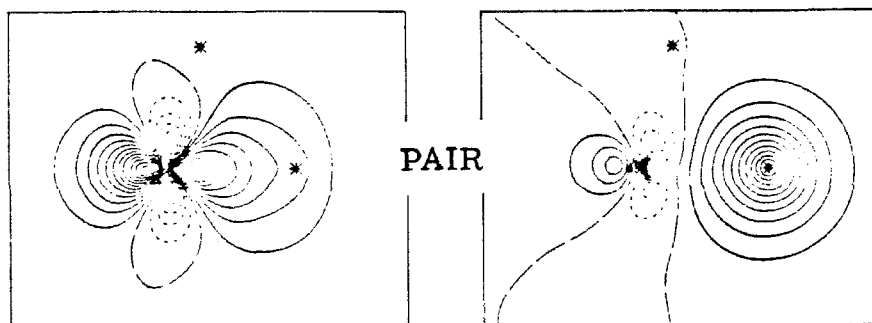


Figure 14.  $\text{Cl}_2\text{TiH}_2$  Ti-H sigma bond orbital contour plots.

Figure 15.  $\text{CH}_4$  C-H sigma bond orbital contour plots.



Ti H



C H

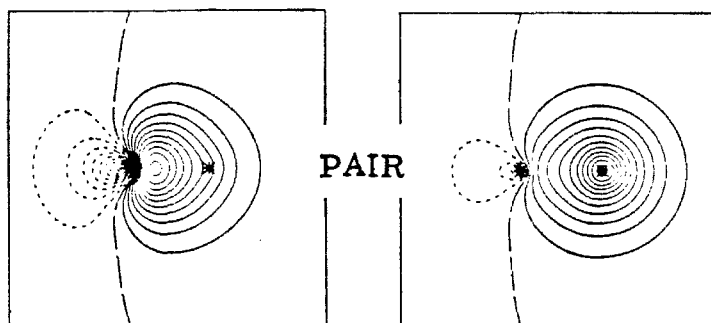
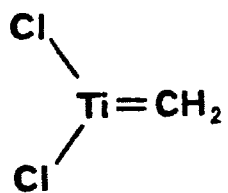
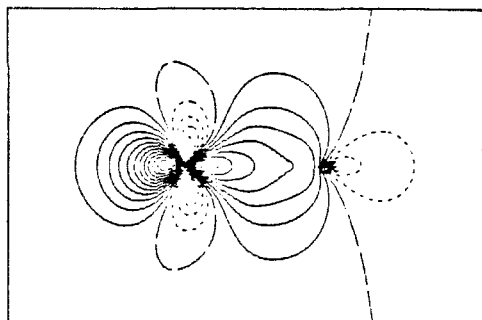


Figure 16.  $\text{Cl}_2\text{TiCH}_2$  Ti-C sigma and pi bond orbital contour plots.

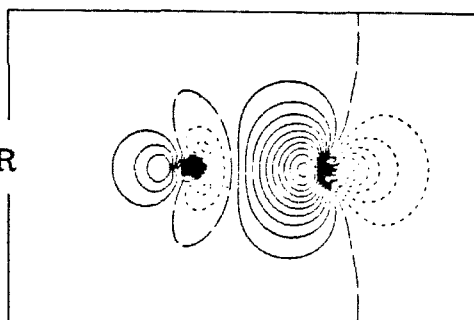
Figure 17.  $\text{C}_2\text{H}_4$  C-C sigma and pi bond orbital contour plots.



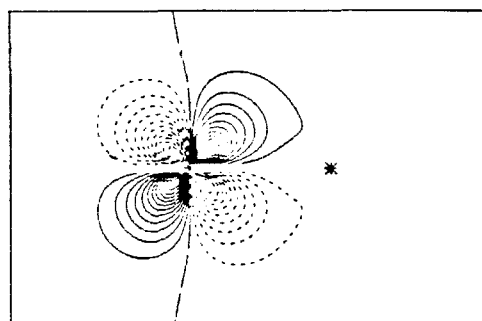
TiC  $\sigma$



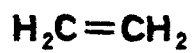
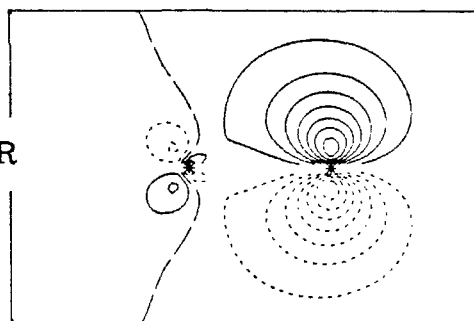
PAIR



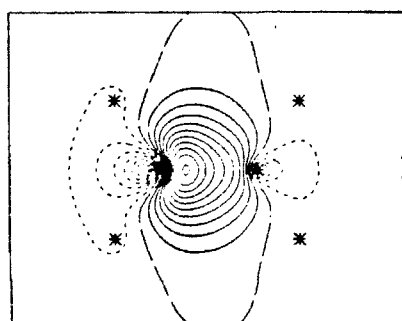
TiC  $\pi$



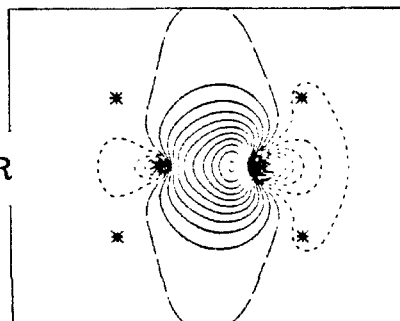
PAIR



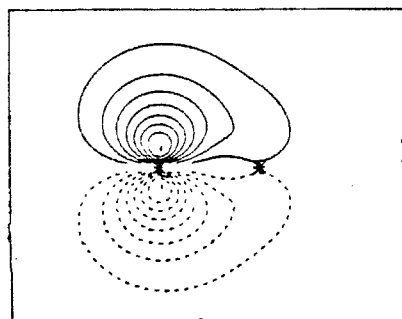
CC  $\sigma$



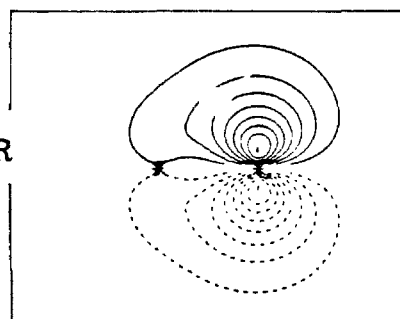
PAIR



CC  $\pi$



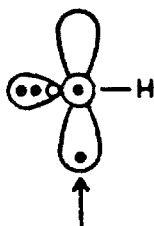
PAIR



$\text{Ti}(\text{Cl}_2)(\text{C}_3\text{H}_6)$  for both a planar metallocycle and one puckered  $10^\circ$  are shown in Table V. The energy difference between planar and puckered  $10^\circ$  is only 0.3 kcal, indicating that there is at most a very small barrier to planarity; in solution the metallocycle will appear planar. Orbital contour plots for one of the Ti-H sigma bonds of  $\text{Ti}(\text{H})_2(\text{Cl})_2$  are shown in Fig. 14. Comparison should be made to a C-H bond of methane shown in Fig. 15.

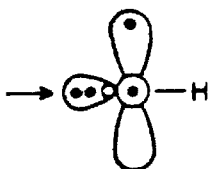
Now consider bonding a single ligand capable of both sigma and pi bonding ( $\text{CH}_2$ ) to  $\text{Ti}(\text{Cl})_2$ . As with two H's, we need to consider which orbital states of  $\text{Ti}(\text{Cl})_2$  methylene will need to bond to. If the  $\text{CH}_2$  plane is oriented perpendicular to the  $\text{TiCl}_2$  plane, the sigma-pi and delta-pi states are needed, and the appropriate combination of these states is 23 kcal above the sigma-delta state. If the  $\text{CH}_2$  is coplanar with  $\text{TiCl}_2$ , the sigma-delta and delta-delta' states are needed, and the appropriate combination of these states is 8 kcal above the sigma-delta state. This latter case is 15 kcal better than the former. Thus, using these simple ideas, we would predict a 15 kcal barrier to rotation about the Ti-C bond. In fact, the calculated barrier is 19 kcal. Note that this is purely an electronic effect; simple steric factors would predict that the perpendicular geometry would be favored. Orbital contour plots for the Ti-C sigma and pi bonds for  $\text{Ti}(\text{Cl})_2(\text{CH}_2)$  are shown in Fig. 16; they should be compared with the sigma and pi bonds of ethylene shown in Fig. 17.

Consider now bonding NH to  $\text{TiCl}_2$ . This ligand has two possible orientations, either like  $\text{CH}_2$



(8)

forming a sigma bond and a pi bond, or in a new mode



(9)

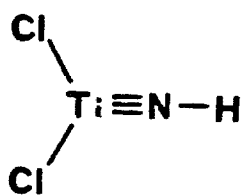
forming two pi bonds and a dative sigma bond. In fact, the latter orientation is favored; bending the H to  $120^\circ$  is 7 kcal above the linear case. Orbital contour plots for the linear case sigma and two pi bonds are shown in Fig. 18.

Finally, consider binding oxygen atom. As with NH, there are two possible orientations and as with NH, the form with two pi bonds and a dative sigma bond is the best. The geometrical and energetic parameters for these three molecules are given in Table VI. These bond energies can be used to calculate energy differences for the processes outlined in Table VII, suggesting that in addition to the exchange process

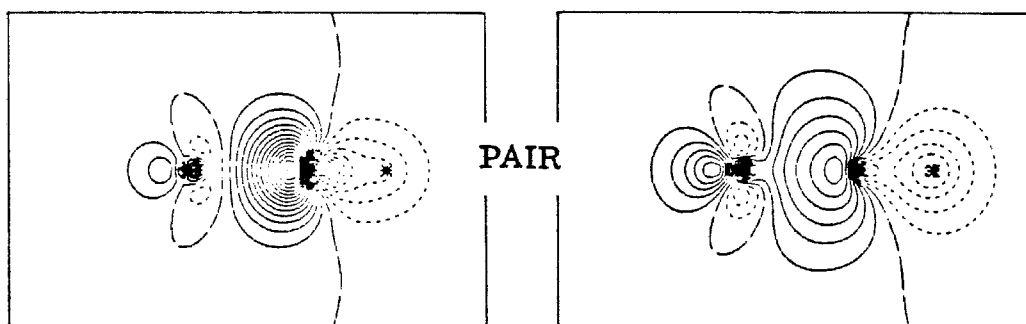


already being experimentally exploited,<sup>13</sup> there are several other processes that should occur. It is interesting that bimolecular

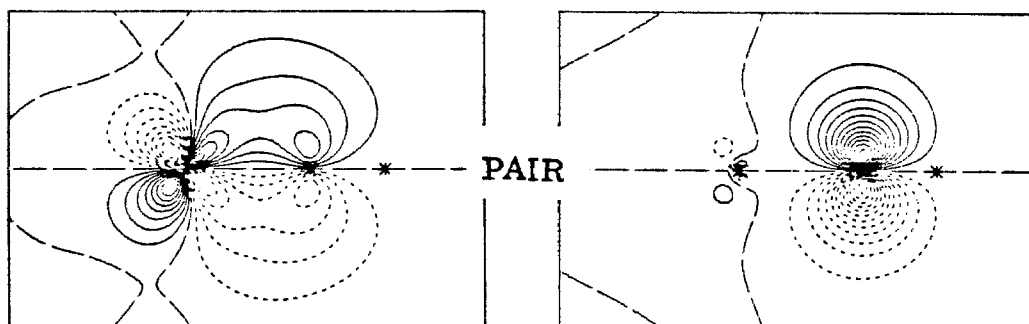
Figure 18.  $\text{Cl}_2\text{TiNH}$  Ti-N sigma and pi bond orbital contour plots.



TiN  $\sigma$



TiN  $\pi_x$



TiN  $\pi_y$

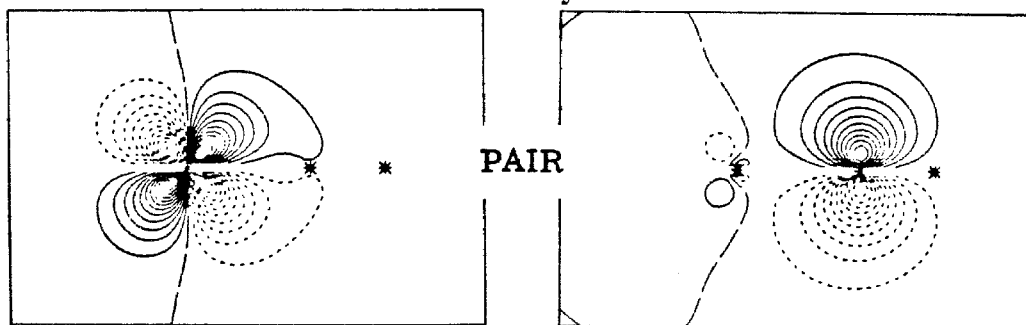




TABLE VI. Bond Distances and Bond Energies for  $\text{Cl}_2\text{TiX}$ .

X =	R(Ti-X) (Å)	Bond Energy (Ti-X) (kcal/mol)
$\text{CH}_2$	1.84	78
NH	1.64	102
O	1.56	140

TABLE VII. Titanium Ligand Exchange Processes.

				$\Delta E$
$\text{Cl}_2\text{TiCH}_2 + \text{H}_2\text{CNH}$	$\rightarrow$	$\text{Cl}_2\text{TiNH} + \text{H}_2\text{CCH}_2$		-35
$\text{Cl}_2\text{TiCH}_2 + \text{H}_2\text{CO}$	$\rightarrow$	$\text{Cl}_2\text{TiO} + \text{H}_2\text{CCH}_2$		-56
$\text{Cl}_2\text{TiCH}_2 + \text{HNNH}$	$\rightarrow$	$\text{Cl}_2\text{TiNH} + \text{HNCH}_2$		-58
$\text{Cl}_2\text{TiNH} + \text{HNO}$	$\rightarrow$	$\text{Cl}_2\text{TiO} + \text{HNNH}$		-38
$\text{Cl}_2\text{TiNH} + {}^1\text{O}_2$	$\rightarrow$	$\text{Cl}_2\text{TiO} + \text{ONH}$		-45
$\text{Cl}_2\text{TiCH}_2 + \text{CO}_2$	$\rightarrow$	$\text{Cl}_2\text{TiO} + \text{OCCH}_2$		-13
$\text{Cl}_2\text{TiCH}_2 + \text{RNO}_2$	$\rightarrow$	$\text{Cl}_2\text{TiO} + \text{RNOCH}_2$		+31-X <sup>a</sup>
$\text{Cl}_2\text{TiCH}_2 + \text{RNO}_2$	$\rightarrow$	$\text{Cl}_2\text{TiO} + \text{RNONH}$		+55-Y <sup>b</sup>
$\text{Cl}_2\text{TiCH}_2 + \text{HNO}$	$\rightarrow$	$\text{Cl}_2\text{TiNH} + \text{H}_2\text{CO}$		-76
$\text{Cl}_2\text{TiCH}_2 + \text{HNO}$	$\rightarrow$	$\text{Cl}_2\text{TiO} + \text{HNCH}_2$		-96

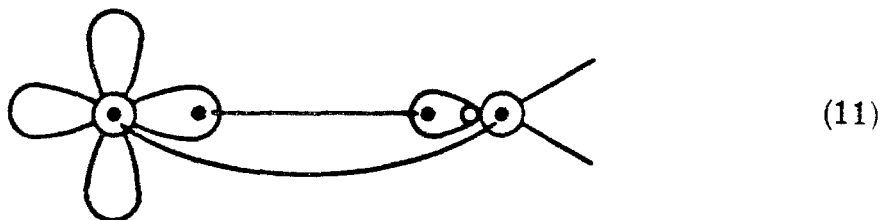
<sup>a</sup> X is the N-C bond strength in  $\text{RN} \begin{array}{c} \text{O} \\ \parallel \\ \text{CH}_2 \end{array}$ .

<sup>b</sup> Y is the N-N bond strength in  $\text{RN} \begin{array}{c} \text{O} \\ \parallel \\ \text{NH} \end{array}$ .

decomposition<sup>20</sup> should only be a problem for  $\text{CH}_2$ , as the energetics shown in Table VIII indicate.

These bonding concepts apply for complexes with more than one multiply bonded ligand. The orbital contour plots for the Cr-O and Cr-C bonds of  $\text{Cr}(\text{O})(\text{Cl})_2(\text{CH}_2)$  are shown in Fig. 19.

This section is closed with a brief discussion of carbene bonding. The dominant convention in the literature<sup>21</sup> defines a carbene ligand as one with bond polarization analogous to a ketone and an alkylidene ligand as one with the opposite polarity. Empirically the "carbene"-type ligands are found for low-valent complexes and "alkylidene" ligands are found for high-valent complexes. We suggest an alternate classification of these ligands in terms of the character of the carbene itself. The "carbene" ligands are dominantly those that have a ground state singlet for the free carbene, and the "alkylidene" ligands are those that have a ground state triplet. Pictorially, alkylidene-metal bonds can be described as

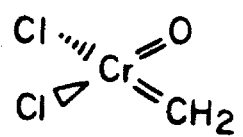


that is, they form a true sigma bond and a true pi bond, whereas the carbene-metal bonds are best described as a simple delocalization of the sigma lone pair into an empty d sigma orbital on the metal. Orbital contour plots for a carbene bonded to  $\text{Cr}(\text{O})(\text{Cl})_2$  are shown in Fig. 20. This bonding mode is analogous to CO or other Lewis bases.

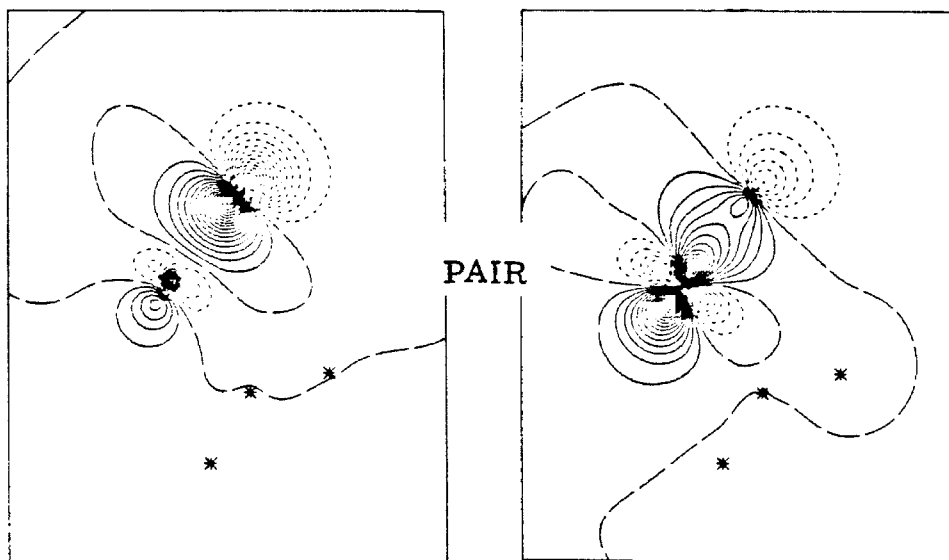
TABLE VIII. Bimolecular Decomposition Processes.

$\text{Cl}_2\text{Ti}-\text{X} + \text{Cl}_2\text{Ti}-\text{Y} \rightarrow 2\text{TiCl}_2 + \text{X}-\text{Y}$		
X	Y	$\Delta E$ (kcal/mol)
$\text{CH}_2$	$\text{CH}_2$	- 14
$\text{CH}_2$	NH	+ 22
$\text{CH}_2$	O	+ 42
NH	NH	+ 80
NH	O	+117
O	O	+162

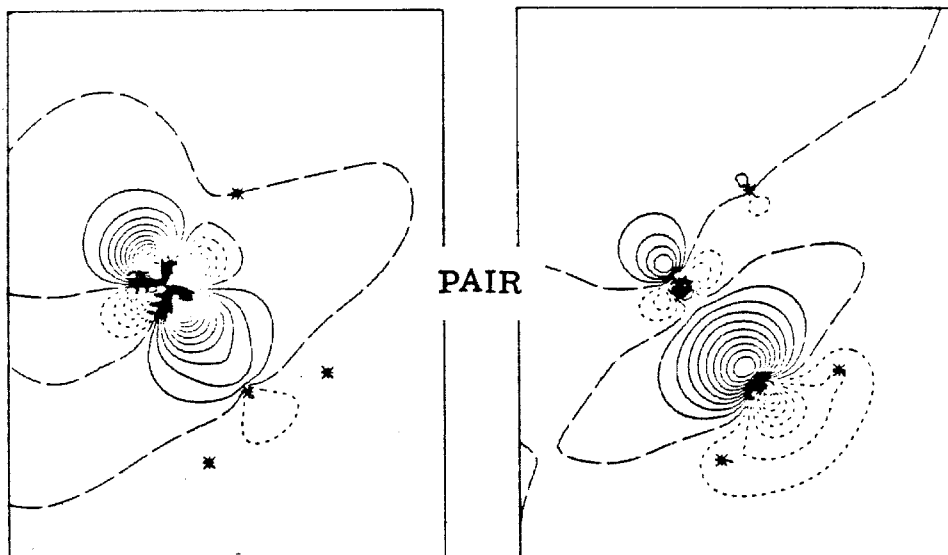
Figure 19.  $\text{Cr}(\text{O})(\text{Cl})_2(\text{CH}_2)$  orbital contour plots.



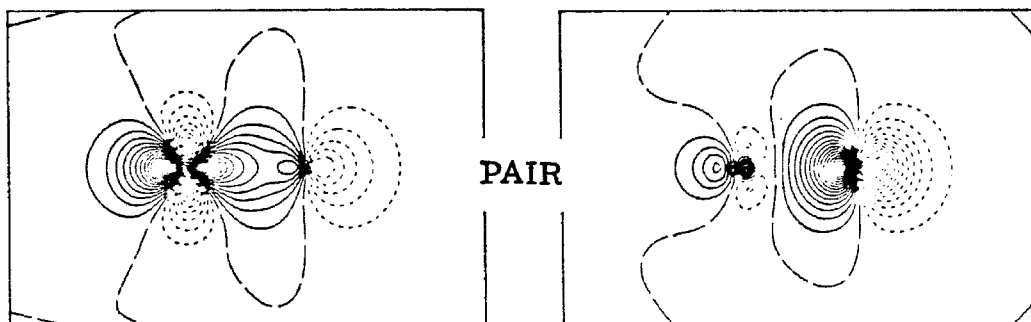
CrO  $\sigma$



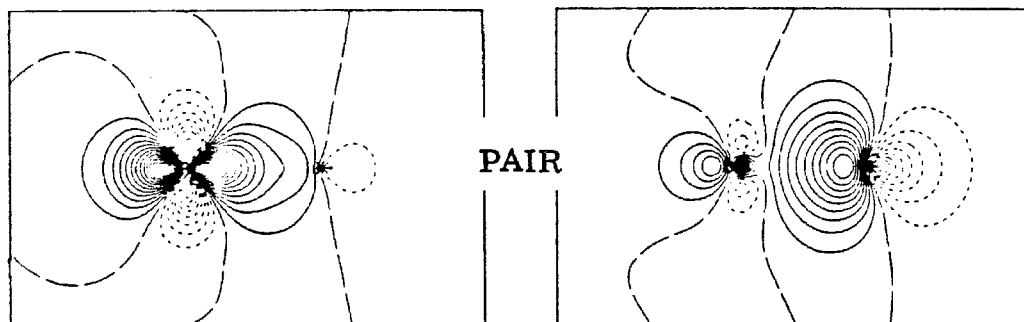
CrC  $\sigma$



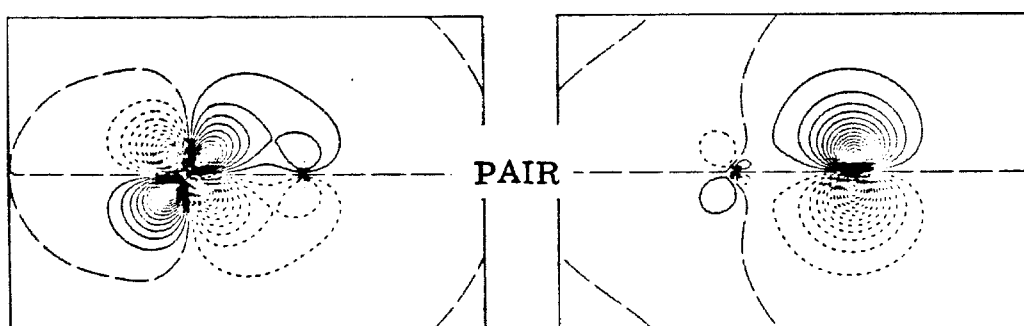
CrO  $\sigma$



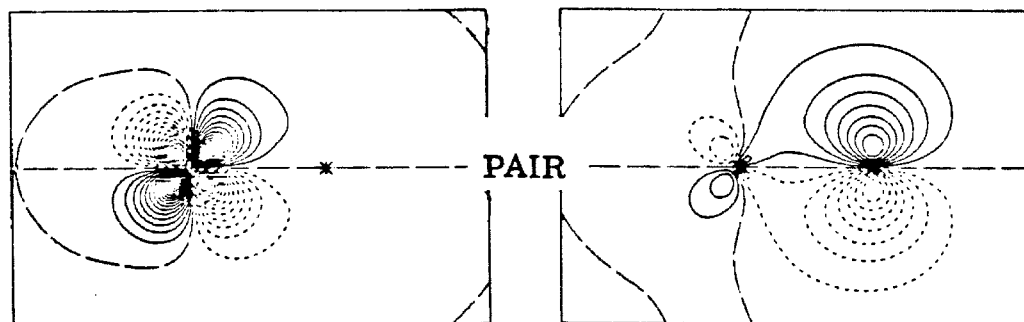
CrC  $\sigma$



CrO  $\pi$



CrC  $\pi$



O L.P.

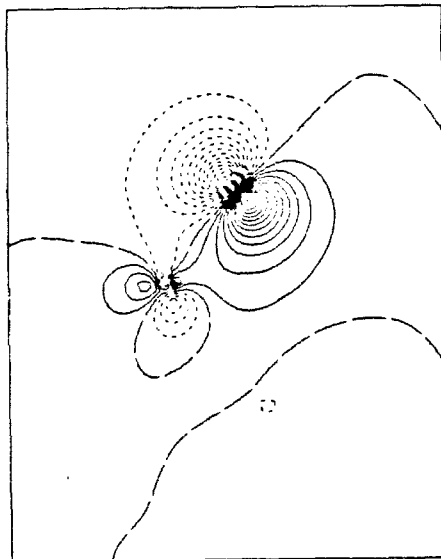
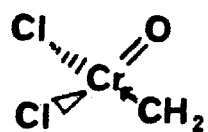
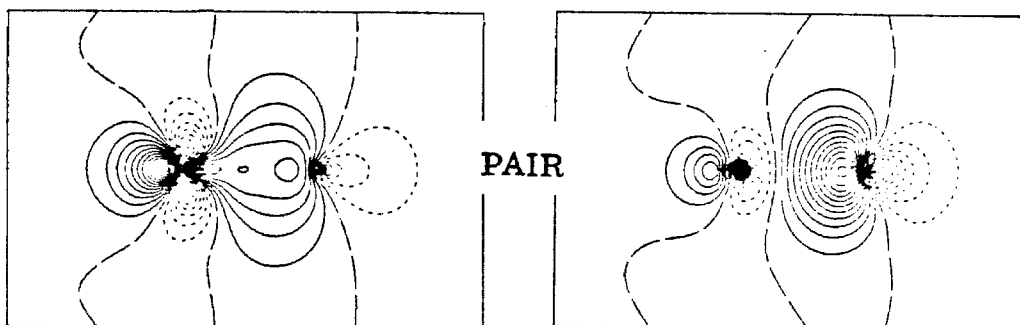




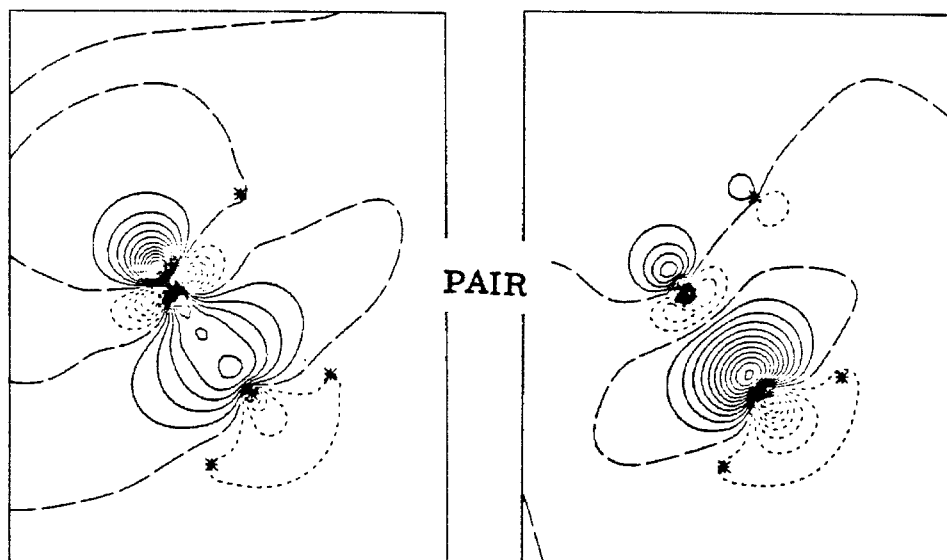
Figure 20.  $\text{Cr}(\text{O})(\text{Cl})_2(\text{CH}_2)$  singlet carbene adduct orbital contour plots.



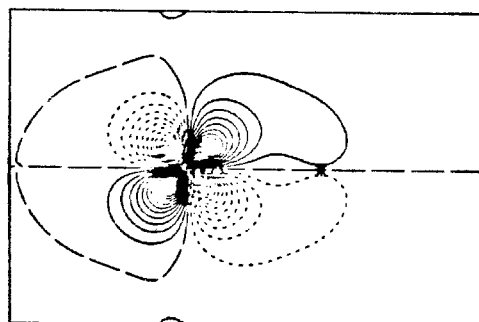
CrC  $\sigma$



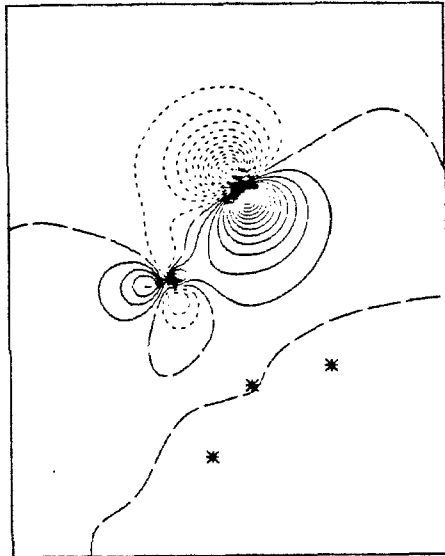
CrC  $\sigma$



Cr d orb



0 L.P.



Energetically, this binding mode forms a significantly weaker bond (it has a bond strength of 25 kcal) than forming a sigma and pi bond (which has a bond strength of 48 kcal), which is the normal mode for  $\text{CH}_2$  bonding to  $\text{Cr(O)(Cl)}_2$ .

## V. Periodic Trends

There is a general trend that transition metal ligand bond strengths decrease as one moves across the periodic table from the left to the right, and they increase as one moves down a column. These effects are shown in Tables IX and X, respectively. A qualitative picture consistent with these trends is that since covalent bonding is a direct function of orbital overlap, the orbital overlaps between the ligand orbitals and the metal orbitals must decrease as one goes across a row of the periodic table and that the overlaps increase as one goes down a column. Table XI shows the sigma and pi bond overlaps for three complexes, verifying the anticipated effect. The Mo-O and Mo-C orbitals for  $\text{Mo}(\text{O})(\text{Cl})_2(\text{CH}_2)$  are shown in Fig. 21 for comparison with the Ti-C orbitals of Fig. 16 and the Cr-C orbitals of Fig. 19; clearly the trend anticipated is followed.

TABLE IX. Horizontal Bond Strength Trends (kcal/mol).

Molecule	Bond Strength
(Cl) <sub>2</sub> Ti-O	140
(Cl <sub>2</sub> O)Cr-O	51
(Cl <sub>2</sub> )Ti-CH <sub>2</sub>	78
(Cl <sub>2</sub> O)Cr-OH <sub>2</sub>	48
Ti-(O tBu) <sub>4</sub>	416 <sup>a</sup>
V-(O tBu) <sub>4</sub>	360 <sup>a</sup>
Cr-(O tBu) <sub>4</sub>	308 <sup>a</sup>

TABLE X. Vertical Bond Strength Trends (kcal/mol).

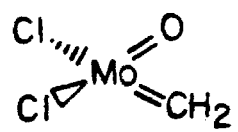
Molecule	Bond Strength
(Cl <sub>2</sub> O)Cr-O	51
(Cl <sub>2</sub> O)Mo-O	79
(Cl <sub>2</sub> O)Cr-CH <sub>2</sub>	48
(Cl <sub>2</sub> O)Mo-CH <sub>2</sub>	71
Ti-(O isoC <sub>3</sub> H <sub>7</sub> ) <sub>4</sub>	424 <sup>a</sup>
Zr-(O isoC <sub>3</sub> H <sub>7</sub> ) <sub>4</sub>	504 <sup>a</sup>
Hf-(O isoC <sub>3</sub> H <sub>7</sub> ) <sub>4</sub>	520 <sup>a</sup>

TABLE XI. GVB Orbital Overlaps for Metal-Carbene Bonds.

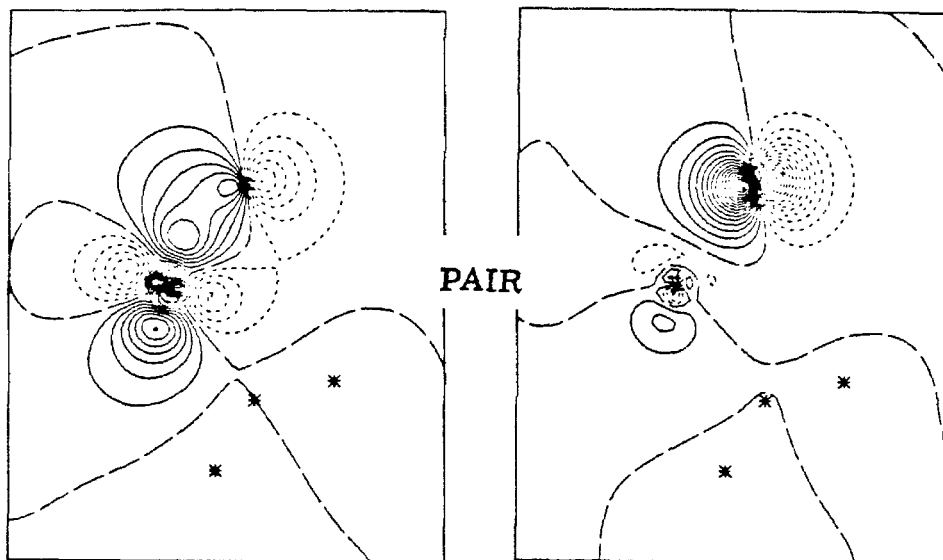
	Sigma Bond	Pi Bond
Cl <sub>2</sub> Ti-CH <sub>2</sub>	0.74	0.41
Cl <sub>2</sub> OCr-CH <sub>2</sub>	0.60	0.39
Cl <sub>2</sub> OMo-CH <sub>2</sub>	0.74	0.53

<sup>a</sup> From Ref. 25.

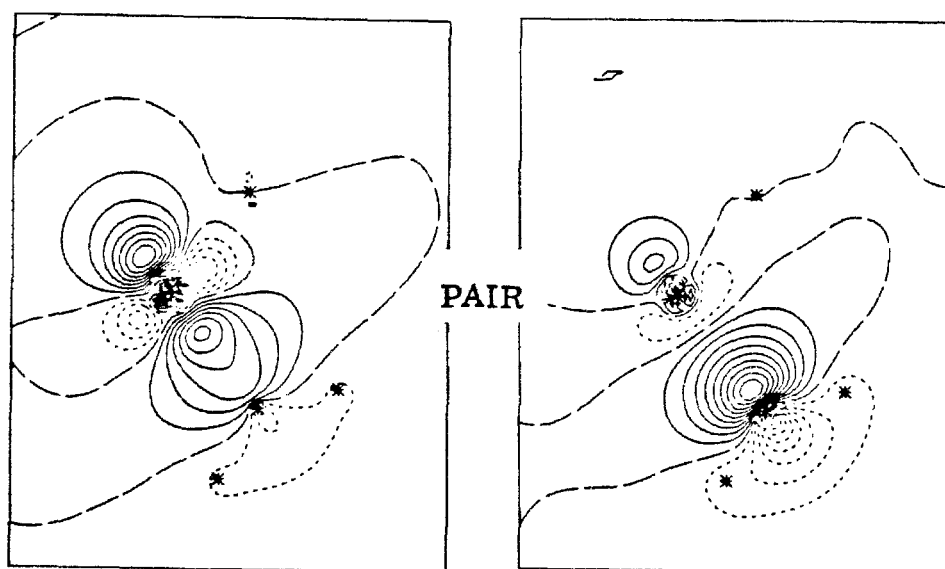
Figure 21.  $\text{Mo}(\text{O})(\text{Cl})_2(\text{CH}_2)$  orbital contour plots.



MoO  $\sigma$

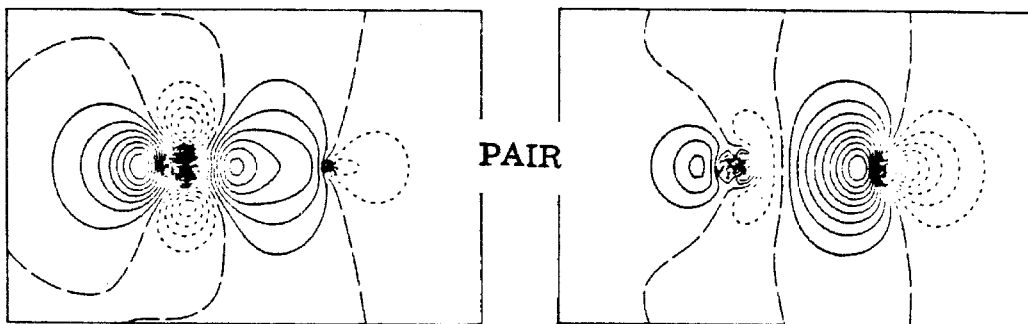


MoC  $\sigma$

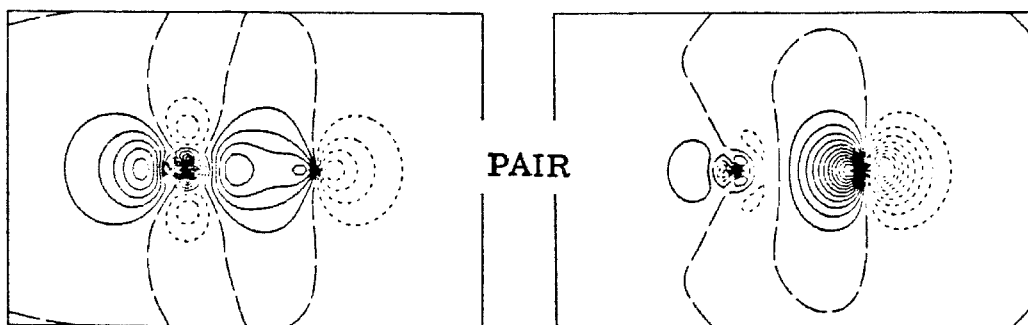




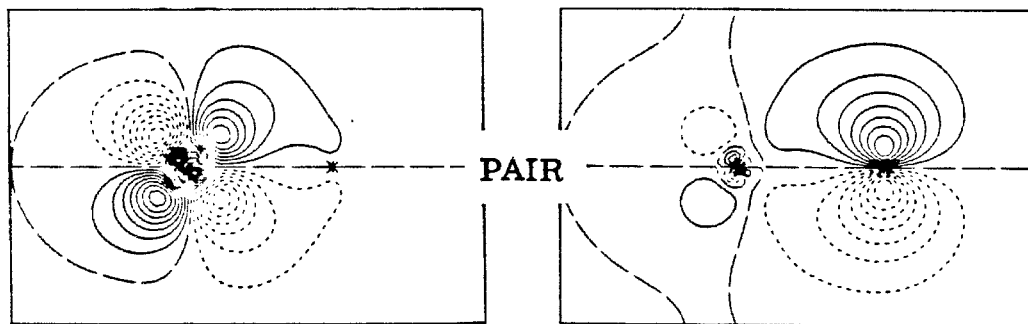
MoC  $\sigma$



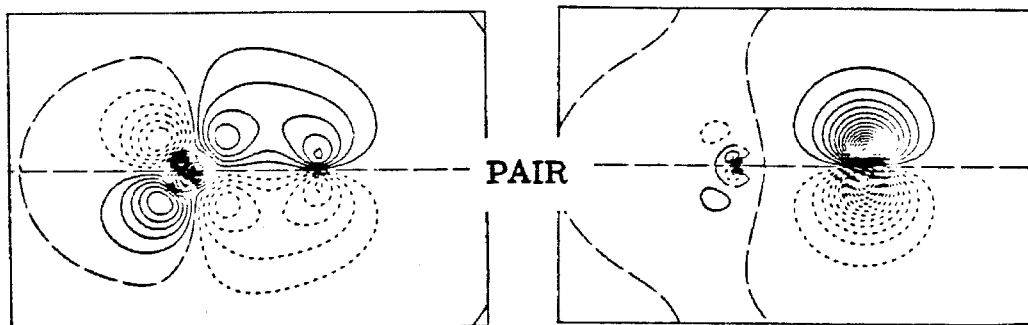
MoO  $\sigma$



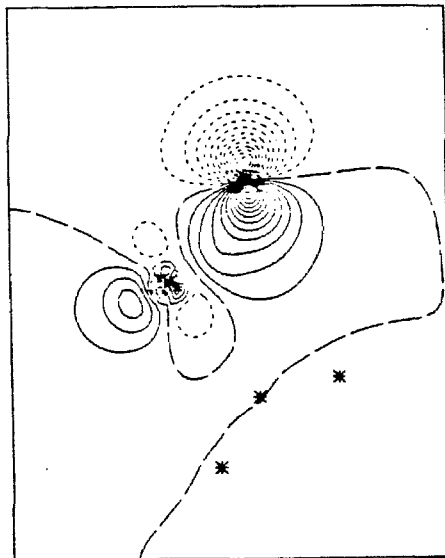
MoC  $\pi$



MoO  $\pi$



O L.P.



## References

1. L. Pauling, The Nature of the Chemical Bond (Cornell University Press, Ithaca, New York, 1960), Third Edition.
2. W. A. Goddard III and L. B. Harding, Ann. Rev. Phys. Chem., 29, 363-396 (1978).
3. C. J. Ballhausen, Introduction to Ligand Field Theory (McGraw-Hill, New York, 1962); C. K. Jorgensen, Absorption Spectra and Chemical Bonding in Complexes (Pergamon Press, 1962); C. J. Ballhausen and H. B. Gray, Molecular Orbital Theory (Benjamin, New York, 1964).
4. C. J. Ballhausen and J. P. Dahl, Acta Chem. Scand., 15, 1333-1336 (1961); N. W. Alcock, J. Chem. Soc. A, 2001-2009 (1967); J. C. Green, M. L. H. Green, and C. K. Prout, Chem. Commun., 421-422 (1972); J. W. Lauher and R. Hoffmann, J. Am. Chem. Soc., 98, 1729-1742 (1976); J. L. Peterson and L. F. Dahl, ibid., 96, 2249-2250 (1974); ibid., 97, 6416-6433 (1975); J. L. Peterson, D. L. Lichtenberger, R. F. Fenska, and L. F. Dahl, ibid., 97, 6433-6441 (1975); E. G. Muller, S. F. Watkins, and L. F. Dahl, J. Organomet. Chem., 111, 73-89 (1976); E. G. Muller, J. L. Peterson, and L. F. Dahl, ibid., 111, 91-112 (1976).
5. L. Pauling, J. Am. Chem. Soc., 59, 3570-3582 (1932).
6. (a) C. E. Moore, Nat. Stand. Ref. Data Ser., Nat. Bur. Stand., 35, Vol. 1 (1971); (b) For example, for Ti the  $s^2d^2 \rightarrow s^2d^1$  ionization is 9.9 eV.
7. H. Hotop and W. C. Lineberger, J. Phys. Chem. Ref. Data, 4, 539-576 (1975).

8. R. J. Cave and W. A. Goddard III, unpublished results.
9. H. Köpf and P. Köpf-Maier, Angew. Chem. Int. Ed. Engl., 18, 477-478 (1979).
10. F. N. Tebbe, G. W. Parshall, and G. S. Reddy, J. Am. Chem. Soc., 100, 3611-3613 (1978).
11. F. N. Tebbe, G. W. Parshall, and D. W. Ovenall, J. Am. Chem. Soc., 101, 5074-5075 (1979).
12. G. Fink, R. Rottler, D. Schell, and W. Zoller, J. Appl. Polym. Sci., 20, 2779-2790 (1976).
13. S. H. Pine, R. Zahler, D. A. Evans, and R. H. Grubbs, J. Am. Chem. Soc., 102, 3271-3272 (1980).
14. S. Kano, Y. Tanaka, and S. Hibino, Chem. Commun., 414-415 (1980).
15. F. Sato, H. Ishikawa, and M. Sato, Tetrahedron Lett., 21, 365-368 (1980); F. Sato, T. Jinbo, and M. Sato, ibid., 2171-2178 (1980).
16. E. C. Ashby and S. A. Noding, J. Org. Chem., 45, 1035-1044 (1980).
17. J. J. Barber, C. Willis, and G. M. Whitesides, J. Org. Chem., 44, 3603-3604 (1979).
18. W. J. Hunt, P. J. Hay, and W. A. Goddard III, J. Chem. Phys., 57, 738-748 (1972); B. J. Moss and W. A. Goddard III, ibid., 63, 3523-3531 (1975); B. J. Moss, F. W. Bobrowicz, and W. A. Goddard III, ibid., 63, 4632-4639 (1975).
19. S. W. Benson, Thermochemical Kinetics (Wiley, New York, 1976).

20. R. R. Schrock and P. R. Sharp, J. Am. Chem. Soc., 100, 2389-2399 (1978).
21. R. H. Grubbs, Prog. Inorg. Chem., 24, 1-50 (1978).
22. K. P. Huber and G. Herzberg, Molecular Spectra and Molecular Structure (Van Nostrand Reinhold, New York, 1979), Vol. IV.
23. H. M. Rosenstock, K. Draxl, B. W. Steiner, and J. T. Herron, J. Phys. Chem. Ref. Data, 6, 736-772 (1977).
24. G. B. Ellison, P. C. Engelking, and W. C. Lineberger, J. Am. Chem. Soc., 100, 2556-2558 (1978).
25. V. I. Tel'noi and I. B. Rabinovich, Russian Chemical Reviews (English Translation), 46, 689-705 (1977).

## APPENDIX A

### I. Introduction

There is a common folklore (backed by systematic study<sup>1</sup>) about the type of method,<sup>2</sup> basis set,<sup>3</sup> and the quality of wavefunction needed to obtain reasonable results for geometries,<sup>4-6</sup> isomeric differences,<sup>4,7,8</sup> and even bond energies<sup>9,10</sup> for nonpathological organic molecules (consisting of C, O, N, and H); however, no such "feel" exists for systems containing a transition metal. This section will attempt to document a study of high-valent early transition metal systems where the metal is fully ligated. The systems studied are dichloro-titanium, chromium, and molybdenum complexes with ligands such as CH<sub>2</sub>, NH, O, or two hydrogens used to complete the coordination sphere. Since it is well established that minimum basis set (MBS) calculations perform marginally well for determining geometries of straightforward systems<sup>4</sup> and generally perform poorly for determining energetic quantities,<sup>4</sup> we have concentrated our investigation on studying the effects of electron correlation and polarization functions at a split-valence [valence double zeta (VDZ)] level of basis set. The basis utilized is a new style gaussian basis, similar perhaps to several in the literature for select elements.<sup>11-13</sup> The basis consists of four optimized primitive gaussians to describe 1s, 2p, and 3d atomic orbitals and two optimized functions to describe each remaining atomic orbital. This basis is then contracted to a split-valence basis (minimal basis for core orbitals and two contracted basis functions for valence orbitals). The basis sets for H-Ba and a more detailed discussion will be presented elsewhere.<sup>14</sup> For reference, this style basis introduces an error of 3.2 kcal (relative to the standard Dunning-

Huzinaga VDZ basis<sup>3</sup> in the C-O bond strength of the CO diatomic.

The effect of electron correlation on geometrical parameters will be examined first. This is followed by a discussion of electron correlation effects on bond energies and an analysis of the partitioning of the electronic correlation into various classes (GVB-PP,<sup>15</sup> interpair terms,<sup>16</sup> and perfect-pairing breakdown terms<sup>15</sup>). These effects are unified in an extension of retention of bondedness<sup>7</sup> (isodesmic<sup>17</sup>) concepts to transition metal systems. Finally, we provide a summary of a scheme that has proven to be useful for studying reactions of transition metal systems.

## II. Geometrical Tests

Geometrical tests of electron correlation were carried out on  $\text{Ti}(\text{Cl})_2\text{X}$ ,  $\text{X} = \text{CH}_2$ ,  $\text{NH}$ , and  $\text{O}$ , where the chlorine is described by an MBS basis with an effective potential<sup>18</sup> replacing the 1s, 2s, and 2p core electrons. Table I presents the results for the Ti-X bond length as one progresses from Hartree-Fock (HF) through generalized valence bond-perfect paired (GVB-PP) to a full configuration interaction (CI) among the uniquely defined GVB orbitals (GVB-CI). The results are consistent with the general trends found for small molecules; that is, HF underestimates bond distances, GVB-PP tends to overestimate bond distances, and adding the GVB-CI has a small effect on the bond distance (if adjacent bonds are correlated, GVB-CI will significantly shorten GVB-PP bond distances, usually resulting in quite adequate bond distances). Comparable results for ethylene, methylenimine, and formaldehyde are presented in Table II. Table III indicates that (as one would expect) correlation in the Ti-X bond has little effect on the Cl-Ti-Cl angle. Addition of f functions ( $\zeta = 0.3$ ) to the Ti basis has a negligible effect on the Ti-O bond length of  $\text{Ti}(\text{O})(\text{Cl})_2$ ; the f functions lengthen the bond by 0.004 Å. Finally, a warning is in order. In spite of the reasonable results presented above for HF geometries, HF may perform disastrously for transition metal systems with more than one covalent ligand (the chlorine bonds in the above systems were quite ionic). For example, the geometry for  $\text{Cr}(\text{H})(\text{O})(\text{Cl})_2(\text{OH})$  optimized at the HF level is in error by 15 kcal relative to the GVB-CI optimized geometry!



TABLE I.  $\text{Cl}_2\text{Ti-X}$  Bond Length Test of Electron Correlation (MBS Cl; VDZ Ti; VDZ + Pol. X). Bond lengths are given in ångstroms.

X	HF	GVB-PP	GVB-CI
O	1.53	1.57	1.56
NH	--	1.71	1.64
$\text{CH}_2$	1.84	1.90	1.89

TABLE II.  $\text{CH}_2\text{-X}$  Bond Length Test of Electron Correlation (VDZ + Pol.  $\text{CH}_2$ ; VDZ + Pol. X). Bond lengths are given in ångstroms.

X	HF	GVB-PP	GVB-CI	Exper.
O	1.183	1.215	1.221	1.2078
NH	1.251	1.280	1.285	--
$\text{CH}_2$	1.327	1.357	1.362	1.339

TABLE III.  $\text{Cl}_2\text{T-X}$  ( $\text{Cl}_2\text{Ti}$ ) Bond Angle Test of Ti-X Correlation (MBS Cl; VDZ + Ti; VDZ + pol. X).

X	HF	GVB-PP	GVB-CI
O	129.6	131.5	131.8
$\text{CH}_2$	137.9	143.4	144.4

### III. Bond Strength Tests

As with geometrical variations, one would anticipate correlation effects on bond strengths for transition metal systems would parallel those for organic molecules with the only anticipated difference being an amplification of the effect. This is borne out by comparison of Tables IV and V. For double bonds, the differential correlation error between  $\text{H}_2\text{C-X}$  and  $\text{Ti}(\text{Cl})_2\text{X}$  systems is between 30 and 40 kcal. Clearly, while HF may be acceptable for some organic applications (at least as a reference configuration<sup>19</sup> for standard CI calculations), it is totally unacceptable for transition metal systems. Tables VI and VII indicate that polarization functions have comparable effects for transition metal and organic systems; f functions on the metal contribute 5 kcal and d functions on the ligand contribute 15 kcal to a bond strength. Tables VIII through XVIII present the dominant correlation terms for several analogous organic and transition metal systems. Again there are no surprises, just amplification of effects previously discussed for organic systems. An interesting point is that molybdenum systems have smaller correlation errors in general than do analogous chromium systems. This is due to the increased overlap between the metal d orbitals and the p orbitals on the ligands.

TABLE IV.  $\text{Cl}_2\text{Ti-X}$  Bond Strength Test of Electron Correlation  
(MBS Cl; VDZ Ti; VDS + Pol. X). Bond energies in kcal/mol.

X	HF	GVB-PP	GVB-CI	$\Delta\text{HF}$
				GVB-CI
O	20.6	67.7	119.8	99.2
NH	-9.9	50.3	77.9	87.8
$\text{CH}_2$	-14.6	59.7	51.5	66.1

TABLE V.  $\text{CH}_2\text{-X}$  Bond Strength Test of Electron Correlation  
(VDZ + Pol.  $\text{CH}_2$ ; VDZ + Pol. X). Bond Energies in kcal/mol.

X	HF	GVB-PP	GVB-CI	$\Delta\text{HF}$	Exper.
				GVB-CI	
O	105.8	138.2	165.0	59.2	180.4
NH	100.1	130.8	146.2	46.1	--
$\text{CH}_2$	123.8	149.2	157.8	34.0	176.7

TABLE VI.  $\text{Cl}_2\text{Ti}=\text{O}$  Bond Strength Test of Polarization Basis Functions (MBS Cl; VDZ Ti; VDZ O).

Basis	Bond Energy (kcal/mol)
--	104.4
+ Pol. on O	119.8
+ Pol. on O + Pol. on Ti	125.0

TABLE VII.  $\text{H}_2\text{C}=\text{CH}_2$  Bond Strength Test of Polarization Basis Functions (VDZ  $\text{CH}_2$ ).

Basis	Bond Energy (kcal/mol)
--	145.2
+ Pol. on C	157.8

TABLE VIII.  $\text{Cl}_2\text{TiCH}_2$  GVB-CI Configurations (cutoff: 1 kcal/mol).

$\sigma$	$\sigma^*$	$\pi$	$\pi^*$	Energy Contribution (kcal/mol)
2	0	2	0	--
2	0	0	2	29.0
1	1	1	1	14.4
0	2	0	2	9.5
0	2	0	2	4.0

TABLE IX.  $\text{C}_2\text{H}_4$  GVB-CI Configurations (cutoff: 1 kcal/mol).

$\sigma$	$\sigma^*$	$\pi$	$\pi^*$	Energy Contribution (kcal/mol)
2	0	2	0	--
2	0	0	2	15.6
1	1	1	1	9.6
0	2	2	0	5.1

TABLE X.  $\text{Cl}_2\text{TiO}$  GVB-CI Configurations (cutoff: 1 kcal/mol).

$\sigma$	$\sigma^*$	$\pi_x$	$\pi_x^*$	$\pi_y$	$\pi_y^*$	Energy Contribution (kcal/mol)
2	0	2	0	2	0	--
1	1	2	0	1	1	18.8
1	1	1	1	2	0	13.9
2	0	1	1	1	1	13.3
2	0	2	0	0	2	9.7
0	2	2	0	2	0	9.5
2	0	0	2	2	0	6.7
1	1	1	1	0	2	2.0
0	2	1	1	1	1	1.8
1	1	0	2	1	1	1.5

TABLE XI.  $\text{CH}_2\text{O}$  GVB-CI Configurations (cutoff: 1 kcal/mol).

$\sigma$	$\sigma^*$	$\pi$	$\pi^*$	Energy Contribution (kcal/mol)
2	0	2	0	--
2	0	0	2	18.1
1	1	1	1	13.5
0	2	2	0	7.2

TABLE XII.  $\text{Cl}_2\text{TiNH}$  GVB-CI Configurations (cutoff: 1 kcal/mol).

$\sigma$	$\sigma^*$	$\pi_x$	$\pi_x^*$	$\pi_y$	$\pi_y^*$	Energy Contribution (kcal/mol)
2	0	2	0	2	0	--
2	0	1	1	1	1	24.1
2	0	2	0	0	2	16.1
2	0	0	2	2	0	10.5
0	2	2	0	2	0	5.6
1	1	1	1	2	0	3.9
2	0	0	2	0	2	2.6
1	1	2	0	1	1	2.5
1	1	1	1	0	2	1.0

TABLE XIII.  $\text{CH}_2\text{NH}$  GVB-CI configurations (cutoff: 1 kcal/mol).

$\sigma$	$\sigma^*$	$\pi$	$\pi^*$	Energy Contribution (kcal/mol)
2	0	2	0	--
2	0	0	2	16.6
1	1	1	1	10.6
0	2	2	0	6.2

TABLE XIV.  $\text{Cl}_2\text{CrO}_2$  GVB-CI Configurations (cutoff: 1 kcal/mol).

$\sigma_1$	$\sigma_1^*$	$\sigma_2$	$\sigma_2^*$	$\pi_1$	$\pi_1^*$	$\pi_2$	$\pi_2^*$	Energy Contribution (kcal/mol)
2	0	2	0	2	0	2	0	--
2	0	1	1	2	0	1	1	30.3
1	1	2	0	1	1	2	0	30.3
2	0	2	0	0	2	2	0	29.6
2	0	2	0	2	0	0	2	29.6
2	0	0	2	2	0	2	0	14.3
0	2	2	0	2	0	2	0	14.3
2	0	0	2	2	0	0	2	6.4
0	2	2	0	0	2	2	0	6.4
2	0	2	0	0	2	0	2	3.2
2	0	1	1	0	2	1	1	2.9
1	1	2	0	1	1	0	2	2.9
1	1	1	1	1	1	1	1	2.4
2	0	2	0	1	1	1	1	2.0
2	0	0	2	0	2	2	0	1.4
0	2	2	0	2	0	0	2	1.4
1	1	2	0	2	0	1	1	1.2
2	0	1	1	1	1	2	0	1.2
1	1	0	2	1	1	2	0	1.1
0	2	1	1	2	0	1	1	1.1



TABLE XV.  $\text{Cl}_2\text{CrOCH}_2$  GVB-CI Configurations (cutoff: 1 kcal/mol).

$\sigma_c$	$\sigma_c^*$	$\sigma_o$	$\sigma_o^*$	$\pi_c$	$\pi_c^*$	$\pi_o$	$\pi_o^*$	Energy Contribution (kcal/mol)
2	0	2	0	2	0	2	0	--
2	0	1	1	2	0	1	1	29.5
2	0	2	0	0	2	2	0	28.4
1	1	2	0	1	1	2	0	24.2
2	0	2	0	2	0	0	2	23.6
0	2	2	0	2	0	2	0	14.9
2	0	0	2	2	0	2	0	13.6
0	2	2	0	0	2	2	0	8.8
2	0	0	2	2	0	0	2	4.2
2	0	1	1	0	2	1	1	3.3
2	0	2	0	0	2	0	2	3.2
2	0	2	0	1	1	1	1	2.8
1	1	1	1	1	1	1	1	2.4
1	1	2	0	1	1	0	2	2.2
2	0	2	0	1	1	2	0	1.6
1	1	2	0	2	0	1	1	1.5
2	0	0	2	0	2	2	0	1.5
0	2	1	1	2	0	1	1	1.4
2	0	1	1	2	0	0	2	1.4
2	0	1	1	1	1	2	0	1.3
0	2	2	0	2	0	0	2	1.3
1	1	1	1	2	0	2	0	1.3
1	1	0	2	1	1	2	0	1.1
1	1	2	0	0	2	1	1	1.0

TABLE XVI.  $\text{Cl}_2\text{MoO}_2$  GVB-CI Configurations (cutoff: 1 kcal/mol).

$\sigma_1$	$\sigma_1^*$	$\sigma_2$	$\sigma_2^*$	$\pi_1$	$\pi_1^*$	$\pi_2$	$\pi_2^*$	Energy Contribution (kcal/mol)
2	0	2	0	2	0	2	0	--
2	0	1	1	2	0	1	1	23.2
1	1	2	0	1	1	2	0	23.2
2	0	2	0	0	2	2	0	17.3
2	0	2	0	2	0	0	2	17.3
2	0	0	2	2	0	2	0	9.9
0	2	2	0	2	0	2	0	9.9
2	0	0	2	2	0	0	2	2.3
0	2	2	0	0	2	2	0	2.3
1	1	1	1	1	1	1	1	1.2
2	0	1	1	0	2	1	1	1.2
1	1	2	0	1	1	0	2	1.2
2	0	2	0	0	2	0	2	1.0

TABLE XVII.  $\text{Cl}_2\text{MoOCH}_2$  GVB-CI Configurations (cutoff: 1 kcal/mol).

[illegible]

TABLE XVIII.  $\text{Cl}_4\text{CrO}$  GVB-CI Configurations (cutoff: 1 kcal/mol).

$\sigma$	$\sigma^*$	$\pi_x$	$\pi_x^*$	$\pi_y$	$\pi_y^*$	Energy Contribution (kcal/mol)
2	0	2	0	2	0	--
2	0	1	1	1	1	23.4
2	0	2	0	0	2	20.8
2	0	0	2	2	0	20.8
1	1	2	0	1	1	16.0
1	1	1	1	2	0	16.0
0	2	2	0	2	0	7.2
1	1	1	1	0	2	5.4
1	1	0	2	1	1	5.4
2	0	0	2	0	2	5.1
1	1	2	0	2	0	3.4
1	1	0	2	0	2	2.3
0	2	1	1	1	1	2.1
0	2	2	0	0	2	1.3
0	2	0	2	2	0	1.3
2	0	0	2	1	1	1.1
2	0	1	1	0	2	1.1

#### IV. Retention of Bondedness

Accurate calculation of energetics for chemical processes is known to require inclusion of those electronic correlation effects that are differential between reactants and products. Thus, to obtain the most accurate energetics at a given level of correlation, it is wise to consider processes involving formation and dissolution of similar bonds. For example, to accurately (and economically) obtain the Ti-C bond strength of  $\text{Ti}(\text{Cl})_2(\text{CH}_2)$ , we recommend that the energy difference for the process



be calculated and that the experimental (or computationally determined)  $\Delta H_f^\circ$ 's for  $\text{Ti}(\text{Cl})_2$ ,  $\text{C}_2\text{H}_4$ , and  $\text{CH}_2$  be used to obtain a  $\Delta H_f^\circ$  for  $\text{Ti}(\text{Cl})_2(\text{CH}_2)$  and hence the Ti-C bond strength. By considering processes with constant bondedness, even HF calculations may yield moderately reliable bond energies for organic systems. However, since HF leads to much larger correlation errors in pi bonds than sigma bonds, and as we have seen before, transition metal systems than organics, processes that change the number of sigma and pi bonds may lead to large errors for HF. This is exemplified in Table XIX. It is apparent that HF leads to differential errors in sigma and pi bonds of 30-50 kcal. Using a GVB-CI wavefunction, the total spread in error has been greatly reduced to 8 kcal. By considering processes where the number and type of bonds are conserved and by including the dominant electron correlation effect, accurate reaction energetics are essentially guaranteed even for transition metal systems.

TABLE XIX.  $\Delta H$  Tests of Electron Correlation for Organic Reactions  
(energies in kcal/mol).

Process	$\Delta H$ HF	$\Delta H$ GVB-CI	$\Delta H$ Exper.	Error HF	Error GVB-CI
$\text{CH}_2\text{O} \rightarrow \text{CH}_2 + \text{O}$	105.8	165.0	180.4	74.6	15.4
$\text{C}_2\text{H}_4 \rightarrow 2 \text{CH}_2$	110.4	157.8	176.7	66.3	18.9
$\text{H}_2 \rightarrow 2\text{H}$	80.1	92.3	109.5	29.4	17.2
$\text{CH}_4 \rightarrow \text{CH}_3 + \text{H}$	86.7	96.7	112.1	25.4	15.9
$\text{C}_2\text{H}_6 \rightarrow 2 \text{CH}_3$	77.8	82.4	96.2	23.4	13.8
$\text{CH}_3\text{OH} \rightarrow \text{CH}_2 + \text{OH}$	63.6	77.4	98.7	35.1	21.3
$\text{CH}_3 \rightarrow \text{CH}_2 + \text{H}$	86.5	98.2	114.4	27.9	16.2
$\text{CH}_4 \rightarrow \text{CH}_2 + \text{H}_2$	93.1	102.5	117.0	23.9	14.5

## V. General Prescription

We suggest the following scheme for determining accurate energetics for chemical processes. One begins by calculating energy differences for reactions where the number and type of bonds are as similar as possible. A certain amount of creativity is needed for this step. To calculate the enthalpies at OK for these processes, one must add the differential zero point corrections to the calculated energy differences. The thus obtained  $\Delta H_{f_0}$  are combined with previously obtained  $\Delta H_{f_0}$  for the other species in the idealized reactions to calculate  $\Delta H_{f_0}$ 's for the molecules of interest. These  $\Delta H_{f_0}$ 's are combined with vibrational frequencies (experimental, calculated, or estimated) and moments of inertia to obtain  $\Delta H_{f_{300}}$  and  $S_{300}$ . Finally,  $\Delta G_{r_{300}}$  for the reactions of interest are calculated. As is apparent, this technique is analogous to the standard experimental techniques for obtaining free energies.

## References

1. There have been several very methodical studies on small organic molecules; see, for example, Refs. 4-6. This work must be lauded as they have firmed the foundations of ab initio theoretical techniques.
2. We will strictly be dealing with ab initio theoretical techniques as current semi-empirical techniques suffer large deficiencies for transition metal systems.
3. T. H. Dunning, Jr., and P. J. Hay, Modern Theoretical Chemistry, H. F. Schaefer III, Ed. (Plenum Press, New York, 1977), Vol. 3, pp. 1-27.
4. C. A. Parsons and C. E. Dykstra, J. Chem. Phys., 71, 3025-3033 (1979).
5. S. Bell, J. Chem. Phys., 68, 3014-3024 (1978).
6. D. Cremer, J. Chem. Phys., 69, 4440-4455 (1978).
7. C. J. Casewit and W. A. Goddard III, J. Am. Chem. Soc., 102, 4057-4062 (1980).
8. J. A. Pople, R. Krishnan, H. B. Schlegel, and J. S. Binkley, Int. J. Quant. Chem., 14, 545-560 (1978).
9. J. H. Davis, W. A. Goddard III, and L. B. Harding, J. Am. Chem. Soc., 99, 2919-2925 (1977); L. B. Harding and W. A. Goddard III, ibid., 99, 4520-4523 (1977).
10. M. L. Steigerwald and W. A. Goddard III, unpublished results; R. A. Bair and W. A. Goddard III, unpublished results.
11. E. L. Mehler and C. H. Paul, Chem. Phys. Lett., 63, 145-150 (1979).



12. H. Tatewaki and S. Huzinaga, J. Chem. Phys., 71, 4339-4348 (1979).
13. D. F. Feller and K. Ruedenberg, Theoret. Chim. Acta, 52, 231-251 (1979); M. W. Schmidt and K. Ruedenberg, J. Chem. Phys., 71, 3951-3962 (1979).
14. A. K. Rappé and W. A. Goddard III, unpublished results.
15. F. W. Bobrowicz and W. A. Goddard III, Modern Theoretical Chemistry, H. F. Schaefer III, Ed. (Plenum Press, New York, 1977), Vol. 3, pp. 79-127.
16. Interpair terms consist of simultaneous single excitations between pairs of electrons; for example  $(\sigma_1 \rightarrow \sigma_1^*) \times (\sigma_2 \rightarrow \sigma_2^*)$ , which allows dynamic correlation of the electrons in two sigma bonds.
17. For a review on the HF calculation of the energetics of "isodesmic" reactions, see W. J. Hehre, Acc. Chem. Res., 9, 399-406 (1976).
18. A. K. Rappé, T. A. Smedley, and W. A. Goddard III, unpublished results.
19. I. Shavitt, Modern Theoretical Chemistry, H. F. Schaefer III, Ed. (Plenum Press, New York, 1977), Vol. 3, pp. 189-275.